

Otto-von-Guericke-Universität Magdeburg  
Medizinische Fakultät  
Institut für Klinische Chemie und Pathobiochemie  
Direktor: Professor Dr. med. Berend Isermann



**The regulation of endoplasmic reticulum stress by activated  
protein C in diabetic nephropathy**

**Dissertation**

zur Erlangung des Doktorgrades

Dr. rer. medic  
(doctor rerum medicarum)

an der Medizinischen Fakultät  
der Otto-von-Guericke-Universität Magdeburg

vorgelegt von Sanchita Ghosh  
aus Jamshedpur, Indien  
Magdeburg 2019

## **Bibliographical description**

“Ghosh Sanchita; M.Sc. The regulation of endoplasmic reticulum stress by activated protein C in diabetic nephropathy – 2019 – 124 pages, 24 figures, 3 tables.

## **Abstract**

Diabetic nephropathy is the leading cause of chronic kidney disease as well as the primary complication of diabetes worldwide. Although, the molecular function of endoplasmic reticulum (ER) stress in diabetes mellitus (DM) is well-established in the liver and the pancreas, the role of ER stress in diabetic nephropathy remained unknown when starting this project. We uncovered important pathophysiological consequences of insulin resistance and hyperglycemia towards maladaptive ER stress and its contributions to the progression of diabetic nephropathy (dNP). This study establishes causality between defective insulin signaling leading to maladaptive ER stress in podocytes and impaired kidney function in DM. Searching for potential pathways compensating for impaired insulin signaling, we identified a new role of the coagulation system. Coagulation protease signaling rescues defective insulin signaling in podocytes, thus, protecting these cells from the detrimental effects of hyperglycemia. Specifically, the coagulation protease activated protein C (aPC), known for its pleiotropic cytoprotective effects, activates the inositol-requiring enzyme 1 $\alpha$  (IRE-1 $\alpha$ ) - spliced X-box-binding protein 1 (sXBP1) signaling arm of the adaptive unfolded protein response (UPR), restoring ER homeostasis. Insulin- and aPC-dependent signaling, despite acting through disjunct receptors, both signal through p85 $\alpha$ / $\beta$ - phosphatidylinositol 3-kinase (PI3K) to induce nuclear localization of sXBP1. Development of therapeutics that mimic aPC-signaling and restore ER homeostasis, or alternative approaches to restore ER homeostasis in insulin resistant tissues constitute a new therapeutic approach in dNP.

## **Keywords**

Diabetic nephropathy, chronic kidney disease, ER stress, UPR, podocytes, aPC, protease activated receptors, IRE-1 $\alpha$ , sXBP1, PI3K, p85 $\alpha$ / $\beta$

## **Bibliographische Beschreibung**

“Ghosh Sanchita; M.Sc. The regulation of endoplasmic reticulum stress by activated protein C in diabetic nephropathy – 2019 – 124 Bl., 24 Abb., 3 Tab.

## **Kurzreferat**

Die diabetische Nephropathie (dNP) ist weltweit die führende Ursache chronischer Nierenerkrankungen (CKD) und die häufigste Komplikation des Diabetes mellitus (DM). Obwohl molekulare Zusammenhänge zwischen ER-Stress und DM gut untersucht sind, war die Rolle des ER-Stress für die dNP bisher unklar. Wir zeigten eine wichtige pathophysiologische Relevanz der Insulinresistenz und der Hyperglykämie für die Regulation des ER-Stresses in der Niere im Kontext der dNP und Kausalität zwischen der Insulinresistenz in Podozyten und einer eingeschränkten Nierenfunktion im Kontext der dNP. Darüber hinaus zeigten wir, dass Gerinnungsproteasen die gestörte Insulinsignalkaskade in Podozyten kompensieren und somit die Zellen vor den schädlichen Effekten der Insulinresistenz und Hyperglykämie schützen können. Konkret aktiviert die Gerinnungsprotease aktiviertes Protein C (aPC) eine adaptive und zytoprotektive Signaltransduktion via der Inositol-requiring Enzyme 1 $\alpha$  (IRE1 $\alpha$ ) – spliced X-box binding protein 1 (sXBP1) – Signalkaskade, wodurch die ER-Homöostase wieder hergestellt wird. Insulin und aPC binden an unterschiedliche Rezeptoren, induzieren aber beide via einer p85 $\alpha$ / $\beta$  – Phosphatidylinositol 3 – Kinase (PI3K) Signaltransduktion die nukleäre Translokation von sXBP1 und induzieren damit eine adaptive ER-Stress Antwort. Die Entwicklung neuer Therapeutika zur Regulation der ER Homöostase in insulinresistenten Nierenzellen basierend auf diesen Erkenntnissen (z.B. small molecule aPC-Mimetika) könnte ein vielversprechender neuer Ansatz für die Therapie der dNP sein.

## **Schlüsselwörter**

Diabetische Nephropathie, chronische Nierenerkrankung, ER-Stress, UPR, Podozyten, aPC, Protease activated receptors, IRE-1 $\alpha$ , sXBP1, PI3K, p85 $\alpha$ / $\beta$

# Table of Contents

<b>List of Abbreviations.....</b>	<b>6</b>
<b>List of figures.....</b>	<b>13</b>
<b>List of Tables.....</b>	<b>15</b>
<b>1. Introduction.....</b>	<b>16</b>
1.1. Diabetes Mellitus.....	16
1.2. Diabetes and kidney complications.....	17
1.3. Insulin signaling and insulin resistance.....	23
1.4. Endoplasmic reticulum and stress.....	25
1.5. Unfolded protein response (UPR).....	27
1.6. The IRE1 $\alpha$ -XBP1 arm of the UPR.....	27
1.7. The PERK-ATF4 arm of the UPR.....	30
1.8. The ATF6 arm of the UPR.....	32
1.9. ER stress and human pathologies.....	33
1.10. Insulin resistance and microvascular complications.....	35
1.11. Coagulation proteases and protease activated receptors (PARs).....	36
1.12. Coagulation proteases in the kidney.....	40
1.13. Coagulation proteases with therapeutic potential.....	40
<b>2. Aim of the study.....</b>	<b>42</b>
<b>3. Materials and Methods.....</b>	<b>43</b>
3.1. Animals.....	43
3.2. Materials.....	43
3.3. Induction of diabetes using streptozotocin.....	44
3.4. Determination of albuminuria.....	45
3.5. Histology and immunohistochemistry.....	45
3.6. Reverse transcription-quantitative polymerase chain reaction.....	46
3.7. Cell culture.....	50
3.8. Transmission electron microscopy.....	50
3.9. <i>In situ</i> proximity-ligation assay.....	51
3.10. Determination of cell death by TUNEL assay.....	52

3.11. Production of lentiviral particles.....	52
3.12. Immunoblotting.....	53
3.13. Cell fractionation.....	54
3.14. Gene expression analysis in Nephromine database.....	54
3.15. Chromatin immunoprecipitation assay.....	54
3.16. CHIP-SEQ dataset analysis.....	55
3.17. Analysis of human samples.....	55
3.18. Study approval.....	56
3.19. Statistical analysis.....	56
<b>4. Results.....</b>	<b>57</b>
4.1. Human dNP is associated with a maladaptive ER stress response.....	57
4.2. Hyperglycemia differentially regulates UPR in murine models of dNP.....	59
4.3. Regulation of PERK-eIF2 $\alpha$ pathway in hyperglycemia.....	61
4.4. Hyperglycemia-induced maladaptive UPR is linked to dNP.....	64
4.5. XBP1 protects against hyperglycemia-induced ER stress activation.....	66
4.6. p85-sXBP1 interaction in podocytes is required for the adaptive ER stress response in dNP.....	68
4.7. TM – PC signaling regulates UPR.....	73
4.8. Activated protein C rescues maladaptive UPR response in mice models of defective insulin signaling.....	75
4.9. ER-homeostasis by aPC employs the INSR-p85-sXBP1 signaling axis.....	80
4.10. aPC signals through G-protein couple receptors to induce UPR in podocytes.....	83
4.11. Insulin and aPC concordantly regulate XBP1-dependent gene expression....	84
<b>5. Discussion.....</b>	<b>88</b>
5.1. Induction of the UPR and rescue of insulin signaling in podocytes in dNP.....	88
5.2. Glomerular filtration barrier is maintained by sXBP1 in podocytes.....	90
<b>6. Conclusion.....</b>	<b>93</b>
<b>7. Future Outlook.....</b>	<b>97</b>
<b>8. References.....</b>	<b>100</b>
<b>9. Acknowledgement.....</b>	<b>116</b>
<b>10. Declaration.....</b>	<b>119</b>

## List of abbreviations

4-PBA	4-phenylbutric acid
AGEs	Advanced glycation end-products
aPC	Activated protein C
ANOVA	Analysis of variance
AT	Antithrombin
ATF4	Activating transcription factor 4
ATF5	Activating transcription factor 5
ATF6 $\alpha$	Activating transcription factor 6 $\alpha$
ASK1	Apoptosis signaling kinase 1
$\beta$ -actin	Beta actin
BCA	Bicinchoninic acid
Bcl-2	B-cell lymphoma-2
BiP	Binding immunoglobulin protein
BSA	Bovine serum albumin
C1INH	C1 esterase inhibitor
CD2AP	CD2-associated protein
CKD	Chronic kidney disease
ChIP	Chromatin immunoprecipitation
DAG	Diacylglycerol
DAPI	4', 6-Diamidin-2-phenylindol
DAB	3,3'-Diaminobenzidine
db/db	Mice homozygous for the diabetes spontaneous mutation (Lepr <sup>db</sup> )

db/m	Control mice heterozygote for Lepr <sup>db</sup> with Dock7 <sup>m</sup>
DKD	Diabetes kidney disease
DM	Diabetes mellitus
dNP	Diabetic nephropathy
ddH <sub>2</sub> O	Double distilled water
DEPC	Diethylpyrocarbonate
DMEM	Dulbecco's modified eagle's medium
DMSO	Dimethyl sulfoxide
DNA	Deoxyribonucleic acid
DNase	Deoxyribonuclease
dNTPs	Deoxynucleoside triphosphates
DR5	Death receptor 5
DTT	Dithiothreitol
Edem1	ER degradation-enhancing alpha-mannosidase-like protein 1
ECM	Extracellular matrix
EDTA	Ethylenediamine tetraacetic acid
eIF2 $\alpha$	Eukaryotic translation initiation factor 2
EGTA	Ethylene glycol tetraacetic acid
eGFR	Estimated glomerular filtration rate
EGFR	Epidermanl growth factor receptor
ELISA	enzyme-linked immunosorbent assay
EMT	Epithelial-mesenchymal transition
EPCR	Endothelial protein C receptor
eNOS	Endothelial nitric oxide synthase
Ero1b	Endoplasmic reticulum oxidoreductase 1 beta
ER	Endoplasmic reticulum

ERAD	Endoplasmic reticulum-associated degradation
Erk1/2	Extracellular signal regulated kinase 1/2
ERSE	ER stress response element
ESRD	End-stage renal diseases
Esrrb	Estrogen related receptor beta
Esrrg	Estrogen related receptor gamma
ETC	Electron transport chain
FBS / FCS	Fetal bovine serum/ fetal calf serum
FMA	Fractional mesangial area
g	Gravitational acceleration
GFR	Glomerular filtration rate
GADD34	Growth arrest and DNA damage-inducible protein 34
GAPDH	Glyceraldehyde 3-phosphate dehydrogenase
GENCs	Glomerular endothelial cells
GLP-1	Glucagon-like peptide-1
GLUT-4	Glucose transporter type 4
Grb2	Growth factor receptor bound protein 2
GRP78	Glucose regulated protein 78 (also known as BiP)
GS	Glycogen synthase
GSK-3	Glycogen synthase kinase-3
HBP	Hexosamine biosynthesis pathway
HBSS	Hank's balanced salt solution
HEPES	4-(2-hydroxyethyl)-1-piperazineethanesulfonic acid
HK	High-molecular weight kininogen
hp	Human podocytes
HRP	Horseradish peroxidase



IgG	Immunoglobulin G
IGF-1	Insulin-like growth factor-1
IGF1R	Insulin-like growth factor receptor 1
IGF2R	Insulin-like growth factor receptor 2
IκB	Inhibitor of κB
i.p.	Intraperitoneal
IP	Immunoprecipitation
IMS	Mitochondrial intermembrane space
INF-γ	Interferon gamma
IR (INSR)	Insulin receptor
IRS1/2	Insulin receptor substrate 1/2
IRE1α	Inositol-requiring enzyme 1α
ISR	Integrated stress response
ITS	Insulin transferrin selenium
JAK	Janus kinase
JNK	c-Jun N-terminal kinase
JIK	JNK inhibitory kinase
KEAP1	kelch-like ECH-associated protein 1
kb	Kilobase(s)
LacZ	β-galactosidase
MAMs	Mitochondria-associated membranes
MgCl <sub>2</sub>	Magnesium chloride
mp	Mouse podocytes
MMP-1	Matrix metalloproteinase-1
mRNA	Messenger ribonucleic acid
NaCl	Natrium (sodium) chloride

NF-κB	Nuclear factor κB
NRF2	Nuclear factor erythroid 2-related factor 2
NO	Nitric oxide
P58IPK	Protein kinase inhibitor p58
PAGE	Polyacrylamide gel electrophoresis
PAR	Protease activated receptor
PAS	Periodic acid Schiff's staining
PBS	Phosphate buffered saline
PBST	Phosphate buffered saline tween-20
PC	Protein C
PCI	Proten C inhibitor
PCIs	Protease cocktail inhibitors
PCR	Polymerase chain reaction
PDK1	Phosphoinositide-dependent kinase 1
PERK	Protein kinase R-like ER kinase
PFA	Paraformaldehyde
PI3K	Phosphatidylinositide 3-kinases
PIP <sub>3</sub>	Phosphatidylinositol (3,4,5)-triphosphate
PKB	Protein kinase B
PKCs	Protein kinase Cs
PPK	Plasma prekalikrein
PPAR <sub>γ</sub>	Peroxisome proliferator-activator receptor gamma
PVDF	Polyvinylidene fluoride
QC	Quality control
qRT-PCR	Quantitative real time polymerase chain reaction
RAAS	Renin angiotensis aldosterone system

RIDD	Regulated IRE1 $\alpha$ -dependent decay
RIPA	Radio-immunoprecipitation assay
ROS	Reactive oxygen species
RPMI 1640	Rosewell park memorial institute medium
rpm	Revolutions per minute
rtTA	reverse tetracycline-controlled transcriptional activator
RT	Room temperature
RTKs	Receptor tyrosine kinases
RT-PCR	Reverse transcription polymerase chain reaction
S1P1	Sphingosine 1-phosphate receptor 1
S1P	Site-1 protease
S2P	Site-2 protease
sXBP1	splice XBP1
s	Second(s)
s.c.	Subcutaneously
SDS	Sodium dodecyl sulfate
SEM	Standard error of mean
SGLT2	Sodium glucose cotransporter 2
SOS	Son of Sevenless
STZ	Streptozotocin
T1DM	Type 1 diabetes mellitus
T2DM	Type 2 diabetes mellitus
TBST	Tris-buffered saline tween20
TEM	Transmission electron microscope
TGF $\beta$	Transforming growth factor beta
TF	Tissue factor

TFPI	Tissue factor pathway inhibitor
TM	Thrombomodulin
TM <sup>Pro/Pro</sup>	Thrombomodulin with mutation Q404P, impairing PC activation
TRB3	Tribble-related protein 3
TRAF2	TNF receptor associated factor-2
TSS	Transcription start site
TUDCA	Tauroursodeoxycholic acid
TUNEL	Terminal deoxynucleotidyl transferase dUTP Nick-end labeling
TXNIP	Thioredoxin interacting protein
UPR	Unfolded protein response
UPR <sup>Mt</sup>	Mitochondrial unfolded protein response
UPRE	UPR response element
uXBP1	unsliced-XBP1
VEGF	Vascular endothelial growth factor
WT	Wild-type
WT-1	Wilms tumor-1
XBP1	X-box binding protein 1

## List of Figures

Figure 1: The effects of diabetes in the glomerulus.

Figure 2: Insulin signaling cascade adapted from Boucher J, et al.

Figure 3: The ER - response as a master regulator of cellular life or death decision.

Figure 4: The IRE1 $\alpha$ -XBP1 arm of the tripartite UPR.

Figure 5: The PERK-ATF4 arm of the tripartite UPR.

Figure 6: The ATF6 arm of the tripartite UPR.

Figure 7: The coagulation cascade (adapted from Madhusudhan T, et al. 2006)

Figure 8: Maladaptive ER-stress response in human dNP.

Figure 9: Hyperglycemia differentially regulates the tripartite UPR in T1DM mouse model.

Figure 10: Hyperglycemia differentially regulates the tripartite UPR in dNP.

Figure 11: Regulation of PERK-eIF2 $\alpha$  activation and ATF4 expression in hyperglycemia.

Figure 12: Hyperglycemia-induced ER stress response is causally linked to dNP.

Figure 13: Podocyte-specific loss of XBP1 promotes maladaptive UPR in dNP.

Figure 14: Impaired sXBP1-p85 interaction in human and murine dNP.

Figure 15: Insulin signals via INSR-p85 axis independent of IRE1 $\alpha$  phosphorylation in podocytes.

Figure 16: Signaling via INSR-p85 axis in podocytes conveys an adaptive ER stress response in dNP.

Figure 17: Thrombomodulin – dependent PC activation regulates UPR in dNP.

Figure 18: Activated PC rescues defective insulin signaling.

Figure 19: Activated PC rescues defective insulin signaling in dNP.

Figure 20: Human and mouse aPC induce nuclear translocation of sXBP1.

Figure 21: UPR-reprogramming by aPC depends on p85-sXBP1 signaling.

Figure 22: aPC induced nuclear translocation of sXBP1 requires both PAR-3 and PAR-1 receptors.

Figure 23: Insulin and aPC-dependent XBP1 regulatory networks linked to UPR regulation.

Figure 24: Proposed model of cytoprotective signaling of insulin and aPC in podocytes in dNP.

## List of Tables

Table 1: Current antihyperglycemic interventions with the potential to reduce hyperfiltration in dNP

Table 2: Interventions targeting different molecular mechanisms in dNP

Table 3: UPR gene primers for quantitative polymerase chain reaction

# 1. Introduction

## 1.1. Diabetes Mellitus

Diabetes mellitus is defined as a group of metabolic diseases characterized by chronic dysregulation of glucose, carbohydrate, lipid and protein metabolism, resulting from impaired insulin secretion, insulin resistance or a combination of both<sup>1-4</sup>. Individuals at risk of T2DM display an initial state of insulin resistance (in liver and other peripheral tissues) along with a compensatory hypersecretion of insulin (hyperinsulinaemia) by  $\beta$ -cells of the pancreas to maintain normal glucose tolerance. Overtime,  $\beta$ -cells are no longer able to secrete enough insulin leading to overt hyperglycemia and hypoinsulinaemia<sup>4-6</sup>. There has been an increase in diabetes prevalence globally since the 1980s, with a 2015 estimation of 415 million people worldwide who were diabetic and a projected rise to 642 million by the year 2040. As the sixth leading cause of disability in 2015, diabetes places considerable socioeconomic pressures on affected individuals and overwhelming costs to global health economies estimated at US\$825 billion<sup>7</sup>. Of the 415 million people plagued by diabetes, 90% suffer from type 2 diabetes mellitus (T2DM) and the rest from type 1 diabetes mellitus (T1DM), gestational diabetes, or other rare forms of diabetes mellitus (DM). Traditionally, diabetes has been classified into type 1 and type 2 DM based on the presence or absence of autoantibodies against pancreatic islet  $\beta$ -cell antigens and age of onset (younger for T1DM). However, other subgroups have been identified, such as latent autoimmune diabetes in adults (LADA), defined by the presence of glutamic acid decarboxylase antibodies (GADA), is phenotypically similar to T2DM at diagnosis progressively becomes similar to T1DM over time<sup>8</sup>.

While the benefits of intensive glucose, lipids and blood pressure management have been shown in several large randomized controlled trials (such as DCCT/EDIC, UKPDS, ADVANCE, VADT, etc.)<sup>9</sup>, diabetes is a heterogenous disease with regard to clinical presentation and progression. So while early treatment and optimizing blood glucose control is necessary, similar therapeutic strategies might not work for every diabetic patient<sup>8</sup>. Recent clinical studies<sup>8</sup> have suggested a refining of the existing classifications of diabetic patients based on metabolic and laboratory parameters to detect those at a greater risk for specific diabetic complications and therefore enable



individualised treatment regimens. This landmark study also supports the need for new pathophysiological concepts. This study revealed an association of insulin resistance and diabetic kidney disease (DKD)<sup>8</sup>. Moreover, they found that patients with insulin resistance and at higher risk for DKD had reasonably low levels of glycated hemoglobin (HbA1c, a form of hemoglobin covalently bound to glucose) indicating that glucose-lowering therapy is not the only prescription for preventing kidney associated complications. Therefore, new insights into the molecular mechanisms involved in the etiology and progression of diabetic nephropathy are urgently needed in order to identify new therapeutic targets and develop improved therapeutic strategies for DKD.

## **1.2. Diabetes and kidney complications**

Prolonged hyperglycemia in DM is associated with chronic metabolic and hemodynamic changes promoting structural renal abnormalities and with the development of diabetic kidney disease (DKD). DKD, also known as diabetic nephropathy (dNP), is the leading cause of end-stage renal disease (ESRD) in the world<sup>4,5</sup>. While hyperglycemia is the leading risk factor, other factors such as gender, obesity, hypertension, chronic inflammation, insulin resistance, hypovitaminosis D, dyslipidemia, and several genetic variants and polymorphisms, have been associated with an increased risk of developing dNP<sup>5</sup>. Increased glucose uptake results first in augmented glycolytic flux and glucose oxidation. A byproduct of mitochondrial substrate metabolism, i.e., electron transport and oxidative phosphorylation, is superoxide, ( $O_2^{\cdot-}$ ). The increased reactive oxygen species production by mitochondria and the associated mitochondrial dysfunction leading to an accumulation of glycolysis associated metabolites cause activation of other pathways. Some of these pathways are the aldose reductase or polyol pathway, the formation of advanced glycation end products (AGEs), the formation of diacylglycerol (DAG) leading to protein kinase C (PKC) activation, and the increased flux via the hexosamine biosynthesis pathway (HBP), involved in posttranslational protein modification by glycosylation<sup>1-3</sup>. Discoveries about 2 decades ago proposed a single unifying process linking all these hyperglycemia-induced pathological mechanisms to the overproduction of superoxide by the mitochondrial electron transport chain and mitochondrial dysfunction<sup>10</sup>. However, translational efforts aiming to restore either excess mitochondrial

ROS generation or to compensate for the activation of these pathways (e.g. aldose reductase inhibitors, PKC-inhibitors) have all fallen short of the expectations and have not been successfully translated into the clinic. Thus, there remains an unmet medical need for new therapeutic approaches based on new mechanistic insights.

dNP is a major chronic complication of both T1DM (insulin insufficiency) and T2DM (insulin resistance). 40-45% of T1DM patients develop dNP and reach ESRD. Major renal structural changes that occur include mesangial extracellular matrix accumulation, glomerular and tubular basement thickening, podocyte foot process fusion and podocyte detachment, interstitial fibrosis and glomerulosclerosis<sup>6,11</sup>. These ultrastructural changes correlate with clinical features such as persistent albuminuria (> 300 mg/24 h) and / or increased serum creatinine and eventually a sustained decline in glomerular filtration rate (GFR), increased cardiovascular events leading to deaths in 50% of cases and progressive renal insufficiency resulting in ESRD in 75% of T2DM patients in dNP who die within 5 years after detection of ESRD<sup>1-3,12</sup>.

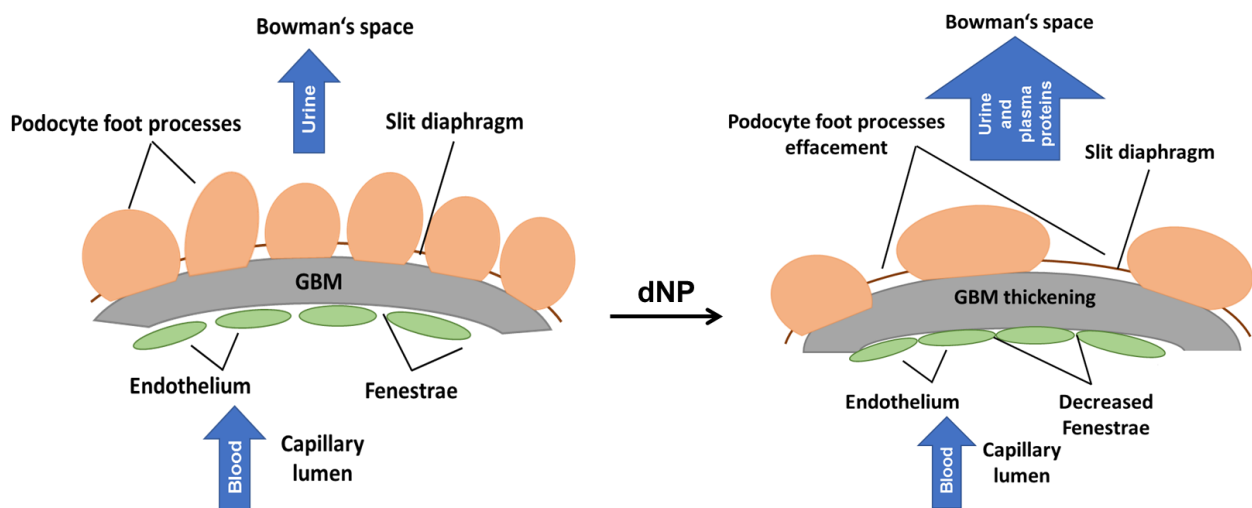


**Figure 1: The effects of diabetes in the glomerulus.** Albuminuria is thought to result from defects in the permeability of the glomerular filtration barrier of the kidney, which comprises fenestrated glomerular endothelial cells (GECs), which are separated from specialized epithelial cells of the glomeruli (podocytes) by the glomerular basement membrane (GBM). Podocytes have extensive interdigitating foot processes connected by a slit diaphragm, which comprise proteins that signal through podocytes' actin cytoskeleton. The structure and integrity of the glomerulus is maintained by a complex local autocrine/paracrine network between the podocyte and the GECs.

The kidneys are designed to filter large quantities of plasma, reabsorb substances that the body must conserve, and secrete substances that need to be eliminated. These functions are critical for the maintenance of fluid and electrolyte balance, body fluid osmolality, acid-based balance, excretion of metabolic waste and foreign chemicals, but also for regulating arterial pressure, hormone secretion, and glucose balance<sup>13</sup>. The basic urine-forming unit of the kidney is the nephron that consists of a filtering apparatus (the glomerulus) that is connected to a long tubular portion that reabsorbs and conditions the glomerular ultrafiltrate<sup>6</sup>. Fluid filtered from the glomerular capillaries flows into the tubular portion, which comprises in essence the proximal tubule, the Loop of Henle, and the distal tubule, all of which assist in reabsorbing essential substances and converting filtered fluid into urine<sup>6</sup>. Albuminuria results from tubular dysfunction and defects in the permeability of the glomerular filtration barrier of the kidney, which comprises fenestrated glomerular endothelial cells (GECs), separated from specialized epithelial cells of the glomeruli, called podocytes, by the glomerular basement membrane (GBM)<sup>6</sup>. This three-layer filtration barrier serves as a size-selective and charge-dependent molecular sieve facilitating the filtration of cationic molecules, electrolytes, and small and mid-sized solutes but restricting the passage of anionic molecules and macromolecules<sup>14</sup>. This elegant structure has to oppose hydrostatic pressure in the glomerular capillary, which is the natural driving force behind macromolecular filtration. Podocytes have extensive interdigitating foot processes connected by the slit diaphragm (**Fig. 1**), comprising proteins such as nephrin and podocin that interact with cytoplasmic adaptor and signaling proteins (PI3K, CD2AP, AKT, and podocin). Nephrin is additionally linked to the podocyte actin cytoskeleton, mechanistically linking the actin cytoskeleton and intracellular signaling. The structure and integrity of the glomerulus is maintained by a complex local autocrine/paracrine network between the podocyte and the GECs that comprises vascular growth factors and vasoactive peptides. The highly fenestrated GECs with a unique ultrastructure lacking fenestrae diaphragms facilitate the permeability of water and small solutes<sup>6,11,13,15</sup>.

Podocytes within the glomerulus are insulin sensitive cells<sup>15-17</sup>. Podocyte-specific insulin receptor knockout mice develop albuminuria, increased extracellular matrix deposition, glomerulosclerosis, and GBM thickening (**Fig. 1**) in normoglycemic condition, which

suggests that insulin signaling is essential for maintaining normal physiological function of the podocytes. Insulin receptor deletion in tubular epithelial cells also results in the disruption of normal cellular functions leading to reduced natriuresis and hypertension<sup>15,17</sup>. Glomerular hyperfiltration is a result of afferent arteriolar dilatation due to the release of vasoactive mediators, such as IGF-1, glucagon and vasopressin<sup>18,19</sup>, nitric oxide (NO), vascular endothelial growth factor (VEGF), and prostaglandin under hyperglycemic conditions. Alteration in the renal tubular function also take place in the early stage of DM due to the high filtrated load of glucose and increase in reabsorption of both glucose and sodium chloride through the upregulated sodium glucose cotransporter 2 (SGLT2) in the proximal tubules. The delivery of sodium chloride to the macula densa of the distal tubules is decreased causing dilatation of afferent arteriole because of tubuloglomerular feedback. Simultaneously, constriction of efferent arteriole occurs due to overactive renin-angiotensin-aldosterone system (RAAS) leading to high local levels of angiotensin II, causing glomerular hypertension. This leads to hyperfiltration and a transient increase of the GFR<sup>20</sup>. In agreement with this pathophysiological model, RAAS inhibitors (RAASi) are a mainstay for therapy in dNP. Yet, even RAASi only delay and fail to halt disease progression<sup>21</sup>. Concurrent to the hemodynamic changes, hyperglycemia, insulin resistance and compensatory hyperinsulinemia independently cause endothelial dysfunction by promoting increased ROS production, activation of protein kinase Cs (PKCs) and advanced glycation end-products (AGE)-induced proinflammatory signaling<sup>10,22</sup>. Mitochondrial dysfunctions, altered energy metabolism, and increased endoplasmic reticulum (ER) stress are also associated with insulin resistance within the glomeruli. Microarray analyses of human biopsies from patients with established dNP show upregulated unfolded protein response (UPR) genes proportionally to the severity of diabetic renal lesions<sup>23,24</sup>.

Treatment of dNP involves normalizing hyperglycemia, hypertension, dyslipidemia, and making lifestyle modifications<sup>25</sup>. The available interventions (Table 1) that control blood glucose and blood pressure slow the progression of microalbuminuria to macroalbuminuria and the GFR decline in patients with T1DM, T2DM and DKD<sup>26-29,30-46</sup>. While these interventions seem promising and may be beneficial for some, a cluster of insulin resistant patients with DKD feature low HbA1c suggesting that glucose lowering

therapy is not sufficient to halt the progression of DKD<sup>8</sup>. Many more classes of drugs with different molecular targets and mechanism of actions were tested but failed to successfully pass clinical trials (Table 2). Additional molecular insights are required to develop interventions that are able to specifically and locally rescue, and protect from the effects of insulin resistance<sup>25</sup>, mitochondrial dysfunction, and ER stress, all of which contribute to progressive kidney disease<sup>6</sup>.

<b>Interventions</b>	<b>Molecular target/ mechanism</b>	<b>Patient population</b>
<i>SGLT2 inhibitors:</i>		
Empagliflozin (EMPA-REG OUTCOME)	Inhibition of SGLT-2 decreases glucose reabsorption	T2DM and high CV risk
Canagliflozin (CANVAS)		T2DM and high CV risk
<i>RAAS inhibitors:</i>		
Paricalcitol (VITAL study)	Inhibition of RAAS	T2DM with RAAS inhibitors
Losartan (NIDDM)		T2DM and dNP
Finerenone		T2DM and albuminuria with RAAS
<i>Angiotensin receptor blockers:</i>		
Irbesartan (IDNT)	Angiotensin receptor blockers	T2DM, dNP and hypertension

**Table 1: Current and emerging antihyperglycemic interventions with the potential to reduce hyperfiltration in dNP<sup>9,26-46</sup>.**

<b>Interventions</b>	<b>Molecular target/ mechanism</b>	<b>Patient population</b>
<i>Glucagon-like peptide -1 receptor agonists (GLP-1 Ras):</i>		
Liraglutide (LEADER)	Enhance GLP-1 expression to increase insulin secretion	T2DM and high CV risks
Semaglutide (SUSTAIN-6)		T2DM and CV risks or CKD stage 3
<i>Dipeptidyl peptidase 4 (DPP-4) inhibitors:</i>		
Linagliptin	Inhibition of DPP-4 to preserve GLP effect	T2DM with microalbuminuria or higher and receiving stable dose of RAAS inhibitors
Saxagliptin (SAVOR-TIMI 53 trial)		T2DM with albuminuria
<i>Thiazolidinediones:</i>		
Rosiglitazone	Activation of PPAR $\gamma$ to increase insulin sensitivity of tissue	T2DM with albuminuria
<i>Phosphodiesterase inhibitors:</i>		
Pentoxifylline (PREDIAN trial)	Inhibition of cell proliferation, kidney inflammation and accumulation of extracellular matrix	T2DM and CKD stage 3 & 4 with RAAS inhibitors
<i>Vitamin D analogs:</i>		
Pyridoxamine	Remove free radicals and carbonyl products; block syntheses of AGEs	T1DM and T2DM with overt dNP
<i>Endothelium A receptor antagonists:</i>		
Atrasentan	Selective endothelin receptor A antagonist	T2DM and CKD stage 2 & 3
<i>Protein kinase C inhibitor:</i>		
Ruboxistaurin	Inhibition of protein kinase C- $\beta$ and reduce of oxidative stress	T2DM and albuminuria
Sulodexide	Restores the anionic heparan sulfate charges on the glomerular basement membrane	T1DM and T2DM with albuminuria
<i>TGF-<math>\beta</math> blockade:</i>		
Pirfenidone	Antagonize MAPK pathway to attenuate EMT and fibrosis	Animal study
<i>Anti-inflammation:</i>		
Bardoxolone methyl	Activation of Nrf2 and inhibit NF- $\kappa$ B pathway	T2DM and impaired renal function
<i>Janus kinase (JAK) inhibitor:</i>		
Baricitinib JAK-2 inhibitor to	Selective JAK-1 and JAK-2 inhibition to reduce innate immune kidney cells	T2DM and DKD

**Table 2: Interventions targeting different molecular mechanisms in dNP** <sup>26-46</sup>.

### 1.3. Insulin signaling and insulin resistance

Insulin and insulin-like growth factors (IGFs) control metabolism, growth and survival in mammals. The insulin receptor (IR) and insulin-like growth factor-1 and -2 receptors (IGF1R and IGFR2R) belong to a subfamily of receptor tyrosine kinases (RTKs). Glucose homeostasis is maintained primarily by insulin, which is secreted by pancreatic islet  $\beta$  cells, and glucagon, secreted by pancreatic islet  $\alpha$  cells. The primary role of insulin is to facilitate glucose uptake by peripheral tissues while glucagon's mechanism of action is to stimulate glucose production by the liver and the muscles through increased gluconeogenesis (glucose synthesis) and glycogenolysis (breakdown of glycogen into glucose)<sup>47</sup>. In individuals with normal glucose tolerance, hepatic glucose production is compensated by insulin-mediated glucose uptake by insulin target tissues like liver, adipose, muscle, and brain<sup>48</sup>.

Insulin signaling is mediated by a complex, highly integrated network that controls several processes<sup>49</sup>. In response to insulin, the insulin receptor phosphorylates insulin receptor substrate proteins (IRS) that are linked to the activation of two main signaling pathways; the phosphatidylinositol 3-kinase (PI3K) - AKT/protein kinase B (PKB) pathway, responsible for most of the metabolic actions of insulin, and the Ras-mitogen-activated protein kinase (MAPK) pathway (**Fig. 2**). Class Ia PI3-kinases are heterodimers consisting of a regulatory (p85) and catalytic (p110) subunit, each of which occurs in several isoforms. Recruitment and activation of the PI3K depends on the binding of the two SH2 domains in the regulatory subunits to tyrosine-phosphorylated IRS proteins. This results in activation of the catalytic subunit, which rapidly phosphorylates phosphatidylinositol 4,5-bisphosphate (PIP<sub>2</sub>) to generate the lipid second messenger phosphatidylinositol (3,4,5)-triphosphate (PIP<sub>3</sub>). The latter recruits Akt to the plasma membrane, where it is activated by phosphorylation and induces downstream signaling<sup>50</sup>. In addition to PKB/ Akt, PIP<sub>3</sub> targets include phosphoinositide-dependent kinase 1 (PDK1), and the atypical protein kinase C,  $\zeta$  and  $\lambda$  isoforms. Upon PKB-mediated phosphorylation, glycogen synthase kinase (GSK-3) is inactivated. This inactivation in parallel to protein phosphatase-1 (PP1) activation relieves the inhibitory phosphorylation of glycogen synthase (GS) promoting glycogen synthesis. PKB also regulates the insulin-stimulated translocation of the glucose

transporter type 4 (GLUT-4) at the plasma membrane, resulting in increased glucose uptake. Parallel to the PKB axis, activated IRS1/2 recruit growth factor receptor - bound protein 2 (Grb2), which associates to Son of Sevenless (SOS) and activates the extracellular signal regulated kinase 1/2 (Erk1/2) - MAPK pathway. Alterations of the activation status of the proximal insulin signaling enzymes (IR, IRS1/2, PI3K) and their downstream targets contribute to the defects in the insulin signaling cascade in insulin resistant-tissues<sup>51,52</sup>. This ability of insulin to elicit cellular responses is impaired in T2DM, including renal tissue and is termed “cellular insulin resistance”.

Insulin resistance correlates with the development of microalbuminuria both in T1DM and T2DM patients. Furthermore, insulin resistance has been implicated in the development of glomerular hypertension and hyperfiltration contributing to higher salt sensitivity, which is associated with increased blood pressure, albuminuria, and a decline in renal function<sup>53-56</sup>. Obesity, hyperglycemia, hyperlipidemia, and hypertension, all of which are associated with dysfunctional insulin signaling are clustered together under the umbrella of “metabolic disorders”<sup>57-59</sup>. At the cellular levels, these metabolic disorders are linked by aberrant endoplasmic reticulum associated signaling<sup>60-65</sup>.



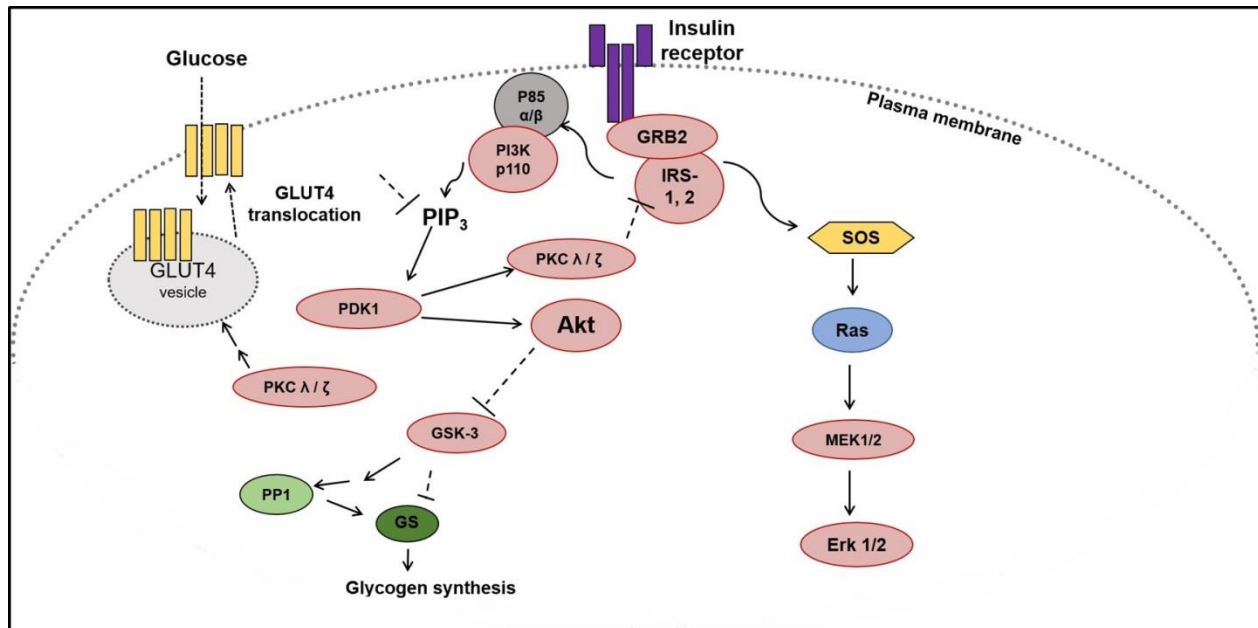


**Figure 2: Insulin signaling cascade adapted from Boucher J, et al.<sup>50</sup>.** In the presence of insulin, the insulin receptor phosphorylates insulin receptor substrate proteins (IRS) activating two main signaling pathways: the phosphatidylinositol 3-kinase (PI3K) - AKT/protein kinase B (PKB) pathway and the Ras-mitogen-activated protein kinase (MAPK) pathway. Phosphorylated IRS1/2 recruit the heterodimeric p85/p110 PI3K at the plasma membrane, where it produces the lipid second messenger phosphatidylinositol (3,4,5) - triphosphate (PIP<sub>3</sub>). phosphoinositide-dependent kinase 1 (PDK1); atypical protein kinase C (PKC), ζ and λ isoforms; glycogen synthase kinase (GSK-3); phosphatase-1 (PP1); glycogen synthase (GS); glucose transporter type 4 (GLUT-4); growth factor receptor - bound protein 2 (Grb2); Son of Sevenless (SOS); extracellular signal regulated kinase 1/2 (Erk1/2).

#### 1.4. Endoplasmic Reticulum and stress

The Endoplasmic Reticulum (ER) is a cellular organelle responsible for the synthesis and folding of secreted and membrane-bound proteins. Newly synthesized proteins are translocated to the ER, where they are folded and assembled in the specialized environment with the assistance of several ER chaperones and oxidoreductases. Additionally, the ER serves as the major store of intracellular calcium and is the site of lipid biosynthesis. The lumen of the ER constitutes a unique cellular environment with the highest concentrations of calcium, calcium-dependent molecular chaperones, and an oxidative environment crucial for the formation of disulphide bonds in proteins. Additionally, various post-translational modifications of proteins, including glycosylation and lipidation, occur in the ER. Lipid-membrane biosynthesis and cholesterol production

are also key functions performed by the ER. Thus, the ER is highly sensitive to stresses such as the accumulation of unfolded or misfolded proteins, disturbances in cellular redox regulation caused by hypoxia, glucose deprivation that interferes with N-linked protein glycosylation, and aberrations in calcium homeostasis. ER transmembrane sensors detect disturbances in the ER to activate three distinct branches of the **unfolded protein response (UPR)** that determine cell fate. The initial function of the UPR is to reestablish ER and cellular homeostasis and activate adaptive transcriptional programs that induce expression of genes capable of enhancing the protein folding capacity of the ER and genes for **ER-associated degradation (ERAD)**, which promote clearing of misfolded or unfolded proteins from the ER and export them to the cytosol for degradation. However, when these adaptive mechanisms fail to restore ER homeostasis due the magnitude of stress or its duration (**Fig. 3**), cell death is induced, involving both caspase-dependent apoptosis and caspase-independent necrosis<sup>66</sup>.

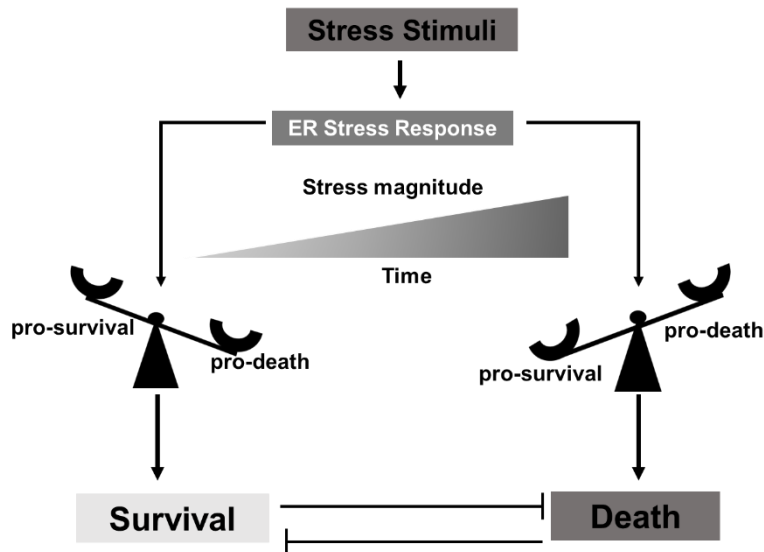


**Figure 3: The ER- response as a master regulator of cellular life or death decision (adapted from Corazzari et al. 2017<sup>67</sup>).** Cell fate following the initiation of the unfolded protein response is determined by the magnitude and the duration of stress stimuli. Both pro-survival and pro-death factors are concomitantly transduced. Pro-survival factors are in surplus initially, efficiently inhibiting the activity of pro-death factors. Prolonged or sustained stress allows accumulation of pro-death factors<sup>67</sup>.

### **1.5. Unfolded protein response (UPR)**

Accumulation of unfolded and misfolded proteins in the ER activates the three major regulators of the UPR, mediated by inositol-requiring enzyme 1 $\alpha$  (IRE1 $\alpha$ ), protein kinase R-like ER kinase (PERK), and activating transcription factor 6 $\alpha$  (ATF6 $\alpha$ )<sup>68</sup>. The luminal domains of IRE1 $\alpha$ , PERK, and ATF6 interact with the ER chaperone GRP78 (also known as BiP). Accumulation of unfolded proteins cause dissociation of BiP from these molecules, leading to their oligomerization (IRE1 $\alpha$  and PERK) or cleavage and nuclear translocation (ATF6 $\alpha$ ), initiating the UPR. Together these proteins trigger downstream signaling events that result in the amelioration of ER associated stress by increasing the expression of ER chaperones, inhibiting most *de novo* mRNA translation, and by accelerating the retrograde export of proteins from the ER to the cytosol for ubiquitylation and proteasome-mediated degradation<sup>66,69</sup>. While the classical understanding of ER stress has meant accumulation of unfolded proteins in the ER, new studies have found that depletion of membrane lipid component inositol or by deletion of genes involved in lipid homeostasis<sup>70</sup>, UPR can be activated. ER stress can also induce autophagy, which has been shown to activate other mechanisms of clearing unfolded proteins and protein aggregates independently of the ubiquitin/proteasome system. Although the UPR is classically linked to protein folding stress under both physiological and pathological conditions, it contributes significantly in regulating various important processes such as lipid and cholesterol metabolism, energy homeostasis, inflammation and cell differentiation. Thus, the UPR is responsible for the maintenance of homeostasis in an environment rife with fluctuating and diversified signal inputs<sup>69</sup>.

### **1.6. The IRE1 $\alpha$ - XBP1 arm of the UPR**

Inositol-requiring enzyme 1 $\alpha$  (IRE1 $\alpha$ ) is a type I transmembrane protein with a serine/threonine kinase domain and an endoribonuclease domain. It is a highly conserved arm of the ER stress pathways, with almost identical signaling outcomes found in yeast and higher mammals. Upon sensing ER-stress, IRE1 $\alpha$  undergoes a conformational change, triggering autophosphorylation and subsequently, trans-autophosphorylation, and oligomerization which generates an active endoribonuclease site, as well as a structurally and functionally independent kinase domain. The endoribonuclease domain

cleaves a 26 nucleotides-intron from the X-box-binding protein 1 (XBP1) mRNA (**Fig. 4**), normally transcriptionally regulated by ATF6 $\alpha$ <sup>71</sup>, resulting in a frame-shift and translation of spliced XBP1 (sXBP1). sXBP1 translocates to the nucleus and functions as a transcription factor. sXBP1 binds to the promoters of several genes and chaperones involved in ER maintenance, ER expansion and ERAD, which together promote restoration of ER-homeostasis. Unspliced XBP1 (uXBP1) is extremely unstable and is subjected to proteasome-dependent and -independent degradation soon after translation. Unspliced XBP1 also interacts with and sequesters sXBP1 and ATF6 in the cytosol, mediating their degradation by the proteasome<sup>72,73</sup>. Thus, uXBP1 functions as a negative regulator of the UPR-specific transcription factors, sXBP1 and ATF6, by shutting off transcription of genes during the recovery phase of ER stress as well as creating a negative feedback loop for the IRE1 $\alpha$  (endoribonuclease function) and ATF6 arms of the UPR.

Besides splicing XBP1 mRNA, IRE1 $\alpha$  has been shown to downregulate several microRNAs and mRNAs through a process known as “regulated IRE1-dependent decay” (RIDD) under conditions in which IRE1 $\alpha$  is activated strongly and for prolonged duration or in the absence of XBP1 mRNA (**Fig. 4**). Degradation of Death Receptor 5 (DR5) mRNA by IRE1 $\alpha$  allows for the establishment of a time window for adaptation to ER stress. IRE1 $\alpha$  also cleaves several miRNAs including miRNA-17, -34a, -96, and -125b, which promote inflammation and cell death through the stabilization and translation of thioredoxin interacting protein (TXNIP) and caspase-1 activation<sup>74</sup>. IRE1 $\alpha$  activates the c-Jun N-terminal kinase (JNK) pathway through formation of a complex with TNF receptor associated factor-2 (TRAF2)<sup>74</sup>. JNK inhibitory kinase (JIK) and apoptosis signaling kinase (ASK)1 are activated downstream of TRAF2. The IRE1 $\alpha$ /TRAF2 also recruits the inhibitor of  $\kappa$ B (I $\kappa$ B) kinase, which allows the activation of the inflammatory pathway by nuclear factor  $\kappa$ B (NF $\kappa$ B). Activation of the UPR in obese state contributes to the decrease in insulin sensitivity through IRE1 $\alpha$ -dependent activation of JNK, leading to phosphorylation of IRS-1 on its inhibitory serine residues<sup>75</sup>. Taken together, while XBP1 splicing by IRE1 $\alpha$  is a cytoprotective response to ER stress, the RIDD and IRE1 $\alpha$ /JNK pathways together convey dual and contrasting effects, either preserving ER homeostasis or inducing inflammation and cell death<sup>76</sup>. In addition, IRE1 $\alpha$  has been

linked with insulin signaling, though its relevance for the action of insulin in the kidney remained unknown hitherto.

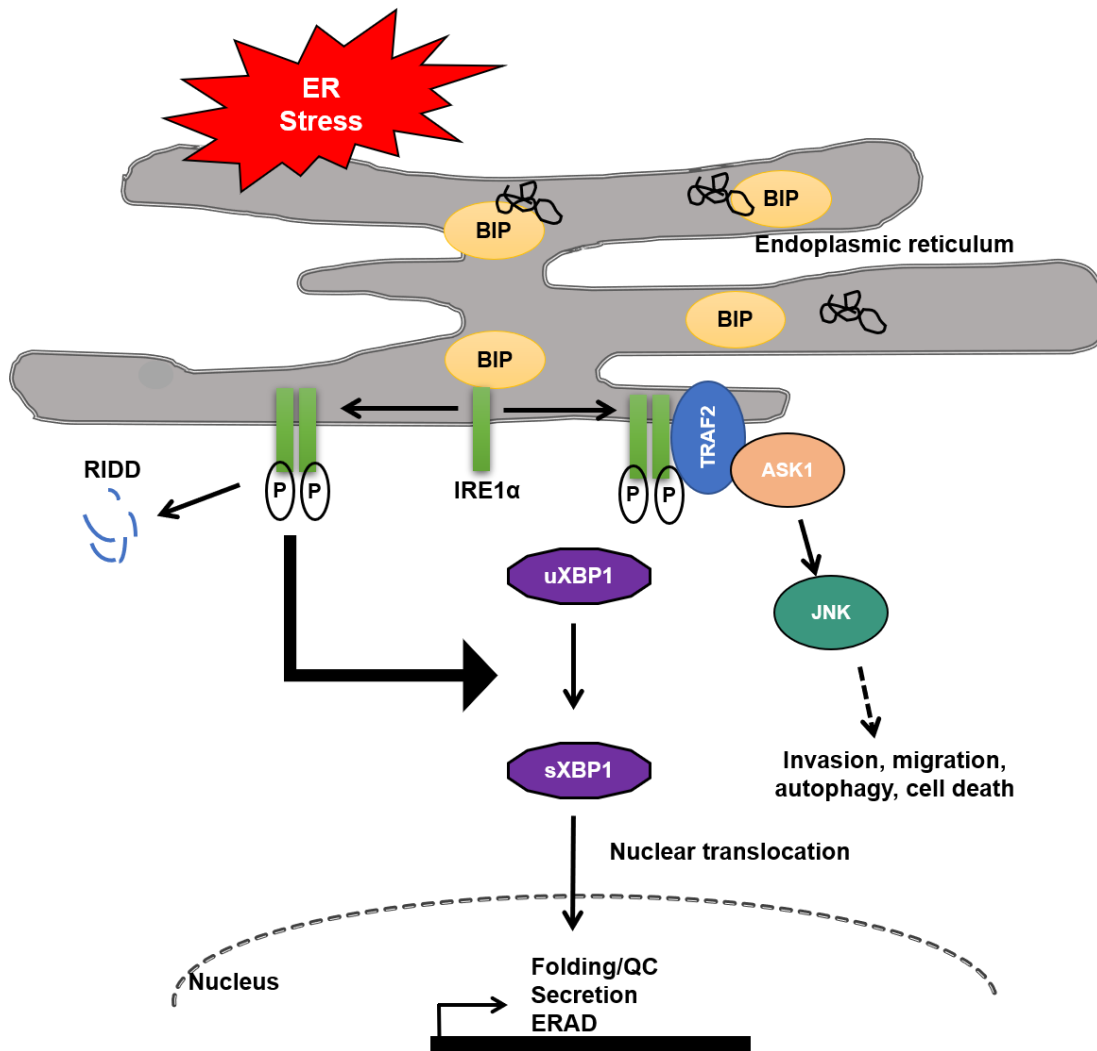


**Figure 4: The IRE1 $\alpha$ -XBP1 arm of the tripartite UPR.** Accumulation of misfolded proteins trigger IRE1 $\alpha$  dissociation from BiP, and oligomerization exposing an endoribonuclease and a kinase domain. The endoribonuclease domain cleaves a mRNA, resulting in a spliced mRNA and translation of splice X-box binding protein 1 (sXBP1). sXBP1 translocates to the nucleus to activate ER-associated degradation (ERAD) genes, ER chaperones involved in protein folding and quality control (QC) as well as secretion. IRE1 $\alpha$  also downregulates several microRNAs and mRNAs through a process known as “regulated IRE1-dependent decay” (RIDD). IRE1 $\alpha$  also activates the c-Jun N-terminal kinase (JNK) and Apoptosis signaling kinase 1 (ASK1) pathway through oligomerization with TNF receptor associated factor-2 (TRAF2).

## 1.7. The PERK-ATF4 arm of the UPR

Like IRE1 $\alpha$ , PERK is a serine/threonine protein kinase activated by dimerization and trans-autophosphorylation upon dissociation from GRP78 (BiP). Activated PERK phosphorylates the  $\alpha$ -subunit of the eukaryotic initiation factor 2 (eIF2 $\alpha$ ) directly via its kinase domain. The eukaryotic initiation factors regulate translation of mRNA by allowing them to bind to the pre-initiation complex. Phosphorylated eIF2 $\alpha$  acts as an inhibitor of its own nucleotide exchange factor, eIF2B, preventing its activation and thus blocking the translation initiation process leading to translational arrest of most mRNAs and a reduction in ER protein load<sup>77</sup>. However, following eIF2 $\alpha$  phosphorylation, due to its unique coding structure, activating transcription factor 4 (ATF4) translation occurs preferentially, allowing continuous transcription of specific UPR targets (**Fig. 5**). Induction of the eIF2 $\alpha$  kinases leading to ATF4 activation is collectively referred to as the integrated stress response (ISR)<sup>78</sup>. ATF4 target-genes include factors involved in restoring ER homeostasis, amino acid metabolism, the oxidative stress response, ER- quality control related as well as pro-apoptotic factors including the transcription factor C/EBP-homologous protein (CHOP, also known as GADD153). Some recent studies suggest that ATF4 is dispensable for induction of CHOP during ER stress<sup>79</sup>. Together, ATF4 and CHOP induce the expression of growth arrest and DNA damage-inducible protein 34 (GADD34), which directs dephosphorylation of phosphorylated eIF2 $\alpha$ <sup>79</sup>. ATF4 and CHOP also induce the expression of a related transcription factor, activating transcription factor 5 (ATF5). As a transcription factor, CHOP is known to regulate numerous pro- and anti-apoptotic genes, such as B-cell lymphoma-2 (Bcl-2) and tribbles-related protein 3 (TRB3)<sup>80</sup>. In addition, CHOP, together with ATF4, regulates genes involved in cellular amino acid metabolism<sup>78</sup> and CHOP expression allows cells to re-establish cellular homeostasis before the initiation of apoptosis. Early studies reported that CHOP deficient mice are resistant to diabetic nephropathy<sup>81</sup>.

PERK also activates the transcription factor nuclear factor-erythroid 2-related factor 2 (NRF2). After phosphorylation by PERK, NRF2 dissociates from its negative regulator kelch-like ECH-associated protein 1 (KEAP1) and induces transcription of genes involved in the cytoprotective antioxidant signaling and autophagy (**Fig. 5**).

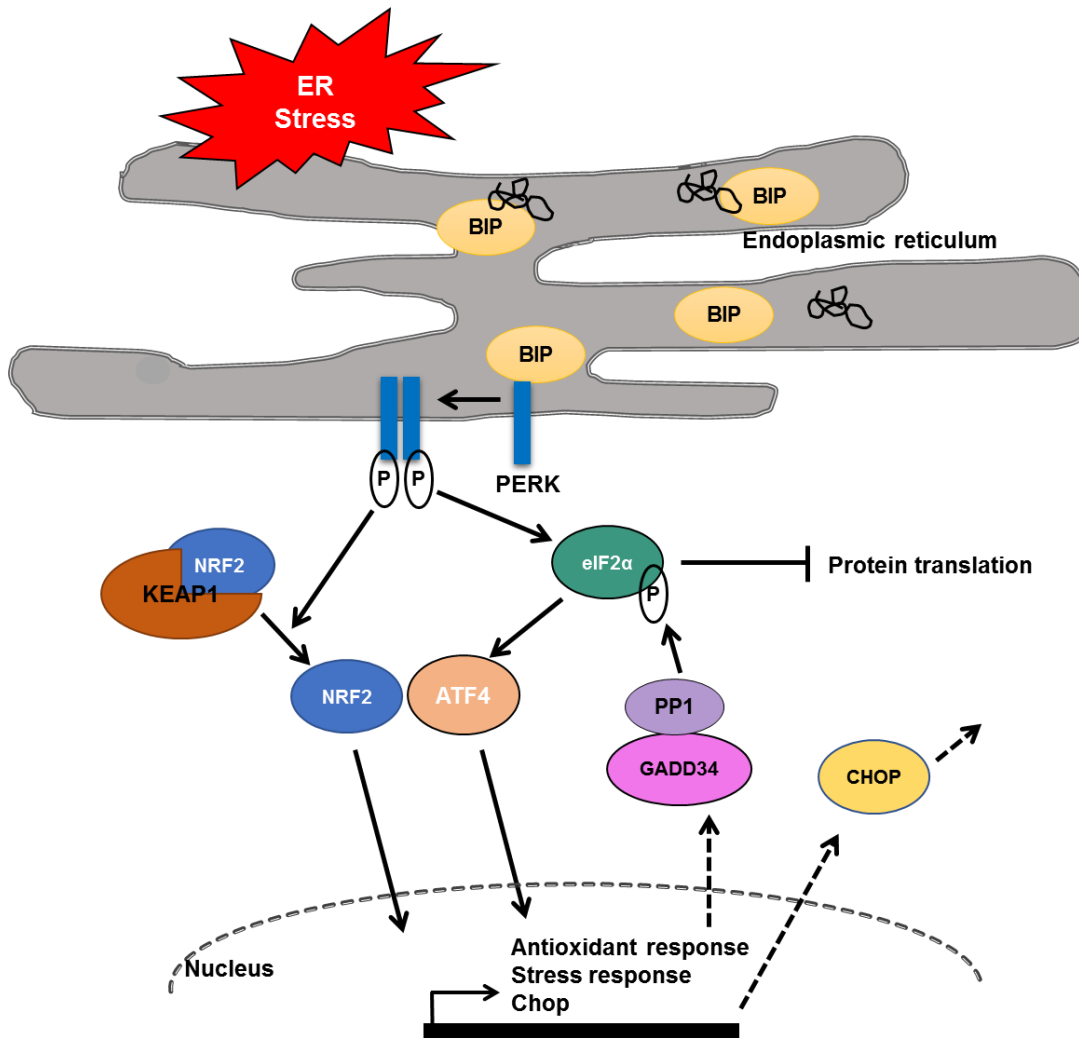


**Figure 5: The PERK-ATF4 arm of the tripartite UPR.** Similar to IRE1 $\alpha$ , PERK dissociation from BiP and oligomerization, results in phosphorylation of the eukaryotic initiation factor 2 (eIF2 $\alpha$ ) via its kinase domain. Phosphorylated eIF2 $\alpha$  inhibits translation initiation process leading to translational arrest of most mRNAs, but preferentially allowing the translation of activating transcription factor 4 (ATF4). ATF4 induces expression of CHOP and together they induce the expression of GADD34, which directly dephosphorylates phosphorylated eIF2 $\alpha$ . PERK also triggers the dissociation of nuclear factor-erythroid 2-related factor 2 (NRF2) from its negative regulator kelch-like ECH-associated protein 1 (KEAP1) and induces transcription of genes involved in cytoprotective antioxidant signaling.

## 1.8. The ATF6 arm of the UPR

Activating transcription factor 6 is a type II transmembrane protein that is retained in the ER membrane by its physical association with GRP78 (or BiP) under normal physiological conditions. Upon development of ER stress, ATF6 dissociates from BiP and translocates to the Golgi, where it is cleaved by site-1 protease (S1P) and site-2 protease (S2P) (**Fig. 6**). The cleaved N-terminal ATF6, which is an active transcription factor, translocates to the nucleus and upregulates the transcription of UPR target genes involved in ER protein processing and ERAD including XBP1. Furthermore, ATF6 collaborates with XBP1 in transcriptional activation of ER chaperone that contain the cis-acting ER stress response element (ERSE) in their promoter regions<sup>82,83</sup>. Another ER stress responsive cis-acting element was identified in mammals, designated the UPR element (UPRE). However, it was found that XBP1 binds to UPRE as a homodimer without assistance from the transcription factor nuclear factor-Y (NF-Y) while ATF6 exhibits much lower affinity for UPRE and instead prefers NF-Y-dependent binding to the ERSE. The activity of ATF6 and its specificity for ER stress response elements in the promoter regions of target genes is determined by its direct interaction with different transcription factors, including NF-Y, Yin Yang 1, TATA-box binding protein and sXBP1<sup>69,83</sup>.

Additionally, there is considerable crosstalk between the three arms of the UPR. Protein kinase inhibitor p58 (p58IPK), a co-chaperone whose expression is upregulated under stress conditions by ATF6 and sXBP1, directly interacts with PERK and inhibits its kinase activity<sup>84</sup>. While the activation of ATF4 is thought to play a dominant role in the induction of CHOP, ATF6 and XBP1 can also upregulate CHOP under stress conditions<sup>85</sup>.



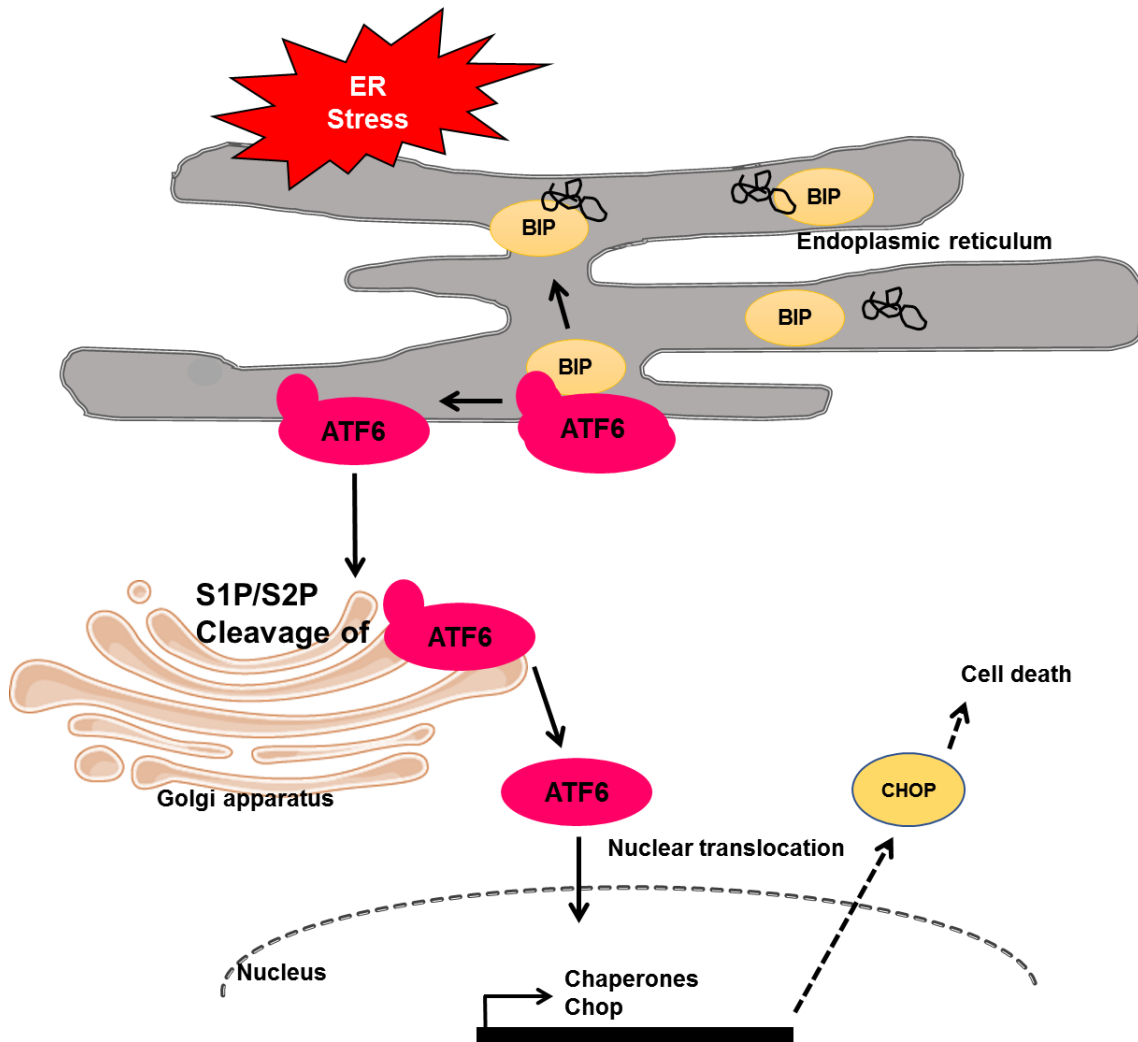


**Figure 6: The ATF6 arm of the tripartite UPR.** Activating transcription factor 6 (ATF6) is retained in the ER membrane by its physical association with BiP under normal physiological conditions. Upon ER stress, ATF6 dissociates and translocates to the Golgi, where it is cleaved by S1P and S2P. The cleaved N-terminal ATF6, which is an active transcription factor, translocates to the nucleus and upregulates the transcription of UPR target genes and ER chaperones.

### 1.9. ER stress and human pathologies

The physiological importance of the UPR is related to the specific cellular function; e.g. secretory cells such as plasma cells, hepatocytes, islet  $\beta$ -cells, adipocytes, macrophages, and oligodendrocytes are particularly dependent on a well-regulated UPR machinery. Aberrant metabolic conditions such as hyperlipidemia, hyperglycemia, excessive cytokine production and reactive oxygen species (ROS) can differentially affect ER trafficking and

therefore, it is imperative to study the ER stress response in a cell- and tissue context-specific manner<sup>86</sup>. In neurons, the chronic expression of folding- defective secretory proteins can put unsustainable demands on the protein folding machinery leading to ER stress<sup>87</sup>. In Alzheimer's disease, intracellular deposits of tau protein are observed in neurofibrillary tangles, while in Parkinson's disease, ubiquitinated protein deposits called Lewy bodies are seen in neuronal cytosol. There is research currently underway targeting the UPR in order to treat these conditions<sup>88</sup>.

In pancreatic  $\beta$ -cells, ER stress can occur as a result of increased levels of insulin intermediates (and the ensuing demand on the ER folding capacity) needed to maintain blood glucose following the loss of most islet cells from autoimmune attack by T lymphocytes in T1DM<sup>80</sup>. In T2DM, peripheral insulin resistance forces islet  $\beta$ -cells to increase insulin production as a compensatory mechanism<sup>89</sup> putting an unusual amount of stress on the protein folding and secretory machinery of the ER, eventually contributing to  $\beta$ -cell failure. Pancreatic XBP1 was shown to play a role in glucose homeostasis, as  $\beta$ -cell specific deletion of XBP1 decreased insulin processing and secretion from the islets, resulting in hyperglycemia and glucose intolerance<sup>90</sup>. Similarly, PERK null mice develop growth retardation and metabolic dysfunction due to loss of pancreatic islet cells<sup>91,92</sup>. Wolcott-Rallison syndrome, a rare genetic disorder in humans caused by mutations of PERK, showcase similar pathologies as in mouse models with growth retardation, and early-onset diabetes by non-autoimmune-mediated  $\beta$ -cell destruction<sup>93</sup>.

Insulin receptor signaling has been shown to positively regulate sXBP1 activity in hepatocytes as well. sXBP1 physically interacts with the regulatory subunits of PI3K ( $p85\alpha/\beta$ ), which facilitates nuclear translocation of sXBP1. In obese and diabetic murine livers, sXBP1 fails to translocate to the nucleus due to impaired association with  $p85\alpha/\beta$ <sup>94</sup>. Neuronal XBP1 deletion creates hypothalamic ER stress and leptin resistance<sup>95</sup>, leading to weight gain upon high fat diet feeding through increased food intake and decreased energy expenditure. Chemical chaperones such as 4-phenylbutric acid (4-PBA) and tauroursodeoxycholic acid (TUDCA), alleviate hypothalamic ER stress in high fat diet-fed mice, reducing food consumption and body weight<sup>95-97</sup>. Peripherally, increased ER stress in the liver and adipose tissues of obese mice has been shown to cause insulin resistance<sup>97-99</sup>. Peripheral administration of chemical chaperones has been shown to

alleviate ER stress in the liver and adipose tissue, improving insulin sensitivity and glucose homeostasis in obese and diabetic mice. 4-PBA and TUDCA have been demonstrated to improve insulin sensitivity in human obese subjects, indicating to ER stress as a potential cause behind human metabolic disorders<sup>99,100</sup>.

Key features of the human T2DM, including dyslipidemia, hyperinsulemia and hyperglycemia are probably best recapitulated in the db/db mice. The spontaneous autosomal recessive mutation diabetes, db, was discovered in the Jackson Laboratory, in 1966<sup>101</sup>. Mice homozygous for the diabetes spontaneous mutation in the leptin receptor (*Lepr<sup>db</sup>*) become obese starting 2-4 weeks of age and display decreased insulin receptor sensitivity accompanied by peripheral insulin resistance (IR)<sup>101,102</sup>. Insulin resistance precedes the development of T2DM by several years in humans<sup>103</sup>.

### **1.10. Insulin resistance and microvascular complications**

Progressive IR leads to microvascular changes in peripheral organs including the kidney, leading to dNP. Diabetes induces pathognomonic changes in the microvasculature affecting the glomerular capillary. The highly specialized glomerular endothelial cells, component of the glomerular capillary and the glomerular filtration barrier, express thrombomodulin (TM), which allows thrombin-dependent protein C activation<sup>104</sup>. Clinical data from diabetic patients show elevated plasma levels of soluble TM, reflecting loss of endothelial TM-function and reduced levels of activated protein C (aPC)<sup>105</sup>. Coagulation protease, aPC, has been shown to inhibit pro-fibrogenic cytokines, growth factors and renal fibrosis in a model of dNP<sup>106</sup>. aPC has also been shown to prevent mitochondrial ROS in the glomeruli under hyperglycemic conditions via regulation of p66<sup>Shc107,108</sup>. p66<sup>Shc</sup> is a cytosolic growth factor adaptor protein involved in the cellular response to oxidative stress and has recently been found to be localized in the mitochondria-associated ER membranes (MAMs). While previous studies have established that coagulation protease have cytoprotective anti-ROS and anti-apoptotic effects in the glomerular compartment, they have eluded to the possibilities of coagulation proteases locally regulating calcium ions and the redox machinery, key cellular functions performed by the ER. However, the impact of coagulation proteases, in particular of aPC, on ER-stress response remains largely elusive.

### 1.11. Coagulation proteases and protease activated receptors (PARs)

In vertebrates the coagulation system was initially identified as a tightly regulated system controlling hemostasis, but additional functions for inflammation and tissue remodeling are now established. The coagulation system is a cascade-like system with two principle activation pathways: the tissue factor (TF) pathways also known as extrinsic pathway and the contact pathways also known as the intrinsic pathway (**Fig. 7**). TF is a type 1 transmembrane receptor, which is physiologically expressed in particular by perivascular cells, and TF encounters blood components only upon vascular injury or inflammation. TF lacks intrinsic proteolytic activity<sup>109</sup>. However, it binds factor VII or factor VIIa in a Ca<sup>2+</sup>-dependent manner, promoting factor VII activation or enhancing the catalytic activity of factor VIIa<sup>110</sup>. The TF/VIIa complex interacts with and activates factors IX and X. Activated factor X induces the formation of the prothrombinase complex comprising of factors Xa, Va, calcium, and negatively charged phospholipids of activated cells such as platelets. The prothrombinase complex promotes the conversion of prothrombin to thrombin, also known as factor IIa. Thrombin initiates an amplification loop via factor XIa generation and by activating the non-proteolytic cofactors V and VIII (which positively regulate thrombin by accelerating its production ~1000 fold)<sup>111</sup>. Thrombin activates fibrinogen by limited proteolysis and platelets via the protease activated receptors (PARs) expressed on the surface of platelets, generating fibrin-platelet aggregates, constituting the blood clot<sup>111</sup>. Activation of the blood clotting system is crucial to maintaining vascular integrity. At the same time its activity must be tightly regulated to prevent inadvertent and excess clotting activation, resulting in potentially lethal thrombosis or disseminated intravascular clotting (DIC). Several physiological anticoagulant mechanisms provide negative feedback. Tissue factor pathway inhibitor (TFPI) is Kunitz-type protease inhibitor that constrains the activity of TF/VIIa and prothrombinase complexes, restricting initiation of the coagulation cascade<sup>109,110</sup>. The serine protease inhibitor antithrombin, previously known as antithrombin III, inhibits multiple coagulation factors (in particular VIIa, IXa, Xa, XIa, and XIIa). Antithrombin also inhibits other serine proteases, such as kallikrein, plasmin and trypsin as well as the complement lectin pathway (**Fig. 7**).

Another anticoagulant mechanism is provided by the endothelial protein thrombomodulin. TM induces a specific and important function by modulating the coagulant activity of thrombin. Thrombin loses its pro-coagulant function when bound to thrombomodulin and thrombomodulin-bound thrombin activates protein C. Activated protein C (aPC), inactivates cofactors Va and VIIIa, efficiently dampening the amplification of thrombin generation<sup>111,112</sup>. Endogenous aPC (~40 pmol/L circulating levels in humans) functions as a potent anticoagulant and anti-inflammatory molecule<sup>113</sup>. In healthy individuals, PC has a half-life of 8 hours, whereas aPC has a half-life of 15 to 20 minutes and murine aPC has a half-life of 12 to 14 minutes<sup>112</sup>.

The contact system comprises the zymogens factor XII (FXII), plasma prekallikrein (PPK), factor XI (FXI), high-molecular weight kininogen (HK) and C1 esterase inhibitor (C1INH). FXII initiates the contact system cascade upon binding to negatively charged surface (such as polyphosphates released from platelets<sup>114</sup>), causing a conformational change in the zymogen and leading to the generation of small amounts of FXIIa. FXIIa cleaves PPK generating active PK which positively regulates FXII activation. PK then activates the kallikrein-kinin system<sup>115</sup>.

In addition to its hemostatic function, the coagulation system has non-hemostatic functions in regulating inflammation and tissue remodeling mediated through the protease activated receptors (PARs). PARs are class A family of rhodopsin-like G protein-coupled receptors (GPCRs) and are predominantly organized within lipid rafts. Four different PARs have been identified: PAR1, PAR2, PAR3, and PAR4<sup>116</sup>. PARs form heterodimers allowing them to activate diverse signaling pathways in tissue-, context-, and temporal-specific manner. PARs transmit cellular responses initiated by several coagulation regulators, such as factor IIa, aPC, factor Xa or plasmin, as well as non-coagulation proteases, such as matrix metalloproteinase-1 (MMP-1), tryptase or matryptase, cathepsin G and cathepsin S<sup>117</sup>. Following cell-surface localization, the proteases cleave PARs at the extracellular N-terminus, unmasking a cryptic N-terminal sequence, which acts as a tethered ligand inducing conformational rearrangement and irreversible activation of heterotrimeric G proteins. This mechanism of activation of PARs is unique and distinct from most other GPCRs, which can be reversibly activated.

PARs expression is highly heterogenous with species-specific expression and more than one PAR being expressed on many cell types. For example human podocytes predominantly express PAR2 and PAR3, while murine podocytes predominantly express PAR1 and PAR3<sup>111,118</sup>. Similarly, human platelets express PAR1 and PAR4 while murine platelets predominantly express PAR3 and PAR4<sup>111</sup>. While both aPC and thrombin can activate PAR1 and PAR3, they convey opposing cellular effects<sup>118</sup>. This biased and cell-specific PAR-mediated signaling is thought to result from distinct cleavage sites resulting in different neo-N-termini, and cell-specific supramolecular receptor complexes. PARs form both homodimers and heterodimers, either constitutively or upon activation, depending on the cell type, extracellular protease, specific PAR that is activated and its co-receptors<sup>119</sup>. While a single study suggested that PAR3 can signal autonomously upon thrombin exposure<sup>120</sup>, studies by others and our group showed that PAR3 requires the hetero-dimerization with PAR2 (in human podocytes) and PAR1 (in murine podocytes) to transduce aPC-dependent inhibition of apoptosis<sup>118,121</sup>. Additionally, PARs can interact with other receptors, such as sphingosine 1-phosphate receptor 1 (S1P1), epidermal growth factor receptor (EGFR), allowing PARs to affect diverse signaling pathways and modulate cellular responses in a highly context- and cell-specific fashion in addition to regulating hemostasis<sup>111</sup>.

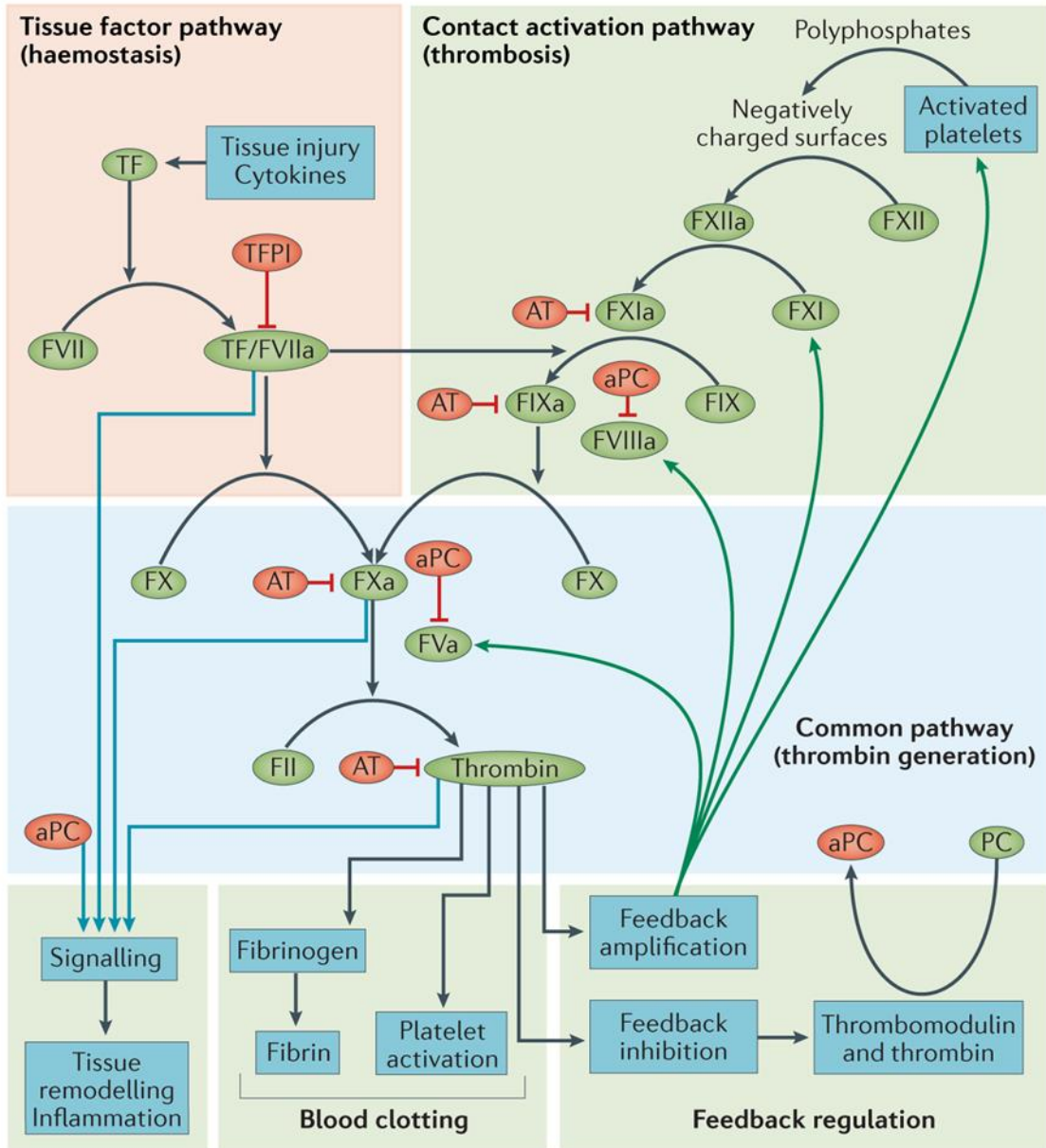


**Figure 7. The coagulation cascade (adapted from Madhusudhan et al. 2016<sup>11</sup>).** The cascade is traditionally divided into the intrinsic, extrinsic, and common pathway. Active forms of coagulation factors are denoted by 'a' along with a roman numeral. The tissue factor and contact pathways lead to generation of thrombin. Thrombin (FIIa) triggers formation of blood clots, provides feedback amplification or inhibition of the coagulation activation processes and receptor-mediated signaling. Excess coagulation activation is prevented through TFPI, AT, and aPC. aPC is generated by the FIIa/Thrombomodulin complex on cell surfaces. TF, tissue factor; TFPI, tissue factor pathway inhibitor; AT, antithrombin.

**1.12. Coagulation proteases in the kidney**

Coagulation regulators and receptors are widely expressed in renal cell types<sup>105,111</sup>. Thrombomodulin and endothelial protein C receptor (EPCR) are expressed in the glomerular endothelial cells. The expression of thrombomodulin and EPCR is reduced in acute inflammatory states such as sepsis, as well as in chronic conditions such as DM<sup>104,112</sup>. Increased TF expression has been detected in acute and chronic kidney diseases in humans and rodents. Since TFPI is expressed in interstitial blood vessels, but not in the glomeruli, glomerular TF expression is not regulated by concomitant TFPI expression<sup>111</sup>. Protein C and protein C inhibitor (PCI) are also expressed in renal cells<sup>111</sup>. Plasma protein C expression is reduced in mice with systemic inflammation or diabetes<sup>104,122</sup>. Renal PAR1 activation results in vasoconstriction and reduces glomerular filtration rate, while PAR2 activation causes vasodilation, partially reversing the vasoconstriction induced by PAR1 agonists or angiotensin II, increasing GFR<sup>111</sup>. Renal endothelial cells express PAR1, PAR2, and EPCR, while podocytes express PAR3, but lack EPCR, demonstrating the distinct cell-specific signaling pathways. In human podocytes, PAR3 dimerizes with PAR2 following aPC-mediated PAR3 activation, whereas in murine podocytes, aPC signaling is transduced by PAR1 and PAR3 heterodimerization<sup>111,112</sup>.

### **1.13. Coagulation proteases with therapeutic potential**

Classical inhibitors of coagulation proteases such as heparin, hirudin, Vitamin-K antagonists (VKAs) and novel direct oral anticoagulants or DOACs are widely prescribed to patients at a risk of venous and – more recently - arterial thromboembolic events<sup>123</sup>. The anticoagulant's mechanisms of action involve direct inhibition of specific or multiple coagulation proteases, while VKAs inhibit the synthesis of vitamin K-dependent clotting factors. Dabigatran, a DOAC, directly inhibits thrombin, while rivaroxaban, apixaban and edoxaban are direct FXa inhibitors<sup>123</sup>. While these coagulation inhibitors have been studied in the context of their hemostatic effects, their intracellular cytoprotective signaling have not been explored<sup>124</sup>.

A new family of small molecules known as parmodulins<sup>125</sup> are being studied for their antiinflammatory and antithrombotic effects<sup>126</sup>. Parmodulins bind to the cytosolic parts of



PAR1 and have been shown to counteract thrombin-dependent platelets activation<sup>127,128</sup>. While parmodulin's modulation of PAR1 signaling are promising new therapeutics restricting platelet activation, their cytoprotective signaling requires further exploration<sup>128</sup>. Our group has recently showed that parmodulin can phenocopy the cytoprotective effect of aPC in the context of ischemia reperfusion injury of the heart or the kidney<sup>129</sup>. However, the underlying mechanism remains largely unknown.

Besides being a potent anticoagulant, aPC has cytoprotective activities including anti-apoptotic and anti-inflammatory functions, and endothelial barrier protection in association with altered gene expression<sup>113</sup>. APC initiates cell signaling that drives cell proliferation and differentiation as well as cell and tissue regeneration in ischemic stroke and wound healing<sup>112,126,130,131</sup>. Given the potent anti-inflammatory effects aPC was approved for sepsis treatment, but withdrawn from the market after 10 years due to limited efficacy arising from bleeding complications<sup>105</sup>. Detailed structure-function analyses were carried out establishing that the molecular requirements of aPC for its anticoagulant and cytoprotective properties are largely disjunct<sup>105</sup>. These insights yielded aPC variants conveying predominantly cytoprotective effects<sup>132,133</sup>. Due to aPC's cytoprotective effects<sup>134</sup> in heart, lung, kidney, gastrointestinal tract, spleen, eye, bone marrow, and skin, recombinant wild type APC and APC mutants are being evaluated in clinical studies for the treatment of ischemic stroke<sup>135</sup>, wound healing and retinal injury<sup>112</sup>. These recombinant proteins are, however, expensive and can only be used for parenteral application. Another approach would be to better understand the underlying cytoprotective signaling mechanisms with the aim of developing functional mimetics.

## 2. Aim of the study

Endoplasmic reticulum (ER) stress is associated with diabetes and dNP, but its pathophysiological relevance in podocytes (glomerular epithelial cells) remain unclear. Considering the known association of ER-stress and diabetic nephropathy, the interaction of insulin- and ER-signaling, the established role of insulin in podocytes and the pivotal role of podocyte injury for DKD, we hypothesized that **insulin signaling regulates the ER-response in podocytes and hence the course of DKD**. To this end we first investigated the role of insulin signaling and the lack thereof in promoting ER stress in the podocytes. As demonstrated in previous studies in insulin sensitive tissues such as the liver, fat and pancreatic  $\beta$  cells, we confirmed that defective insulin signaling in podocytes impairs nuclear translocation of the ER-transcription factor sXBP1 due to deficient interaction with the regulatory subunits of PI3K, p85 $\alpha$  and p85 $\beta$ . The loss of nuclear sXBP1 aggravates hyperglycemia-induced ER stress in the glomeruli. Given the prominent cytoprotective effects of aPC in the context of experimental diabetic nephropathy, I, furthermore speculated that **aPC-PAR signaling interacts with insulin- and ER- signaling in podocytes, potentially restoring impaired ER-homeostasis in the absence of proper insulin-signaling**. We, thus, hoped to identify points of regulatory convergence that may facilitate compensating for insulin resistance and relieve ER stress associated with DKD.

### 3. Methods

#### 3.1. Animals

XBP1<sup>flox/flox</sup> mice (provided by Laurie H. Glimcher), INSR<sup>flox/flox</sup> mice and PI3KR1<sup>flox/flox</sup> (p85 $\alpha$ ) mice (both obtained from The Jackson Laboratory) were crossed with Pod<sup>Cre</sup> mice (provided by Marcus J. Moeller) to generate mice with podocyte specific deletion of XBP1, INSR, and p85 $\alpha$ , respectively<sup>16,75,94</sup>. TM<sup>Pro/Pro</sup> mice and PIK3R2 (p85 $\beta$ ) constitutive knockout mice were obtained from The Jackson Laboratory. Mice had been back crossed onto the C57BL/6J background for at least 7 generations and were routinely maintained on the C57BL/6J background. Only littermates were used as controls and all male mice were used. The presence of targeted genes and transgenes was routinely determined by PCR analyses of tail DNA and podocyte specific genetic deletion of respective genes was confirmed by two independent methods: (1) Analysis of protein levels in isolated podocytes as compared to wild type mice and (2) double immunofluorescence staining using a podocyte specific marker (synaptopodin) and an antibody for the corresponding protein to be inactivated.

APC<sup>high</sup> mice have been previously described<sup>94</sup>. These mice express a transgene in the liver inducing expression of a human protein C (PC) variant (D167F/D172K). The D167F/D172K PC variant can be efficiently activated in the absence of thrombomodulin, resulting in high plasma concentrations of aPC. Wild type C57BL/6J and db/db (C57BL/KSJRj-db) mice were obtained from Janvier, France. Animal experiments were conducted following standards and procedures approved by the local Animal Care and Use Committee (Landesverwaltungsamt Halle, Germany).

#### 3.2. Materials

The following antibodies were used in the current study: mouse monoclonal antibodies: sXBP1 (MAB4257, R&D biosystems), CHOP (#2895, Cell Signaling Technology, and sc-7351, Santacruz, Germany), ATF6 (NBP1-40256, Imgenex); rabbit polyclonal antibodies: XBP1 (sc-7160), ATF4 (sc-200) and WT1 Goat polyclonal (sc-15421) and p85 $\beta$  (sc-100407) antibodies (Santacruz, Heidelberg, Germany); rabbit polyclonal antibodies: p85 $\alpha$

(#05-212, Millipore GmbH, Germany); Lamin A/C (#2032, Cell Signaling Technology, Germany),  $\beta$ -galactosidase (orb344789, Biorbyt Ltd, Cambridgeshire, United Kingdom). The following HRP conjugated secondary antibodies were used for immunoblotting: rabbit IgG and mouse IgG (Cell Signaling Technology, Germany). The following secondary antibodies for immunofluorescence were used: Texas red conjugated anti-mouse (#TI-2000) and FITC conjugated anti-mouse (#FI-2000), FITC conjugated anti-goat (#FI-5000) from Vector Laboratories, CA, USA. The following reagents were obtained from Sigma-Aldrich, Taufkirchen, Germany: Duolink *In situ* proximity ligation assay kit and reagents, streptozotocin, RPMI 1640, 1% collagen, 2% Gelatin, and Bradford reagent. Other reagents used in the current study were: Insulin (Lantus; Sanofi, Frankfurt, Germany); mouse albumin Elisa quantitation kit (Bethyl Laboratories, TX, USA); Dapagliflozin (Bristol-Myers Squibb); Trypsin-EDTA, fetal bovine serum, and HEPES (Thermo Fischer Scientific, Germany); Interferon  $\gamma$  (cell sciences, Canton, MA); *In situ*-cell death detection kit (TUNEL) and protease inhibitor cocktail (Roche diagnostics GmbH, Mannheim, Germany); BCA reagent (Thermo Fisher Scientific, Germany); Vectashield mounting medium with DAPI, (Vector Laboratories, CA, USA); shRNA for XBP1 (Openbiosystems, Heidelberg, Germany); transfection reagent FuGENE (Promega, Germany); and PVDF membrane, immobilization enhanced chemiluminescence reagent and Tauroursodeoxycholic acid (Millipore GmbH, Germany). Human aPC was used throughout the study, which was generated using an established protocol<sup>136</sup>.

### **3.3. Induction of diabetes using streptozotocin**

Diabetes was induced by intraperitoneal administration of streptozotocin (STZ, obtained from Sigma-Aldrich) at 60 mg/kg, freshly dissolved in 0.05 M sterile sodium citrate, pH 4.5, on five successive days in 8-week-old male mice. Mice were considered diabetic if blood glucose levels were above 300 mg/dl (16.7 mM/L) 16–25 d after the last STZ injection. Blood glucose levels were determined in blood samples from the tail vein using ACCU-CHEK glucose meter (Roche Diagnostics). In the first three weeks after onset of diabetes blood glucose values were measured three times per week, afterwards once a week. Mice displaying blood glucose levels above 500 mg/dl (27.7 mM/L) received 1–2 U

insulin (Lantus) to avoid excessive and potentially lethal hyperglycemia. We obtained blood and tissue samples after 26 weeks of persistent hyperglycemia in diabetic mice. We injected a subset of diabetic mice intraperitoneally with either TUDCA (150 mg/kg, dissolved in PBS) or PBS once daily starting 18 weeks after the last streptozotocin (STZ) injection until 1 d before analyses (week 26). In addition a group of diabetic mice received drinking water supplemented with sodium-glucose co-transporter 2 (SGLT2) inhibitor (dapagliflozin, 25 mg/kg, body weight, provided by Bristol-Myers Squibb) starting 18 weeks after the last streptozotocin (STZ) injection until 1 d before analyses (week 26). In other mice we intraperitoneally injected aPC (1 mg/kg bodyweight, every alternate day) or an equal volume of PBS. Additionally, in a subgroup of mice aPC was pre-incubated before injection with the HAPC<sup>1573</sup> antibody at a 1:1 ratio for 10 min under gentle agitation to block its anticoagulant activity<sup>118,137</sup>.

### **3.4. Determination of albuminuria**

The day before blood sample collection and tissue preparation mice were individually placed in metabolic cages for 12 h and urine samples were collected. We determined urine albumin using a mouse albumin ELISA kit (Bethyl Laboratories, Inc.) according to the manufacturer's instructions and urine creatinine with a modified version of the Jaffe method using a commercially available assay (X-Pand automated platform, Siemens, Eschborn, Germany)<sup>104,138</sup>.

### **3.5. Histology and immunohistochemistry**

Animals were sacrificed using a high dose of anesthetics (65 mg/kg Ketamine + 11 mg/kg Xylazine) and subsequently perfused first with ice-cold PBS and then with 4% buffered paraformaldehyde (PFA). Tissues were further fixed in 4% buffered paraformaldehyde for 2 d, embedded in paraffin and processed for sectioning. Extracellular matrix (ECM) deposition in glomeruli was assessed by periodic acid–Schiff (PAS) staining. The fraction mesangial area (FMA) in the kidney sections were scored in a blinded fashion, according to an established scoring system following the current DCC (Diabetic Complication

Consortium) protocol<sup>104,107,139</sup>. The FMA was calculated as the percentage of the glomerular area relative to the tuft area.

Human renal tissue samples were provided by the tissue bank of the National Center for Tumor Diseases (NCT, Heidelberg, Germany) in accordance with the regulations of the tissue bank and the approval of the ethics committee of the University of Heidelberg. Double immunofluorescence staining of sXBP1, ATF6 and CHOP on paraffin sections was performed on human kidney sections with and without diabetic nephropathy. Briefly, sections were fixed in ice cold acetone for 1 min, incubated in PBS (0.1% triton + 0.1% sodium citrate) for 10 min, blocked in 2.5% serum for 1 h, and incubated overnight at 4°C with the primary antibodies against human sXBP1 (1:50), ATF6 (1:50) and CHOP (1:50). Corresponding fluorescently labelled secondary antibodies (anti-mouse IgG-FITC: 1:200, anti-rabbit IgG-Texas red) were added for 60 min and sections were rinsed twice in PBS. Slides were covered with vectashield mounting medium containing nuclear stain DAPI. All specimens were imaged on an Olympus Bx43-Microscope (Olympus, Hamburg, Germany). Confocal images were obtained at 40x magnification using a Zeiss LSM7 microscope (Carl Zeiss, Jena, Germany). Nuclear localization of sXBP1, ATF6 and CHOP was analysed using ImageJ-Fiji software. DAPI stained and fluorescently-labeled images were acquired individually. The exposure settings and gain of laser were kept the same for each condition. Thirty fields were acquired per condition, a single focal plane by field. The ImageJ plugin, colocalization color map was used for automatic quantification and visualization of a pair of co-localized fluorescent signals. Brightness and contrast was adjusted for all images to exclude background signal. Before beginning analysis, images were converted to 8-bit gray scale. "Colocalization" was run to generate the Icorr (index of correlation) values, which represents fraction of positively colocalized pixels. The plugin is based on Jaskolski's algorithm and the method produces a psudeo-color map of correlations between pairs of corresponding pixels from two fluorescent channels of the input images, offering quantitative visualisation of colocalization, described elsewhere<sup>107,140</sup>.

### **3.6. Reverse transcription-quantitative polymerase chain reaction**

Mouse glomeruli from wild type control non-diabetic and diabetic mice were isolated by sequential sieving method<sup>141</sup>. Total RNA was isolated using RNeasy kit (Qiagen, Germany) and reverse-transcribed by RevertAid First Strand cDNA Synthesis Kit (Thermoscientific, Germany). Quantitative polymerase chain reaction was performed in a Bio-Rad real time system (CFX-Connect) using SYBR Green (Thermo Fisher Scientific, Germany). UPR-specific 96-well-format PCR arrays were obtained from SA biosciences-Qiagen and gene expression analysis was performed in real-time PCR (Biorad-CFX connect) according to manufacturer's instructions. For a selective set of UPR genes quantitative polymerase chain reaction was performed using SYBR Green. Primers and further details are given in the **table 3**. The mRNA levels of the genes tested were normalized to  $\beta$ -actin as an internal control.

	<b>Genes</b>	<b>Pimers</b>	<b>Sequences</b>
<b>1</b>	<b>Srebf2</b>	Forward	AGCTGGGCGATGGATGAGAG
		Reverse	TCAGGGA ACTCTCCCACTTGA
<b>2</b>	<b>Creb3</b>	Forward	GAAAGCGGAGATTTGTGGGC
		Reverse	TTGCACGGAGTTCTCGGAAG
<b>3</b>	<b>Bax</b>	Forward	CTGGATCCAAGACCAGGGTG
		Reverse	GTGAGGACTCCAGCCACAAA
<b>4</b>	<b>Nucb1</b>	Forward	CAGGCTGTTCTGCAGATGGA
		Reverse	ACAGGAGCGTCATCTGTGTC
<b>5</b>	<b>Ganab</b>	Forward	GGAGCAAACCCGGTACAAGA
		Reverse	ACTTAACCAAGACCGCCTCC
<b>6</b>	<b>Edem1</b>	Forward	GCGCTTCAAATAATGCCCG
		Reverse	CCGAAGACCAACCAGAGCAC
<b>7</b>	<b>Dnajc3</b>	Forward	TCGAAGGAGAGGATCTGCCA
		Reverse	GAGCATTACATTGTCGGGC
<b>8</b>	<b>Eif2a</b>	Forward	GGTGAATGGACCACCACACT
		Reverse	GCTTTTGGGAGGTCGAAGGA
<b>9</b>	<b>Rnf5</b>	Forward	CCCTATTCCTGTTCTCGCC
		Reverse	TAAGGGGGTGGTCCAAAAGC
<b>10</b>	<b>Sec62</b>	Forward	GTCACACGGTGGTTTTGCTT
		Reverse	TACCGTTCCATCCACACAGG
<b>11</b>	<b>Sec63</b>	Forward	TTCCAGTACGATGACAGCGG
		Reverse	GAATTTGCTCCGCGTTCTGG
<b>12</b>	<b>Ufd1</b>	Forward	CAGTGCAGCATGAGGAGTCA
		Reverse	GAACCAGAGAAGGCACGGAA
<b>13</b>	<b>Dnajb9</b>	Forward	AGAGGCAATGGGAGTCCTTT
		Reverse	CCTGGAAGTGATGCCTTTGT
<b>14</b>	<b>Pdia4</b>	Forward	GTGGTCATCATTGGGCTCTT



		Reverse	CTTCTCAGGGTGTGTCAGCA
15	<b>Ero1B</b>	Forward	CAGCAAACAGCACCAAAGAA
		Reverse	TGGTCCTGCGAATCATCATA
16	<b>Total XBP1</b>	Forward	GGTCTGCTGAGTCCGCAGCAGG
		Reverse	AGGCTTGGTGTATACATGG
17	<b>sXBP1</b>	Forward	GGTCTGCTGAGTCCGCAGCAGG
		Reverse	GAAAGGGAGGCTGGTAAGGAAC
18	<b>ATF4</b>	Forward	CATGCCAGATGAGCTCTTGA
		Reverse	GCCAATTGGTTCACTGTCT

**Table 3: UPR gene primers for quantitative polymerase chain reaction**

### **3.7. Cell culture**

Conditionally immortalized mouse podocytes (obtained from Jochen Reiser's laboratory, Rush University, Chicago) and human podocytes were cultured as described elsewhere<sup>138</sup>. In brief, podocytes were routinely grown on cell culture-grade plates at 33°C in the presence of interferon  $\gamma$  (10 U/ml) to enhance expression of a thermosensitive T antigen. Under these conditions, cells proliferate and remain undifferentiated. To induce differentiation, podocytes were grown at 37°C in the absence of interferon  $\gamma$  for 14 d. Experiments were performed after 14 d of differentiation. Differentiation was confirmed by determining expression of synaptopodin and Wilms tumor-1 (WT-1) protein. Mouse glomerular endothelial cells were obtained from (Cell Biologics, Chicago, IL, USA) and cultured at 37°C in a humidified 5% CO<sub>2</sub> incubator in M1168 mouse endothelial cell medium with growth factors as provided by the manufacturer. Cells were starved overnight before treatment with high concentrations of glucose (25 mM) or mannitol (25 mM). At desired time points post glucose and mannitol treatment, cytosolic and nuclear lysates were prepared for immunoblotting analysis.

Cells were starved for 3 h before treatment with aPC (20nM) or insulin (20nM; Sigma-Aldrich). At desired time points post aPC or insulin treatments, cytosolic and nuclear lysates were prepared for immunoblot analysis. Likewise, 3 h post aPC, insulin or concomitant aPC and insulin treatment, RNA was isolated<sup>138</sup> and subsequently cDNA was synthesized for gene expression analysis.

### **3.8. Transmission electron microscopy**

Transmission electron microscopy (TEM) was performed at the Institute for Clinical Chemistry and Pathobiochemistry, Otto-von-Guericke-University Magdeburg and at the Institute of Anatomy, University Leipzig, Germany. Renal cortex tissues were fixed with 2.5% glutaraldehyde, 2.5% polyvidone 25, 0.1 M sodium cacodylate pH 7.4. After washing with 0.1 M sodium cacodylate buffer (pH 7.4), samples were post-fixed in the same buffer containing 2% osmium tetroxide and 1.5% potassium ferrocyanide for 1 hour, washed in

water, contrasted en bloc with uranyl acetate, dehydrated using an ascending series of ethanol and embedded in glycidyl ether 100-based resin. Ultrathin sections were cut with a Reichert Ultracut S ultramicrotome (Leica Microsystems, Wetzlar, Germany), contrasted with uranyl acetate and lead citrate, and were viewed with an EM 10 CR electron microscope (Carl Zeiss NTS, Oberkochen, Germany). The glomerular basement membrane (GBM) thickness was analysed by ImageJ-Fiji software<sup>142</sup>.

### **3.9. *In situ* proximity-ligation assay**

A Duolink *In situ* PLA Kit was used according to the manufacturer's instructions (Olink Biosciences, Sigma Aldrich) for *in situ* proximity-ligation assay. Double immunofluorescence staining with primary antibodies was performed as described above, followed by PLA to detect the sXBP1 and p85 protein complexes on paraffin sections of human renal biopsies. For *in vitro* imaging, differentiated mouse podocytes were plated on collagen-coated glass coverslips and fixed in 3.7% PFA and methanol. Coverslips were washed (3x PBS or PBS + 0.2% Triton X-100, each 10 min) and blocked in the blocking buffer provided (DuoLink *in situ* PLA kit) for 1 h. Sections were then incubated (overnight, 4°C) with two primary antibodies raised in different species recognizing the target antigens of interest were used. After washing (2 x buffers A and B provided in the kit, each 10 min) sections were incubated with species-specific secondary antibodies with a unique short DNA strand attached (PLA probes). Antibody attached oligonucleotides were linked by enzymatic ligation, amplified *via* rolling circle amplification using a polymerase, and amplified DNA was detected by fluorescent labelled complementary oligonucleotide probes. For quantification of PLA-data, images were acquired on Olympus microscope (BX43, Germany). The exposure settings and gain of laser were kept the same for each condition. Thirty fields were acquired per condition, a single focal plane by field. Before beginning analysis, images were converted to 8-bit images on ImageJ-Fiji. A threshold range was set to distinguish the objects of interest from the background. Automated particle analysis was used to detect the nuclei count per glomeruli. To exclude "noise", the size of particles was defined between 150-Infinity pixels<sup>2</sup> and roundness values were limited to 0.00-1.00. The accumulative counts for each cell type appeared in the Counters

menu. After counting the cells within the ROI, the size of the ROI was calculated and used to identify the number of cells labeled per glomeruli. To count the PLA-positive signals, *Point Picker* plugin was used. The Point List dialog enabled the calculation of PLA positive signals in the nucleus and cytoplasm.

### **3.10. Determination of cell death by TUNEL assay**

Podocytes were serum starved overnight in serum free medium followed by incubation with high concentrations of glucose (25 mM). At indicated time points post glucose treatment cells were fixed in 4% neutral buffered formalin, washed in PBS, and apoptosis was determined using the TUNEL assay<sup>118</sup>. Cells were incubated with terminal deoxynucleotidyl transferase in the presence of fluorescein-labeled dUTP (60 min at 37°C) and counterstained with Hoechst 33258 (3.5 µg/ml). Random images were obtained and the frequency (in percent) of TUNEL-positive cells was determined using Image-J Fiji software.

### **3.11. Production of lentiviral particles**

HEK293T cells (CRL-11268, ATCC) were grown at 37°C and 5% CO<sub>2</sub> in a humidified atmosphere incubator (Thermo). The culture medium contained Dulbecco's modified Eagle's medium (Gibco), 10% fetal bovine serum, and penicillin-streptomycin (50 µg/ml and 50 µg/ml). The HEK293T cells were seeded at the density of  $11 \times 10^6$  cells per 15-mm<sup>2</sup> dish 24 h before transfection. Lentiviruses were produced by transfecting HEK293T cells with shRNA targeting XBP1, PAR1, and PAR3 plasmids (from Dharmacon), together with two helper plasmids (packaging plasmid psPAX2 and VSV-G-expressing plasmid pMD2.g, both Addgene). The transfections were carried out using the calcium phosphate method (2M calcium chloride and 2 x HBS, pH 7.4) with plasmids in a 3:2:1 ratio (shRNA plasmid:psPAX2:pMDg.2). The virus-containing medium was harvested 48 h and 72 h after transfection and subsequently pre-cleaned with a 0.45 µm filtration (Millipore) as described<sup>143</sup>. The virus-containing medium was mixed with 50% PEG6000, 4M NaCl, and 1 x PBS (without calcium and magnesium) at

26%, 11%, 12% (by volume) and incubated on a shaker at 4°C for 4 h. Following incubation, the solution was aliquoted into 50 mL falcons and centrifuged at the 1600 x g at 4°C for 60 min. After centrifugation, the supernatant was carefully removed without disturbing the viral pellet. Cell culture media was added to the pellet for re-suspension and the 50 mL falcon was placed at 4°C in a shaker for recovery overnight. Viral particles were resuspended in 1/20th of the original volume. The protocol for concentrating viral particles was adapted from Kutner et al.<sup>144</sup>. Cells were treated with 2 rounds of the enriched lentivirus and knockdown efficiency was ascertained after 4 d by immunoblotting.

### **3.12. Immunoblotting**

Cell lysates were prepared using RIPA buffer containing 50 mM Tris (pH7.4), 1% NP-40, 0.25% sodium-deoxycholate, 150 mM NaCl, 1 mM EDTA, 1 mM Na<sub>3</sub>VO<sub>4</sub>, 1 mM NaF supplemented with protease inhibitor cocktail. Lysates were centrifuged (13000 x g for 10 min at 4°C) and insoluble debris was discarded. Protein concentration in supernatants was quantified using BCA reagent. Equal amounts of protein were electrophoretically separated on 10% or 12.5% SDS polyacrylamide gel, transferred to PVDF membranes and probed with desired primary antibodies at a concentration of XBP1 (1:200), ATF6 (1:000), CHOP (1:200), ATF4 (1:200), LaminA/C (1:1000), Actin (1:1000), p85 $\alpha$  (1:1000), p85 $\beta$  (1:200). After overnight incubation with respective primary antibodies at 4°C, membranes were then washed with TBST and incubated with anti-mouse IgG (1:5000), anti-rabbit IgG (1:2000) or anti-Goat IgG (1:2000) horseradish peroxidase conjugated antibodies for 1 h at room temperature. Blots were developed with the enhanced chemiluminescence system. To compare and quantify levels of proteins, the density of each band was measured using Image J-Fiji software. Equal loading for total cell or tissue lysates was determined by  $\beta$ -actin western blot.

### **3.13. Cell fractionation**

For isolation of cytosolic and nuclear fractions renal cortex samples were lysed using tissue homogenizer in buffer-A containing 10 mM HEPES-KOH (pH- 7.9), 10 mM KCl, 1.5 mM MgCl<sub>2</sub>, 1 mM EDTA, 0.6% NP-40, 0.5 mM DTT, protease inhibitor cocktail (Roche) and lysates were incubated for 10 min on ice. After brief vortexing the lysates were centrifuged for 30 s at 13000 x g at 4°C. Supernatants were collected as cytosolic fractions and the pellets were resuspended in 100 µl of buffer-B containing 10 mM HEPES-KOH (pH 7.9), 25% glycerol, 420 mM NaCl, 1.5 mM MgCl<sub>2</sub>, 0.2 mM EDTA, 0.5 mM DTT and protease inhibitors. Lysates were incubated for 20 min on ice followed by centrifugation at 13000 x g at 4°C for 5 min. Supernatants containing the nuclear extracts were collected and stored at -80°C<sup>138</sup>.

### **3.14. Gene expression analysis in Nephromine database**

Gene expression data in healthy and diabetic nephropathy patients was extracted from the Nephromine database (Life Technologies, Ann Arbor, MI, **Website: [www.nephromine.org](http://www.nephromine.org)**). Within Nephromine, data was obtained from “Ju Podocyte” database which is a collection of gene expression profiling of 217 micro-dissected glomerular samples and 219 tubulointerstitial samples from chronic kidney disease (CKD) patients and healthy living donors, used to predict cell-type-specific (podocyte-) transcripts by support vector machine based in silico nano-dissection.

### **3.15. Chromatin immunoprecipitation assay**

Chromatin immunoprecipitation (ChIP) assay was performed with Enzymatic Chromatin IP kit (Magnetic beads) according to the manufacturer’s instructions (Cell Signaling Technology). Briefly, unstressed podocytes on day 14 after complete differentiation were treated with low dose of insulin (20 nM) or aPC (20 nM). 3 h post treatment with insulin or aPC cells were fixed with paraformaldehyde and lysed. Chromatin was fragmented by partial digestion with micrococcal nuclease to obtain chromatin fragments of 1 to 5 nucleosomes. Chromatin immunoprecipitations were performed using antibody against spliced-XBP1 (MAB4257-R&D biosystems) and ChIP-grade Protein-G magnetic beads.

After reversal of protein-DNA cross-links, the DNA was purified using DNA purification spin columns, allowing for efficient recovery of DNA and removal of protein contaminants. The enrichment of specific XBP1 target genes was validated using quantitative real-time PCR. The sequence libraries were generated and sequencing was performed on a HiSeq 2000 Illumina (core facility, Helmholtz Centre for Infection Research, Braunschweig, Germany).

### **3.16. CHIP-SEQ dataset analysis**

ChIP- SEQ data analysis was done with the help of bioinformatician, Mohammad Mobashir (Karolinska Institute, Sweden) . Sequence reads were mapped to the mouse genome data base mm10 reference genome assembly with Bowtie2.0 and the latest version of samtools was used to obtain the BAM file from SAM file<sup>145,146</sup>. To identify significantly enriched transcription factor binding sites (TFBS), MATLAB was used. Peak enrichment for each gene covering  $\pm 500$  bases was determined and binning algorithm was applied to explore the coverage for the whole range of the genome and finally we identified and filtered the regions with artefacts before generating the files with gene names, number of peaks and gene coordinates for the respective experiments.

### **3.17. Analysis of human samples**

Human renal tissue samples were provided by the tissue bank of the National Center for Tumor Diseases (NCT, Heidelberg, Germany) in accordance with the regulations of the tissue bank and the approval of the ethics committee of the University of Heidelberg. Patients (N=67) with type 2 Diabetes (T2DM), according to the criteria of the American Diabetes Association (ADA) (1997b), recruited from the diabetes outpatient clinic at the University Hospital Heidelberg. Microalbuminuria was diagnosed if at least two separate urine samples out of three consecutive urine samples (albumin excretion rate AER > 30 mg/ 24h) were positive. Non-diabetic control subjects (N=33) were recruited at the outpatient clinic of the University Hospital Heidelberg and Magdeburg. Non-diabetic controls had either stable and minor osteoporosis or stable and well-controlled thyroid

function (e.g. after thyroidectomy). Non-diabetic controls were on Vitamin D and calcium substitution only (osteoporosis patients) or thyroid hormones, but no other medication. All diabetic patients and non-diabetic controls were Caucasian. The study complied with the declaration of Helsinki; all patients entered the study, according to the guidelines of the local ethics committees after giving informed consent (Ethic-Committee-No: 204/2004).

### **3.18. Study approval**

All animal experiments and protocols were conducted following standards and procedures approved by the local animal care and use committee (Landesverwaltungsamt Halle, Germany). All human samples (biopsies) from patients were used as per the guidelines of the local ethics committees following approval and informed consent (Ethic-Committee-No:204/2004).

### **3.19. Statistical analysis**

Data are summarized as the mean  $\pm$  SEM (standard error of the mean). The Kolmogorov–Smirnov test was used to determine whether the data are consistent with a Gaussian distribution. Statistical analyses were performed with Student *t* test or ANOVA as appropriate. Posthoc comparisons of ANOVA were corrected with the method of Tukey. Prism 7 ([www.graphpad.com](http://www.graphpad.com)) software was used for statistical analyses. Statistical significance was accepted at values of  $P < 0.05$ .

## **4. Results**

### **4.1. Human dNP is associated with a maladaptive ER stress response**



To assess the pathophysiological relevance of ER stress induction in human dNP, we performed immunofluorescence analyses of UPR regulators in renal biopsies of human subjects. The sXBP1 is a highly active nuclear transcription factor and that upregulates gene expression of ER chaperones, components of the ER-associated degradation machinery and transcription factors involved in increasing ER folding capacity. To assess the nuclear localization of sXBP1, quantification of colocalization of nuclear WT1 (green) and sXBP1 (red) was carried out using an automated colocalization color map plugin (ImageJ) index of correlation (Icorr). Icorr quantifies the fraction of positively correlated pixels from two different fluorescent channels within an area. Nuclear localization of sXBP1 was reduced in renal biopsies of patients with dNP (**Fig. 8b**), primarily within the renal glomeruli as determined by the immunofluorescence staining of sXBP1 in non-diabetic human renal biopsies (**Fig. 8a**). Conversely, immunofluorescence analyses for the nuclear localization of ATF6 and CHOP was significantly increased compared to biopsies from healthy patients reflecting enhanced ER stress (**Fig. 8b**). Gene expression analysis of UPR target genes within the Nephromine database was next conducted to gain additional information. The gene expression datasets were derived from the 'Ju Podocyte' group of the Nephromine database which consists of expression profiling of 217 micro-dissected glomerular samples and 219 tubulointerstitial samples from chronic kidney disease (CKD) and healthy patients. Analyses of these data sets showed increased mRNA levels of UPR target genes known to be involved in expanding the folding capacity of the ER (DNAJB9, DNAJC3, PDIA4, Ero1b) and activating the ER-associated degradation (ERAD: Edem1) in patients with diabetic nephropathy when compared to healthy living donors (**Fig. 8c**). These gene expression datasets corroborate that the ER is activated in dNP.

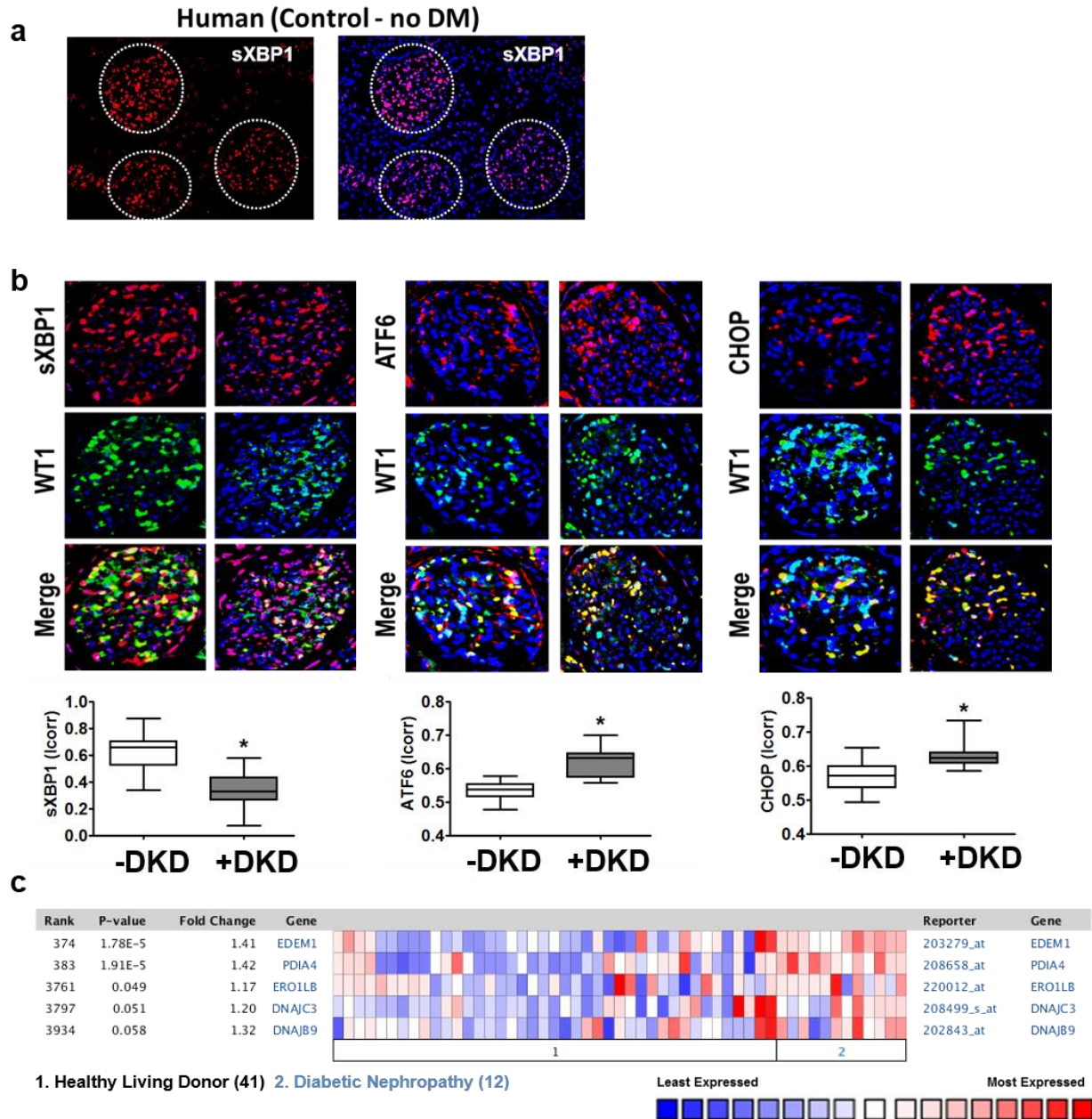


**Figure 8: Maladaptive ER-stress response in human dNP**

Representative image at low magnification (20x) showing immunofluorescent detection of sXBP1 in a non-diabetic human renal biopsy (a). sXBP1 (red) is predominately observed in glomeruli (white dotted line) and only sparsely detected in the tubulointerstitial space. Representative immunofluorescent images of human renal biopsies obtained from diabetic patients without (-DKD) or with (+DKD) diabetic kidney disease, stained for sXBP1, ATF6, CHOP (red) and podocyte marker WT1 (green) with a nuclear counterstain (DAPI, blue). In human diabetic nephropathy, nuclear localization of sXBP1 was reduced primarily in renal glomeruli, while nuclear localization of ATF6 and CHOP were increased when compared to biopsies from

healthy subjects (**b**). Analyses of glomerular specific expression of UPR target genes in healthy human donors (n=41) and patients with diabetic nephropathy (n=12), indicating ER stress in dNP; heat map obtained from 'Ju Podocyte' group of Nephromine database (**c**). Mean  $\pm$  SEM, \* $P$ <0.05 (**b**: t-test).

#### 4.2. Hyperglycemia differentially regulates UPR in murine models of dNP

Two independent mouse models of diabetes were employed to delineate the mechanism controlling the UPR in dNP. We used the model of streptozotocin (STZ) -induced persistent hyperglycemia, reflecting insulinopenic T1DM, and the model of insulin resistance and hyperglycemia in db/db mice, reflecting T2DM. The renal cortex of STZ-treated mice was analyzed by immunoblotting to determine total protein levels of the three stress sensor pathways of the ER - ATF6, sXBP1 and ATF4 – and of CHOP. The total levels of CHOP and active form of ATF6 proteins were significantly upregulated while the expression levels of sXBP1 and ATF4 remained unchanged (**Fig 9a, b**). As one important aspect of the ER stress response is the nuclear translocation of the ER-derived transcription factors, we next analyzed the cytoplasmic and nuclear distribution of these transcription factors. This revealed a significant reduction of nuclear sXBP1 while nuclear CHOP and ATF6 were elevated. The nuclear expression of ATF4 was not altered (**Fig 9c, d**). These protein expression analyses in the T1DM mouse model corroborated the observations made in human diabetic patients without or with dNP (**Fig. 8b**), and underpint a disparate regulation of the tripartite UPR.

To gain further insights into the regulation of ER stress during the progression of dNP, the three arms of the ER stress pathway were analyzed at different stages of the disease in both the STZ-induced and db/db mouse models. The nuclear expression of sXBP1 was downregulated at 10, 18, and 26 weeks post-STZ injections, which correlated with the induction of nuclear ATF6 (50kDa) and CHOP in the renal cortex (**Fig. 9e, f**). The increase in ATF6 and CHOP and the reduction in sXBP1 were associated with the increase in albuminuria in these mice at 10, 18, and 26 weeks post-STZ injections (**Fig. 9g**). The nuclear expression of the transcription factors- sXBP1, ATF6 and CHOP, was strikingly similar in db/db mice. With the onset of albuminuria (4, 8, 12, and 16 weeks of age) (**Fig. 10c**) and disease progression, there was a significant reduction in the nuclear

translocation of sXBP1 that correlated with the upregulation of ATF6 and CHOP (**Fig. 10a, b**). Thus, the observed disparate regulation of the tripartite UPR is seen in both type 1 and type 2 DM models. Of note, no change in the total or nuclear levels of ATF4 were observed in non-diabetic versus diabetic renal cortices (**Fig. 9c, d**). Collectively, these data establish a disparate regulation of the tripartite-UPR in human and murine dNP. Consistent with the previous human dNP data (**Fig. 8b, c**), glomerular specific mRNA levels of UPR-target genes were similarly up regulated in murine dNP indicating ER-stress (**Fig. 10d**).

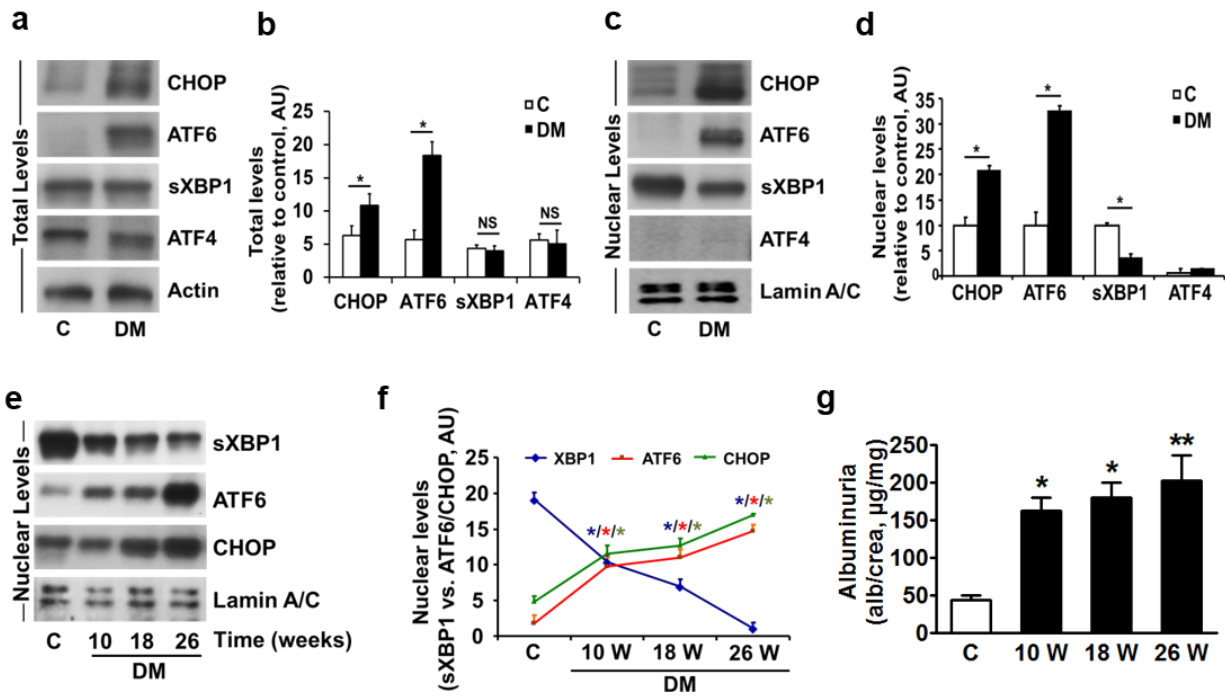


**Figure 9: Hyperglycemia differentially regulates the tripartite UPR in T1DM mouse model**

Representative immunoblots (**a, c**) and bar graphs (**b, d**) showing total (**a, b**) and nuclear (**c, d**) levels of ER transcription factors in renal cortex samples of wild type control (C) and STZ-induced diabetic mice (DM). As loading controls,  $\beta$ -actin was used for total cell extracts (**a**) and lamin A/C for nuclear extracts (**c**, n=6 mice per group). Representative immunoblots (**e**) and line graph (**f**) showing nuclear levels of ER transcription factors in renal cortex samples (**e, f**) and albuminuria (**g**) in wild type control (C) and STZ-induced diabetic (DM) mice at indicated time points post STZ administration (n=8 mice per time point). C=control mice without diabetes, open bars; DM=diabetes, black bars; Mean  $\pm$  SEM, \* $P$ <0.05, \*\* $P$ <0.01 (**b, d, f**: t-test, **g**: one-way ANOVA).

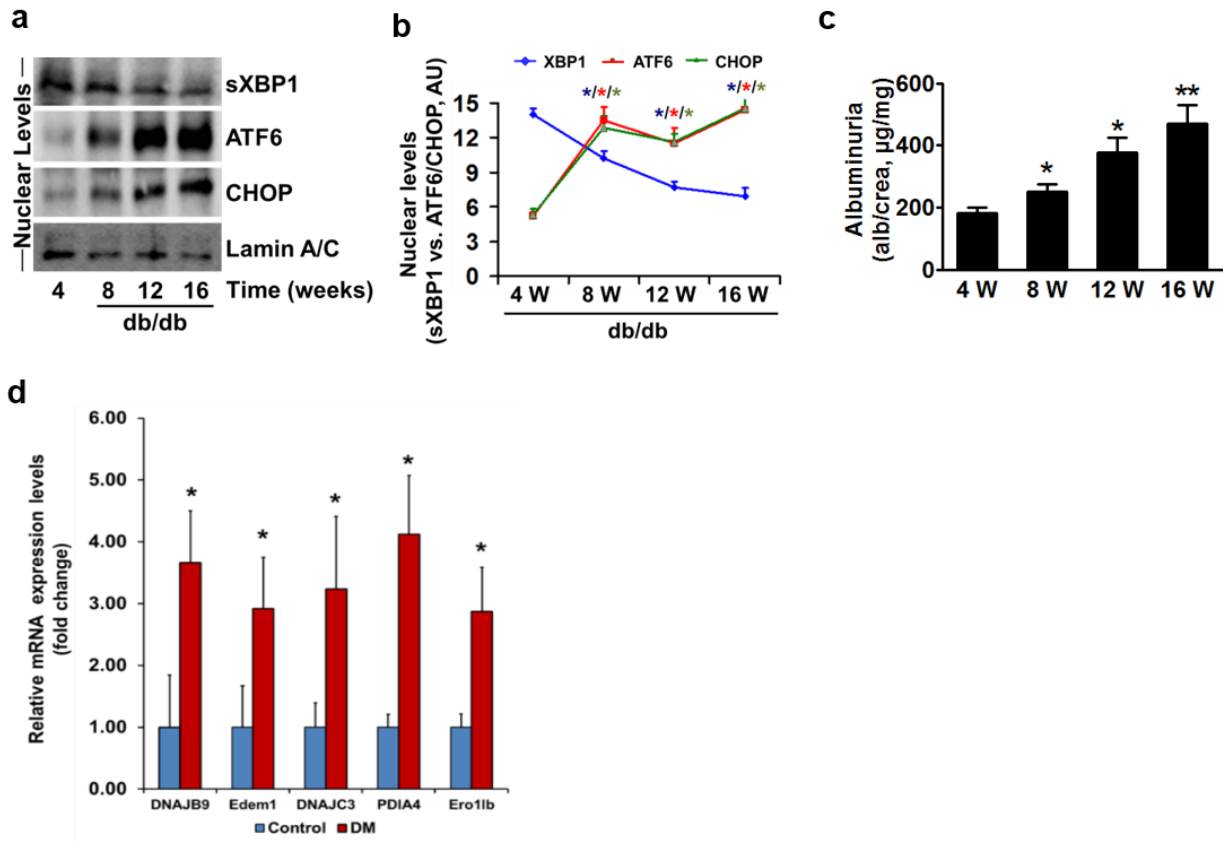


**Figure 10: Hyperglycemia differentially regulates the tripartite UPR in dNP**

Representative immunoblots (**a**) and line graph (**b**) showing nuclear levels of ER transcription factors in renal cortex samples (**a, b**) and albuminuria (**c**) in db/db mice at ages indicated. (n=6 mice per time point). Bar graph (**d**) showing relative mRNA expression levels of UPR target genes in isolated mouse glomeruli from wild type non-diabetic control mice (blue bars) and diabetic mice (26 weeks post-STZ treatment, red bars). The mRNA levels of the genes tested were normalized to 18S as an internal control (n = 5 mice per group were analysed). Mean  $\pm$  SEM, \* $P$ <0.05, \*\* $P$ <0.01 (**b, d**: t-test, **c**: one-way ANOVA).

#### 4.3. Regulation of PERK-eIF2 $\alpha$ pathway in hyperglycemia

An increase in the transcription factors ATF6 and CHOP was evident in the immunoblot analyses of the renal cortices of STZ-injected as well as db/db mice (**Fig. 9 & 10**), but we did not observe a significant change of ATF4 expression. To explore the ATF4 pathway further, the phosphorylation status of its upstream regulators, PERK and eIF2 $\alpha$  were analyzed (**Fig. 11 a, b**). Congruent with the stable ATF4 levels, phosphorylation of PERK

and eIF2 $\alpha$  was not induced at different stages of dNP (**Fig 11. c, d**). These results strongly suggest that the PERK-ATF4 pathway is not contributing to dNP in mouse models of dNP.

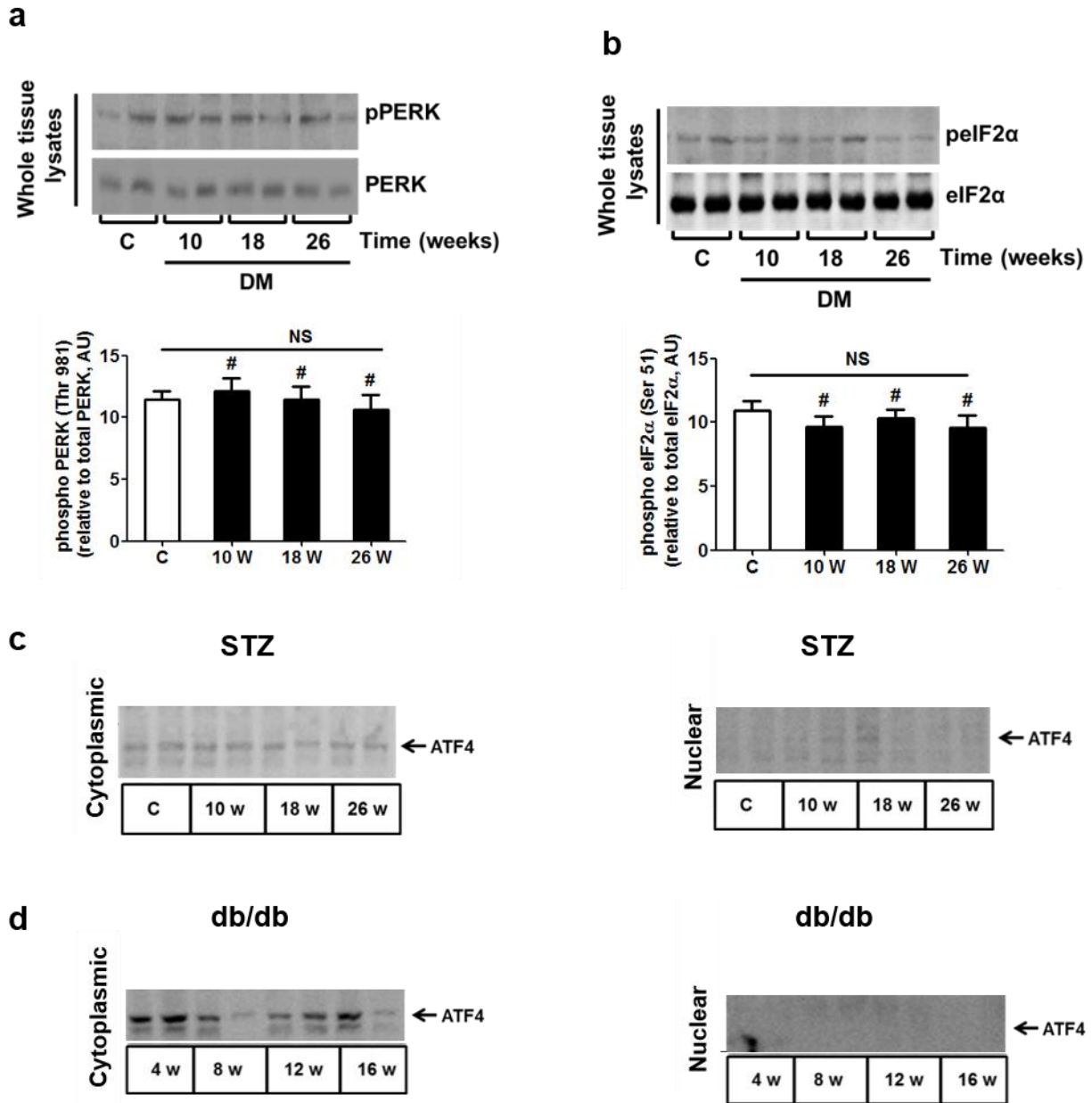


**Figure 11: Regulation of PERK-eIF2α activation and ATF4 expression in hyperglycemia**

Representative immunoblots (**a-b**) showing phosphorylated and total PERK (**a**, upper panel) and phosphorylated and total eIF2α (**b**, upper panel) and in renal cortex samples of wild type control (C) and STZ-induced diabetic mice (DM) at indicated time points post STZ administration. Bar graphs showing phosphorylated levels of PERK (**a**, lower panel) and phosphorylated levels of eIF2α (**b**, lower panel) in renal cortex samples of wild type control (C) and STZ-induced diabetic mice (DM) at indicated time points. Representative immunoblots (**c-d**) showing cytoplasmic levels and nuclear levels of ATF4 in renal cortex samples of wild type control (C) and STZ-induced diabetic mice (DM) at indicated time points post STZ

administration (c) or in db/db mice at ages indicated (d). Cytoplasmic levels of ATF4 remained unchanged and nuclear levels were undetectable. w: weeks; Mean  $\pm$  SEM, (a, b, n = 6 mice per group).

#### 4.4. Hyperglycemia-induced maladaptive UPR is linked to dNP

To determine if hyperglycemia is a sufficient trigger for ER stress, diabetic mice were injected with a sodium-glucose co-transporter 2 inhibitor (SGLT2 inhibitor – dapagliflozin) 18 weeks post stable induction of hyperglycemia and disease onset, to normalize their blood glucose levels (**Fig. 12a, b**). As a positive control, and to evaluate potential therapeutic approaches to the maladaptive ER-stress response in dNP, diabetic mice were also treated with the chemical chaperone TUDCA to attenuate ER stress. Both SGLT2 inhibitor and TUDCA treatment normalized nuclear levels of sXBP1, ATF6 and CHOP and reduced albuminuria and extracellular matrix deposition in the glomeruli (**Fig. 12c-g**). *In vitro*, high-glucose treatment of podocytes and glomerular endothelial cells (GENCs) impaired nuclear translocation of sXBP1 and augmented expression of ATF6 (50kDa) and CHOP (**Fig. 12h-j**). This demonstrates that hyperglycemia selectively disrupts the IRE1-XBP1 arm of the UPR while activating the ATF6 and CHOP branches of ER Stress. Importantly, preventing excess hyperglycemia (SGLT2 inhibitor) or restoring ER homeostasis (TUDCA), both reinstated an adaptive unfolded protein response and alleviated experimental dNP.



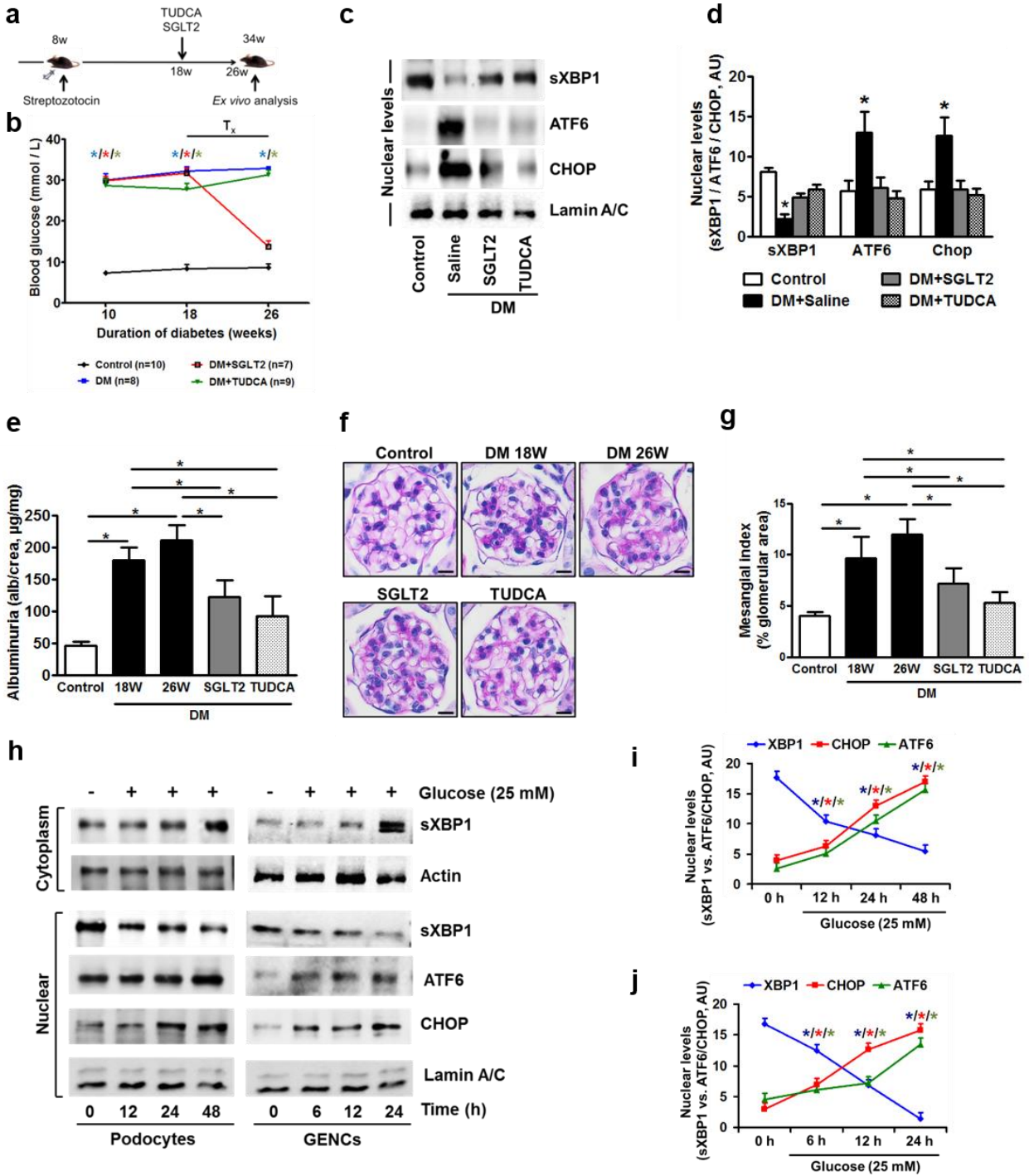


**Figure 12: Hyperglycemia-induced ER stress response is causally linked to dNP**

Schematic illustration of interventional studies in mice with STZ-induced hyperglycemia (a), treatment with a sodium–glucose co-transporter 2 (SGLT2) inhibitor or the chemical chaperone tauroursodeoxycholic acid (TUDCA) was initiated after manifestation of albuminuria at week 18 (a, b). Line graphs reflecting

blood glucose levels in mice with STZ-induced hyperglycemia. Blood glucose was measured at indicated time points. Treatment with the SGLT2 inhibitor dapagliflozin normalizes blood glucose levels, while TUDCA has no impact on the blood glucose levels. Tx: treatment period (**b**). Normalizing glucose levels or attenuation of ER stress normalizes nuclear levels of sXBP1, ATF6, and CHOP (**c**, **d**) and reduces albuminuria (**e**) and extracellular matrix deposition (**f**, **g**); C=control mice without diabetes, open bars; DM=diabetic mice, black bars; SGLT2 inhibitor: dapagliflozin treatment, grey bars; TUDCA treatment, dotted bars; scale bar represents (c: 20mm). Representative immunoblots showing cytoplasmic (**h**, top panel) and nuclear levels (**h**, lower panel) of ER transcription factors in immortalized mouse podocytes (left panel) and human glomerular endothelial cells (right panel) at indicated time points after treatment with high glucose (25 mM). Line graphs (**i**, podocytes and **j**, glomerular endothelial cells) representing the mean  $\pm$  SEM of 6 independent experiments; Mean  $\pm$  SEM, \* $P$ <0.05, \*\* $P$ <0.01 (**b**, **d**, **e**, **g**: one-way ANOVA).

#### 4.5. XBP1 protects against hyperglycemia-induced ER stress activation

The results obtained from the human tissues samples (**Fig. 8b**) and the mouse models of dNP indicate an important function of nuclear XBP1 in alleviating the indices of ER stress in the glomeruli. To scrutinize the functional relevance of XBP-1 for the ER-stress response, we next conducted lentiviral knockdown of XBP1 in podocytes. Reduced XBP-1 expression was sufficient for an upregulation of nuclear levels of ATF6 (50kDa) and CHOP as well as increased cell death in glucose-stressed podocytes *in vitro* (**Fig. 13a-c**). This indicates that XBP1 has a crucial function in maintaining ER homeostasis and protecting podocytes from ER stress induced cell death.

To study the relevance of XBP1 *in vivo*, we then employed a mouse model of STZ-induced hyperglycemia using mice in which XBP1 was specifically knocked out in podocytes (XBP1<sup>flox/flox</sup> x Pod<sup>Cre</sup>, **Fig. 13d**). In these mice, indices of dNP, such as albuminuria, extracellular matrix deposition and glomerular-basement membrane (GBM)-width, were markedly increased compared to wild type control mice, and the disease aggravation was associated with an upregulation of nuclear ATF6 and CHOP levels (**Fig. 13e-g**).

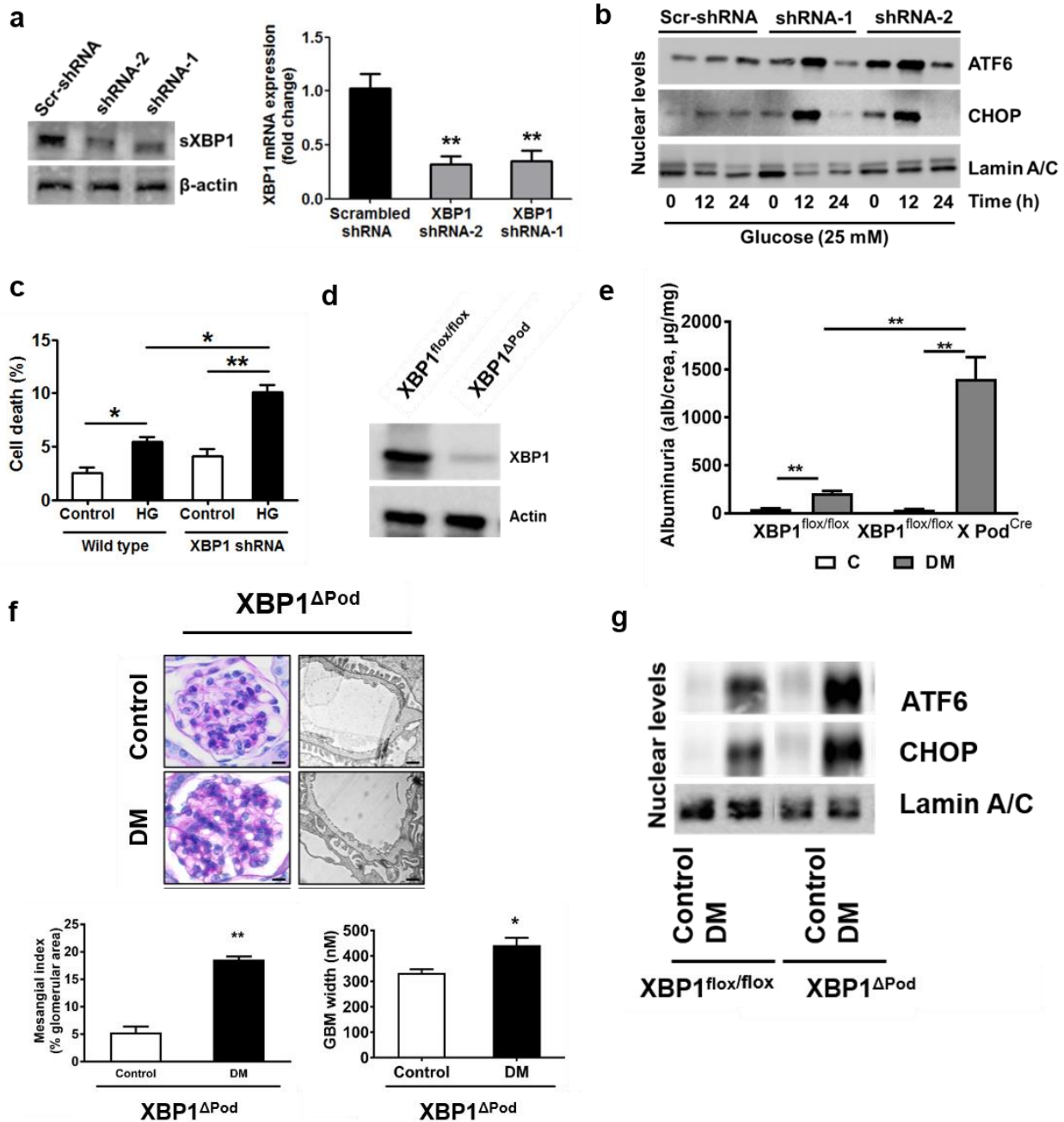


**Figure 13: Podocyte-specific loss of XBP1 promotes maladaptive UPR in dNP**

Representative immunoblot showing shRNA-mediated knockdown of XBP1 in immortalized mouse podocytes (a, left panel). Bar graph showing reduction of XBP1 expression in XBP1KD cell lines, as determined by qRT-PCR (a, right panel). Results for two independent shRNAs (shRNA-1 and -2) and a non-specific scrambled-shRNA (Scr-shRNA) are shown. Representative immunoblots showing nuclear levels of cleaved ATF6 and CHOP in immortalized mouse control (Scr-shRNA) and XBP1 knockdown (shRNA-1 and -2) podocytes at indicated time

points after treatment with high glucose (25 mM) **(b)**. Bar graph summarizing the frequency (mean  $\pm$  SEM of three independent experiments) of apoptotic cells as determined by TUNEL assay in immortalized mouse control and XBP1 knockdown (XBP1shRNA) podocytes 24 h after treatment with high glucose (25mM) **(c)**. Analyses of mice with podocyte-specific loss of XBP1 (XBP1 $\Delta$ Pod) compared with control mice (XBP1<sup>flox/flox</sup>) **(d-g)**. Representative immunoblot showing podocyte-specific complete deletion of XBP1 in podocytes isolated from XBP1 $\Delta$ Pod mice when compared with podocytes isolated from control mice (Xbp1<sup>flox/flox</sup>) **(d)**. Bar graph summarizing albuminuria **(e)**, representative images of extracellular matrix deposition **(f, top panel, PAS staining)** and the disrupted glomerular filtration barrier **(f, bottom panel, transmission electron microscopy, TEM)**, bar graphs reflecting extracellular matrix deposition (below, left), glomerular basement membrane thickness (below, right). Representative immunoblots **(g)** showing nuclear levels of ER transcription factors in renal cortex samples; (n=8 mice per group were analyzed, except for TEM **(f)** where n=3 mice per group were analyzed). C=control mice without diabetes, open bars; DM=diabetes, grey bars; scale bar represents **(f: 20mm for PAS stain, 2 mm for glomerular filtration barrier, TEM)**; Mean  $\pm$  SEM, \* $P$ <0.05, \*\* $P$ <0.01 **(a-c, e,f: t-test)**.

#### 4.6. p85-sXBP1 interaction in podocytes is required for the adaptive ER-stress response in dNP

In the aforementioned data we observed that the loss of XBP1 in podocytes causes a maladaptive UPR and augmentation of diabetic nephropathy. As regulation of sXBP1 nuclear translocation in the liver has been linked with insulin – p85 signaling, we next explored the potential role of insulin receptor - p85 signaling. To determine the pathophysiological relevance of the INSR – p85 pathway in dNP, we first analysed p85 $\alpha$  (PIK3R1) and p85 $\beta$  (PIK3R2) gene expression (mRNA levels) in a large human renal database (Nephromine). We analysed the gene expression (loss of function – under expression) in “Ju Podocyte” database. Gene expression of p85 $\alpha$  (PIK3R1) is slightly decreased ( $P=0.056$ ,  $t$ -test) and that of p85 $\beta$  (PIK3R2) markedly ( $P<0.001$ ,  $t$ -test) reduced **(Fig. 14a)**. Intriguingly, reduced p85 $\alpha$  and p85 $\beta$  gene expression was only observed in renal glomeruli but not in the tubulointerstitial compartment **(Fig. 14b)**. In contrast, when interrogating overexpression glomerular specific-total XBP1 mRNA was upregulated in patients with dNP when compared to healthy controls ( $P=0.007$ ,  $t$ -test) **(Fig. 14a, lower panel)**, similar to our observation made in db/db mice **(Fig. 14c)**. Importantly, the data obtained from nephromine reflect total XBP1 mRNA levels and preclude any conclusions regarding XBP1 splicing or nuclear translocation of sXBP1. To analyse mRNA levels of total-XBP1 and sXBP1 we performed quantitative qRT-PCR in renal cortex samples from

murine dNP. These data show that total XBP1 and sXBP1 expression was not significantly altered in STZ-treated mice (26 weeks post-STZ) when compared to non-diabetic control mice (**Fig. 14d**). These data demonstrate that sXBP1 nuclear translocation is impaired independent of its total expression in dNP (**Fig. 8b**).

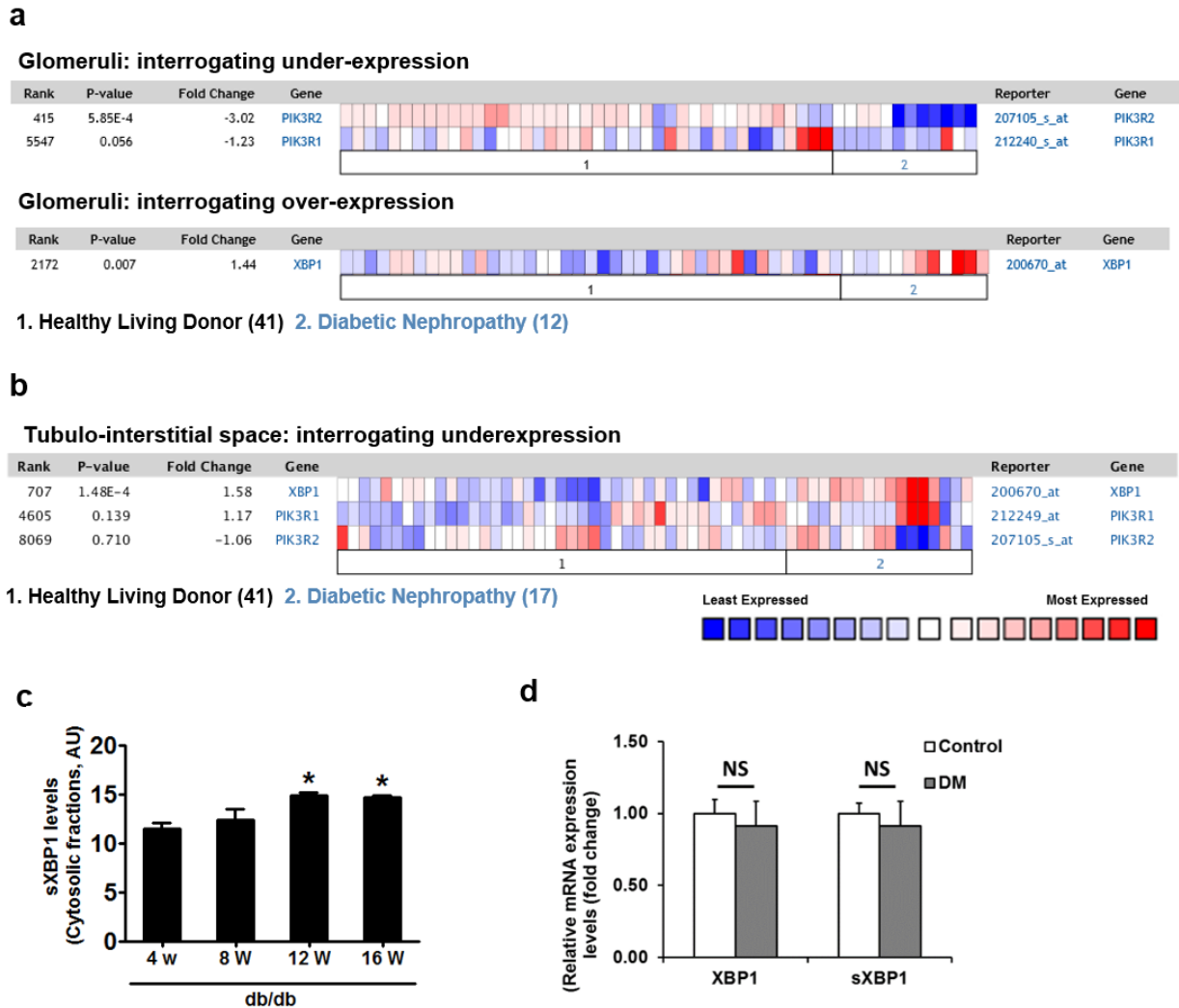


**Figure 14: Impaired sXBP1-p85 interaction in human and murine dNP**

Analyses of glomerular specific expression of p85 $\alpha$  (PIK3R1), and p85 $\beta$  (PIK3R2) and XBP1 in human healthy living donors (n = 41) and patients with diabetic nephropathy (n = 17). Heat map obtained from “Ju Podocyte” group from Nephromine, showing the glomerular specific gene expression levels of p85 $\alpha$  (PIK3R1), p85 $\beta$  (PIK3R2) (**a**, upper panel) and XBP1 (**a**, lower panel) in human healthy living donors (n = 41) and patients with diabetic nephropathy (n = 12). *P*-values shown reflect results if interrogating the Nephromine database for under expression (PIK3R1 and PIK3R2) or over expression (XBP1). Heat map obtained

from “Ju Podocyte” group from Nephromine showing tubulointerstitium specific gene expression levels of XBP1, p85 $\alpha$  (PIK3R1), and p85 $\beta$  (PIK3R2) in human healthy living donors (n = 41) and patients with diabetic nephropathy (n = 17) (**b**). *P*-values shown reflect results if interrogating the Nephromine database for over expression. Bar graphs showing cytoplasmic levels of ER transcription factor, sXBP1 in renal cortex samples of db/db mice at ages indicated (**c**). Bar graph showing relative mRNA expression levels of total (XBP1) and spliced (sXBP1) levels in renal cortex samples from untreated (white bars) and STZ-treated (grey bars) mice (**d**). Mean  $\pm$  SEM, (n = 6 mice per group for **c**; n = 5 independent mice per group, NS: not significant).

Next we determined the interaction of sXBP1 and p85 $\alpha$  or p85 $\beta$  in human renal biopsies (**Fig. 15a**) by PLA. Both p85 $\alpha$  - sXBP1 and p85 $\beta$  - sXBP1 complexes were significantly reduced in renal biopsies from dNP patients compared to non-diabetic controls. Furthermore, *in vitro* treatment of podocytes with high glucose reduced interactions of p85 $\alpha$  and p85 $\beta$  with sXBP1 in a time dependent manner as was determined by immunoprecipitation experiments (**Fig. 15b**). To gain further mechanistic insights, we conducted *in vitro* studies. First, we observed that insulin promoted nuclear translocation of sXBP1 in podocytes (**Fig. 15c**). To investigate whether insulin-induced nuclear translocation of sXBP1 was dependent on its canonical activation pathway regulated by IRE1 $\alpha$  phosphorylation, podocytes were treated with 100 nM of insulin. While it induced nuclear translocation of sXBP1, it failed to induce IRE1 $\alpha$  phosphorylation indicating that insulin-mediated sXBP1 nuclear translocation is independent of IRE1 $\alpha$  activation.

To determine the *in vivo* relevance of insulin signaling in podocytes for sXBP1 – p85 heterodimerization and nuclear sXBP1 translocation, a mouse model with podocyte-specific deletion of INSR was generated. Nuclear localization of sXBP1 was absent in the glomeruli of mice with defective insulin signaling compared to non-diabetic wild type mice (**Fig. 16a**), a finding in agreement with impaired sXBP1 - p85 heterodimerization in human patients with dNP (**Fig. 15a**). Similar to *in vitro* experiments, diabetic mice lacking p85 $\alpha$  specifically in podocytes (p85 $\alpha^{\Delta\text{Pod}}$ ) or whole body p85 $\beta$  knockout mice (p85 $\beta^{-/-}$ ) demonstrated severely impaired nuclear translocation of sXBP1, while nuclear ATF6 and CHOP were increased in these mice to a comparable extent as observed in diabetic INSR $\Delta\text{Pod}$  (**Fig. 16b-d**). These

results demonstrate that INSR-p85-sXBP1 regulates an adaptive UPR response in dNP.

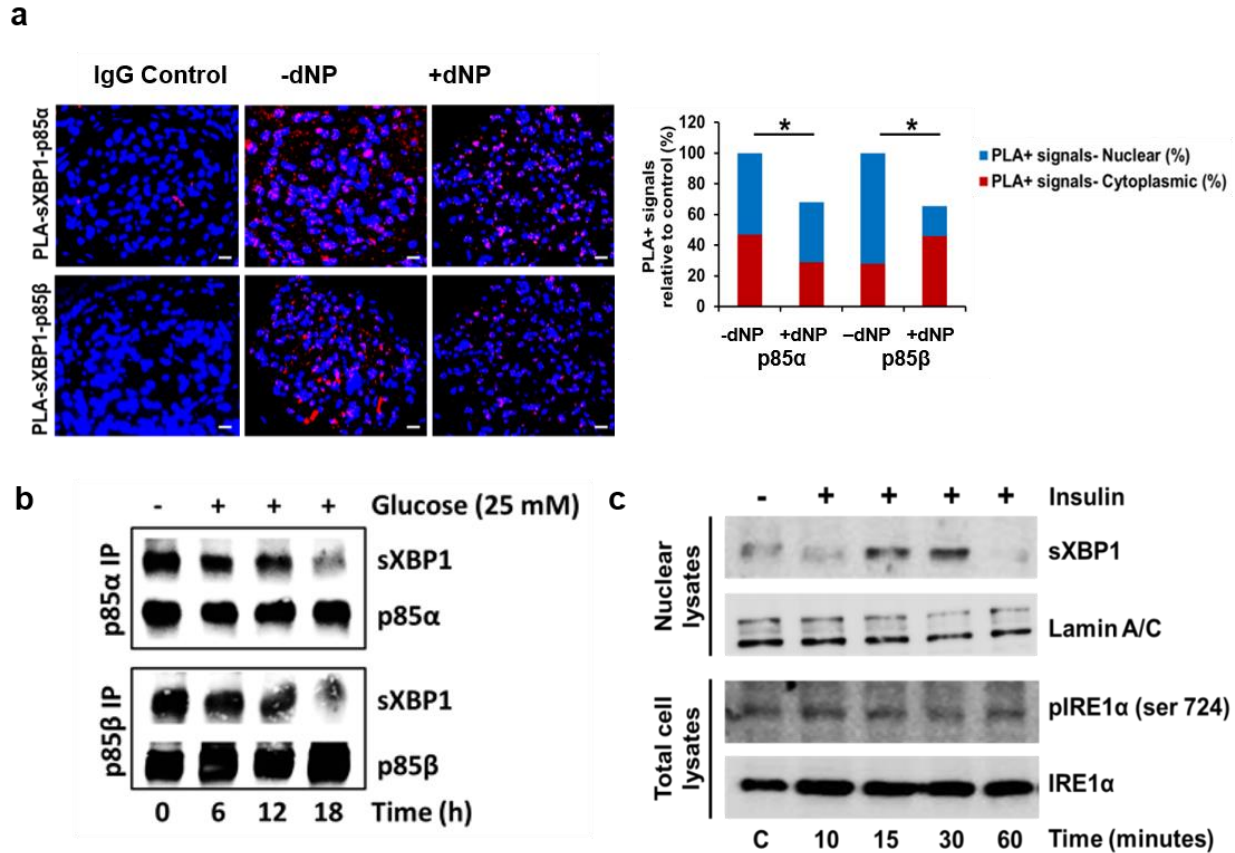


**Figure 15: Insulin signals via INSR-p85 axis independent of IRE1α phosphorylation in podocytes**

Representative images showing protein complexes (red) of sXBP1-p85α (a, upper panel) and sXBP1-p85β (a, lower panel) analyzed by proximity-ligation assay (PLA) in renal biopsies obtained from diabetic humans without (-dNP) or with (+dNP) diabetic nephropathy. Frequency of nuclear and cytoplasmic protein complexes of 5 samples per group were summarized as bar graphs. Scale bar represents (c: 20 μm). Representative immunoblots of immunoprecipitates showing binding of sXBP1 with p85α and p85β in immortalized human podocytes after treatment with high glucose (HG 25mM) at indicated time points (n = 3, independent repeat experiments)(b). Insulin promotes nuclear translocation of sXBP1 in mouse podocytes independent of IRE1α phosphorylation. Representative immunoblot showing nuclear levels of sXBP1 and total levels of IRE1α and phosphorylated form of IRE1α (ser-724) after treatment with insulin (100 nM) at indicated time points. Lamin A/C used as loading control for nuclear lysates (c). Mean ± SEM (a), \* $P < 0.05$ , \*\*  $P < 0.01$  (one-way ANOVA).



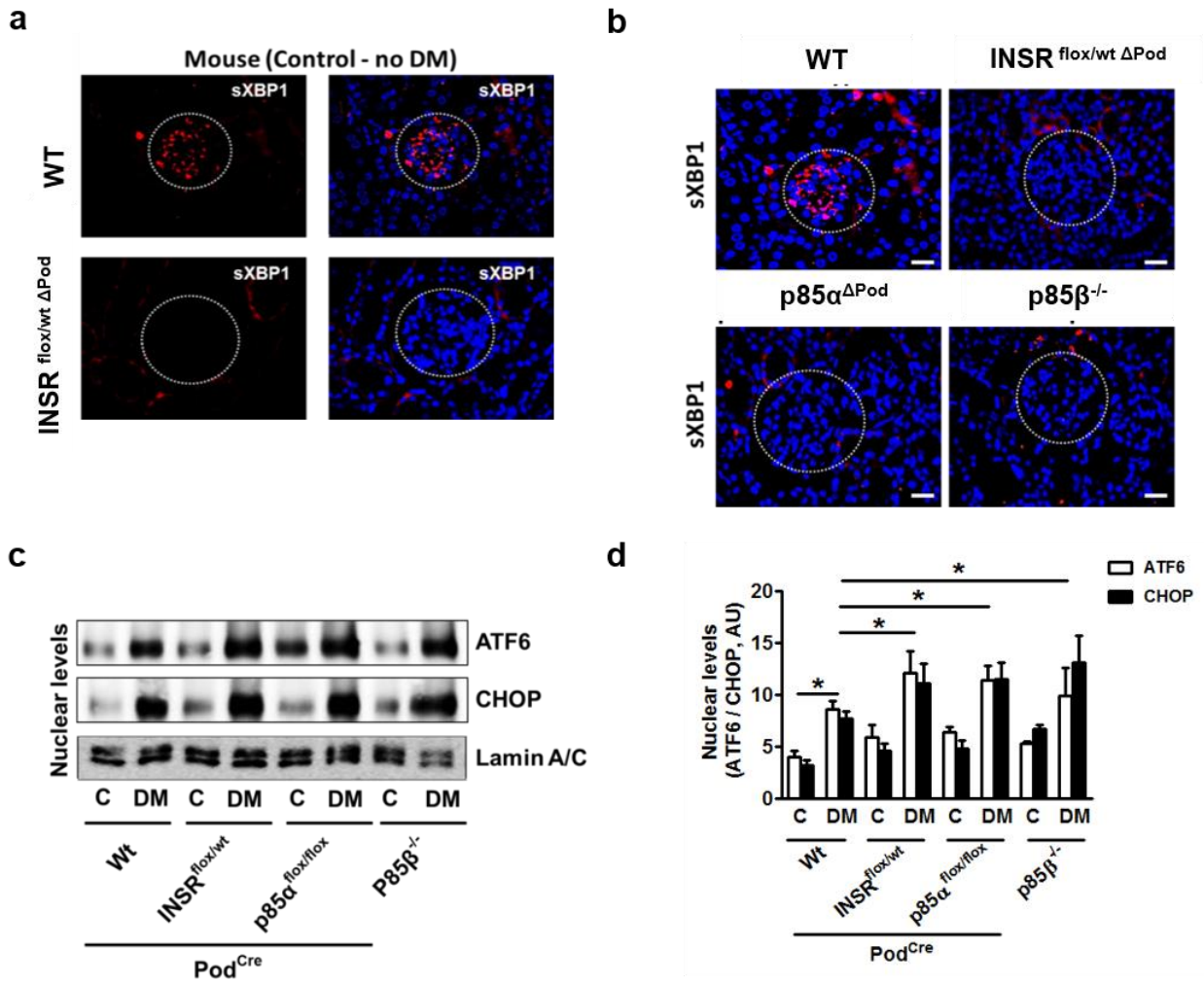


**Figure 16: Signaling via INSR-p85 axis in podocytes conveys an adaptive ER stress response in dNP**

Representative images at low magnification (20x) showing renal immunofluorescent detection of sXBP1 in control mice (wild type, top panel) and mice with podocyte specific deletion of insulin receptor in podocytes ( $INSR^{flox/Wt \Delta Pod}$ , lower panel). sXBP1 (red) is predominately observed in glomeruli (white dotted line) of wild type mice, but not of  $INSR^{flox/Wt \Delta Pod}$  mice (a). sXBP1 is only sparsely detected in the tubulointerstitial space. Representative images showing sXBP1 levels (using an antibody detecting the spliced form of XBP1, in the renal glomeruli of non-diabetic wild type mice and mice with podocyte specific deletion of insulin receptor ( $INSR^{flox/Wt \Delta Pod}$ ) or p85 $\alpha$  (p85 $\alpha^{\Delta Pod}$ ), or whole body p85 $\beta$  deficiency (p85 $\beta^{-/-}$ ) (b). Representative immunoblots (c) and bar graph (d) showing nuclear levels of ER transcription factors in renal cortex samples (n = 8 mice per group were analyzed). C: Control mice without diabetes, open bars; DM: diabetes, black bars. Mean  $\pm$  SEM (g), \*  $P < 0.05$ , \*\*  $P < 0.01$  (one-way ANOVA).



#### 4.7. TM – PC signaling regulates UPR

We have previously shown that hyperglycemia impairs endothelial thrombomodulin – dependent aPC formation resulting in the loss of cytoprotective signaling in the glomerular compartment causing cell death and diabetic nephropathy<sup>104</sup>. Since treatment with aPC conveys protection from diabetic nephropathy in various animal models<sup>105</sup>, we evaluated whether endogenous PC activation can regulate UPR in dNP. We analyzed mice with STZ induced persistent hyperglycemia and either loss (secondary to impaired PC activation,  $TM^{Pro/Pro}$ ) or gain (transgenic mice expressing a hyperactivatable PC-variant,  $APC^{high}$ ) of function within the TM-PC system (**Fig. 17a**). Compared to wild type mice, impaired PC activation in  $TM^{Pro/Pro}$  mice aggravated the maladaptive renal UPR, characterized by impaired nuclear translocation of sXBP1 and heightened nuclear ATF6 and CHOP levels (**Fig. 17b-e**). These changes were associated with aggravated dNP indicated by increased albuminuria, loss of differentiated podocytes indicated by decreased number of WT-1 positive cells in the glomeruli as well as the reduced expression of nephrin and podocin protein levels in the renal cortex of wild-type and  $TM^{Pro/Pro}$  STZ injected mice (**Fig. 17f-i**). The dNP phenotype is more pronounced in the  $TM^{Pro/Pro}$  mice than in wild-type. Conversely, in  $APC^{high}$  mice nuclear levels of sXBP1 were normal, expression of ATF6 and CHOP were reduced, and mice were protected from dNP despite persistent hyperglycemia (**Fig. 17b-e**). Restoring aPC levels in  $TM^{Pro/Pro}$  mice by crossing  $TM^{Pro/Pro}$  with  $APC^{high}$  mice or relieving ER-stress in  $TM^{Pro/Pro}$  mice using TUDCA reduced albuminuria and the maladaptive ER-response (**Fig. 17f, i**). These data identify a function of TM-dependent PC activation in controlling ER-response-patterns in the glomerular compartment and suggest that aPC– similar to insulin – can modulate the UPR in dNP.

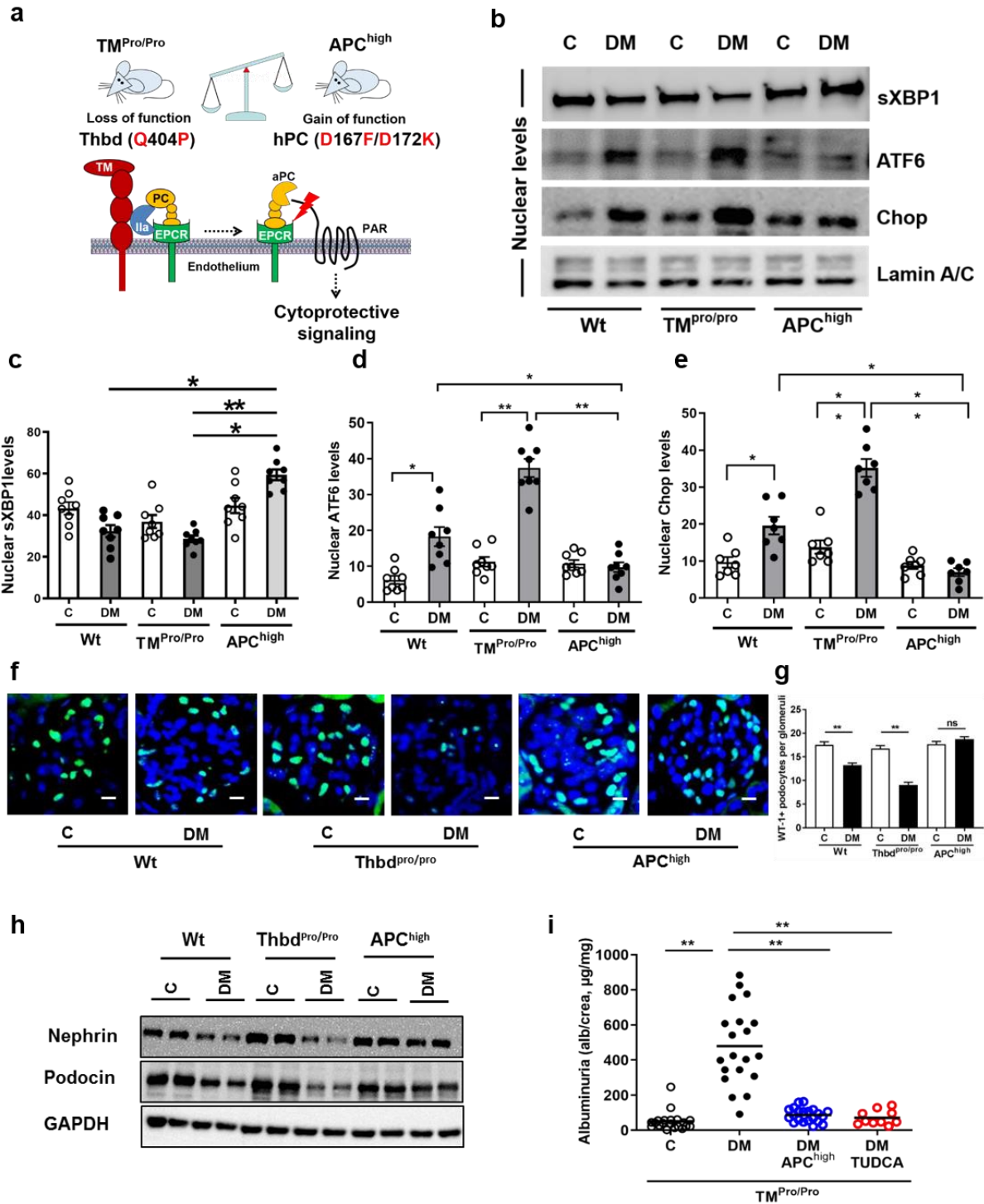


**Figure 17: Thrombomodulin – dependent PC activation regulates UPR in dNP**

Schematic illustration of TM - dependent PC activation on endothelial cells and of molecular defects in employed mouse models with altered TM - dependent PC activation (**a**). Representative immunoblots (**b**) and bar graphs (**c-e**) showing nuclear levels of ER transcription factors in renal cortex samples 26 weeks post STZ-treatment. Representative immunofluorescent images for WT-1 (green) and nuclear DAPI stain (blue) in glomeruli (**f**), bar graph reflecting the number of WT-1

positive podocytes (**g**), and representative immunoblots reflecting nephrin and podocin expression in mouse renal cortex samples (**h**). Restoring aPC levels or inhibiting ER-stress with the chemical chaperone TUDCA protects TM<sup>Pro/Pro</sup> mice against dNP. Dot plot summarizing albuminuria (**i**). C, Control mice without diabetes; DM: diabetic mice; Mean  $\pm$  SEM, n = 6 mice per group(**c-e, h**) and 8 mice per group (**i**); \* $P$ <0.05, \*\* $P$ <0.01 (**c-e, g, i**: one-way ANOVA).

#### **4.8. Activated protein C rescues maladaptive UPR response in mice models of defective insulin signaling**

Since INSR-p85-sXBP1 signaling axis is essential for adaptive UPR response, mice lacking insulin receptor (INSR) in podocytes develop exacerbated dNP, characterized by increased albuminuria, GBM width, extracellular matrix deposition (FMA) and all other indices of dNP (**Fig. 18a-d**). These changes were associated with impaired nuclear translocation of sXBP1 and heightened ATF6-CHOP dependent maladaptive ER-response (**Fig. 18h**). Similar to insulin, aPC signaling via G-protein coupled receptors are known to engage – among others – PI3K signaling pathway, we speculated that aPC may compensate for impaired insulin signaling in podocytes. To this end, we crossed transgenic overexpression of aPC (APC<sup>high</sup> mice) with mice lacking the insulin receptor in podocytes (INSR $\Delta$ Pod mice) or treated INSR $\Delta$ Pod mice with aPC after the onset of persistent hyperglycemia (starting 18 weeks post-STZ, **Fig. 18a**). Overexpressing aPC or injection of aPC into mice with impaired insulin signaling in podocytes resulted in the improvement of pathophysiological manifestation of dNP with decreased albuminuria, GBM width, reduced deposition of extracellular matrix, increase in number of differentiated podocytes in the glomeruli indicated by higher number of WT-1 positive podocytes as well as increased protein expression of nephrin and podocin in the renal cortex (**Fig. 18b-g**). Both interventions restored nuclear sXBP1 levels and prevented the maladaptive ER- response initiated by ATF6 and CHOP in diabetic INSR $\Delta$ Pod mice (**Fig. 18h**), verifying the role of aPC in restoring defective insulin signaling.

We next used a model of obesity induced defective insulin signaling (db/db mice). Db/db mice are a model of T2DM which develop insulin resistance following hyperlipidimia, hyperinsulimia and obesity. To test if aPC would be able to improve the indices of dNP

resulting from insulin resistance, db/db mice were treated with aPC or TUDCA starting at an age of 16 weeks (**Fig. 19a-e**).

To test if aPC's cytoprotective adaptive UPR signaling is independent of its function as an anticoagulant, aPC was pre-incubated with the monoclonal antibody (HAPC1573), which specifically blocks aPC's anti-coagulant function. Treatment of db/db mice with the aPC lacking anticoagulant function did not impede its nephroprotective and UPR-reprogramming effects (**Fig. 19c-h**). aPC and the chemical chaperone TUDCA restored nuclear sXBP1 while averting the ATF6-CHOP (**Fig. 19f-h**) mediated maladaptive UPR in db/db mice. Treating these mice with aPC or TUDCA had no significant effects on blood glucose levels (**Fig. 19b**) demonstrating that normalizing ER-function is sufficient to avert dNP. In both mice models of defective insulin signaling, aPC reprograms the UPR and conveys nephroprotection.

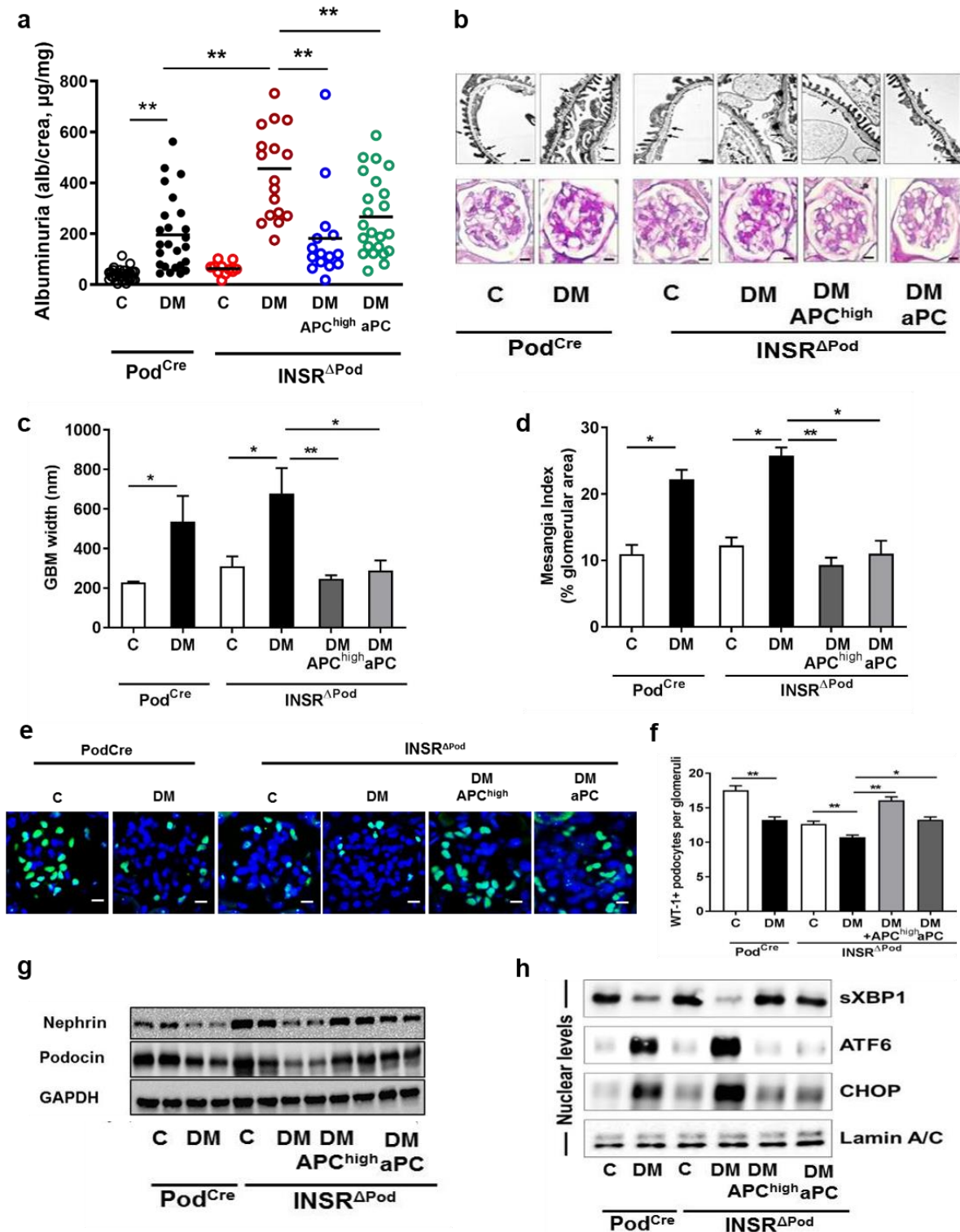


**Figure 18: Activated PC rescues defective insulin signaling**

Dot plot summarizing albuminuria (a), representative images showing (b, upper panel, transmission electron microscopy, TEM; GBM: glomerular basement membrane, arrows; scale bar: 2µm) and bar graph of the glomerular filtration barrier width (c), representative images (b, lower panel, scale bar: 20µm) and bar

graph showing extracellular matrix deposition (**d**). Representative immunofluorescent images for WT-1 (green) and nuclear DAPI stain (blue) in glomeruli (**e**) and bar graphs summarizing the number of WT-1 positive podocytes (**f**). Representative immunoblots reflecting nephrin and podocin expression (**g**) in whole renal cortex, and nuclear levels of ER transcription factors (**h**) in mouse renal cortex samples from non-diabetic and diabetic  $INSR^{\Delta Pod}$  mice with aPC treatment and in  $INSR^{\Delta Pod}$  with transgenic overexpression of aPC ( $APC^{high}$ ). C, Control mice without diabetes; DM: diabetic mice; Mean  $\pm$  SEM of at least 15 (**a**), 10 (**c-d**), or 8 (**e-f**) mice per group; scale bar: 20  $\mu$ M \* $P$ <0.05, \*\* $P$ <0.01 (**c-f**: one-way ANOVA).

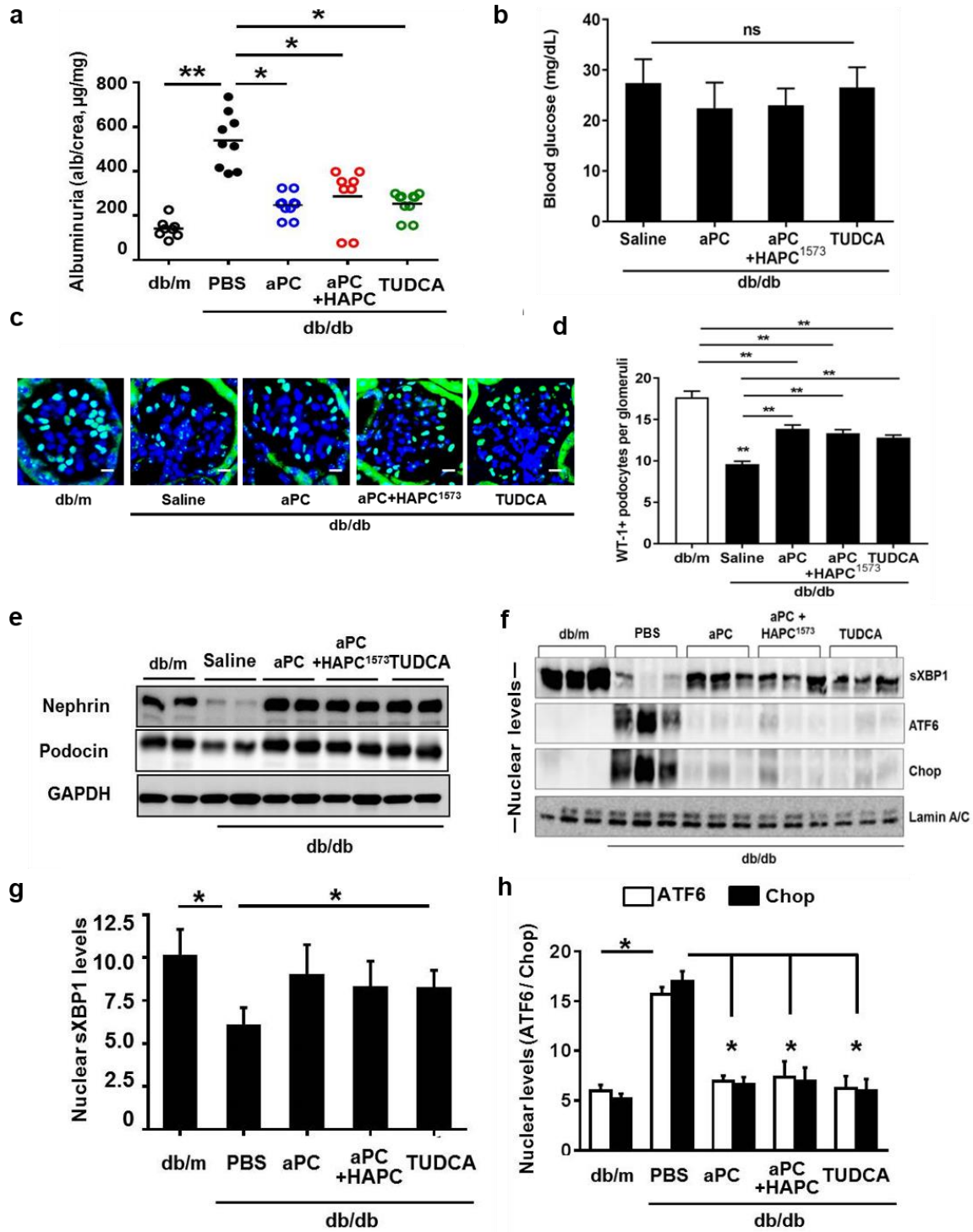


**Figure 19: Activated PC rescues defective insulin signaling in dNP**

Dot plot summarizing albuminuria (**a**), and representative bar graphs summarizing blood glucose levels in db/db mice without or with interventions (**b**). Markers of diabetic nephropathy in db/m control and db/db mice without or with interventions to restore aPC levels (aPC or aPC+HAPC<sup>1573</sup> or the chemical chaperon TUDCA);

representative immunofluorescent images for WT-1 (green) and nuclear DAPI stain (blue) in glomeruli (**c**), and bar graph reflecting the number of WT-1 positive podocytes (**d**). Representative immunoblots reflecting nephrin and podocin expression in whole renal cortex samples (**e**), and nuclear levels of ER transcription factors (**f**) in mouse renal cortex samples from db/db mice post treatment with PBS (vehicle), aPC, aPC + HAPC<sup>1573</sup>, or TUDCA. db/m: Control mice without diabetes; aPC+HAPC<sup>1573</sup>: aPC pre-incubated with the monoclonal HAPC<sup>1573</sup> antibody. Bar graphs (**g**, **h**) summarizing quantification of immunoblot (**f**), mean  $\pm$  SEM of at least 6 (**g**, **h**) or 8 (**b**) mice per group; \* $P$ <0.05, \*\* $P$ <0.01 (**b-h**: one-way ANOVA), scale bar: 20  $\mu$ M(**c**).

#### 4.9. ER-homeostasis by aPC employs the INSR-p85-sXBP1 signaling axis

Given the remarkable nephroprotective and ER-homeostatic effect of aPC in insulin signaling deficient mice (STZ-induced INSR <sup>$\Delta$ Pod</sup> mice and db/db mice), we wanted to investigate aPC's mechanism in regulating stress-dependent physiological UPR in podocytes. Exposure of podocytes to aPC temporally induced nuclear translocation of sXBP1 independent of IRE1 $\alpha$  activation (**Fig. 20e**), while the nuclear levels of ATF6 and CHOP remained unchanged, similar to insulin's effect (**Fig. 20a**). Mouse aPC likewise temporally induced nuclear translocation of sXBP1 without affecting ATF6 and CHOP levels in resting podocytes (**Fig. 20a-d**). aPC temporally induced dissociation of p85 $\alpha$  and p85 $\beta$  and induced complex formation of p85 $\alpha$ /p85 $\beta$  with sXBP1 in resting podocytes (**Fig. 21a**). The lentiviral knockdown of p85 $\alpha$ /p85 $\beta$  in mouse podocytes, resulted in significantly reduced nuclear sXBP1 as determined by the ratio of nuclear and cytoplasmic fluorescent signal of sXBP1 (**Fig. 21b**). To ascertain the physiological relevance of aPC for UPR reprogramming via p85-dependent sXBP1 nuclear translocation *in vivo* APC<sup>high</sup> mice with conditional podocyte specific deletion of XBP1 (APC<sup>high</sup>  $\times$  XBP1 <sup>$\Delta$ Pod</sup>) or p85 $\alpha$  (APC<sup>high</sup>  $\times$  p85 $\alpha$  <sup>$\Delta$ Pod</sup>) or with constitutive p85 $\beta$  deficiency (APC<sup>high</sup>  $\times$  p85 $\beta$ <sup>-/-</sup>) were generated. Deletion of XBP1, p85 $\alpha$  or p85 $\beta$  in APC<sup>high</sup> mice had no effect on baseline albuminuria but abolished the renoprotective effect of aPC by eliciting the maladaptive UPR response, mirroring the response observed in diabetic INSR <sup>$\Delta$ Pod</sup> or db/db mice (**Fig. 21d-e**). Thus, insulin and aPC utilize the same signaling hub to maintain ER-homeostasis and to protect from dNP.



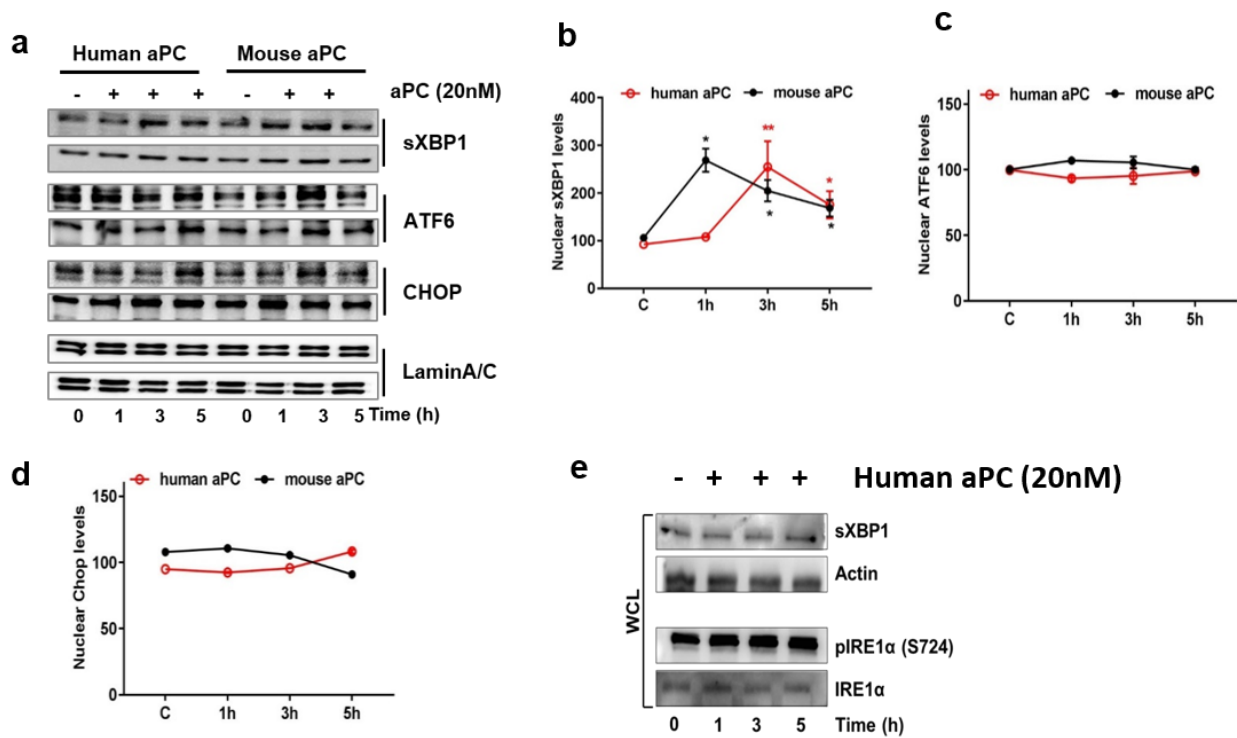


**Figure 20: Human and mouse aPC induce nuclear translocation of sXBP1**

Two exemplary immunoblots (**a**) and line graphs (**b-d**) showing nuclear levels of sXBP1, ATF6 and CHOP in wild type mouse podocytes after treatment with human aPC (20nM) or mouse aPC (20nM) at indicated time points. Representative immunoblots showing  $\beta$ -actin (loading control) and total XBP1 levels or phosphorylated IRE1 $\alpha$  in whole cell lysates (WCL) without or with aPC (20 nM) treatment at indicated time points (**e**). Mean  $\pm$  SEM of at least 3 independent repeat experiments (**a-e**); \* $P$ <0.05, \*\* $P$ <0.01 (**b-d**: t-test).

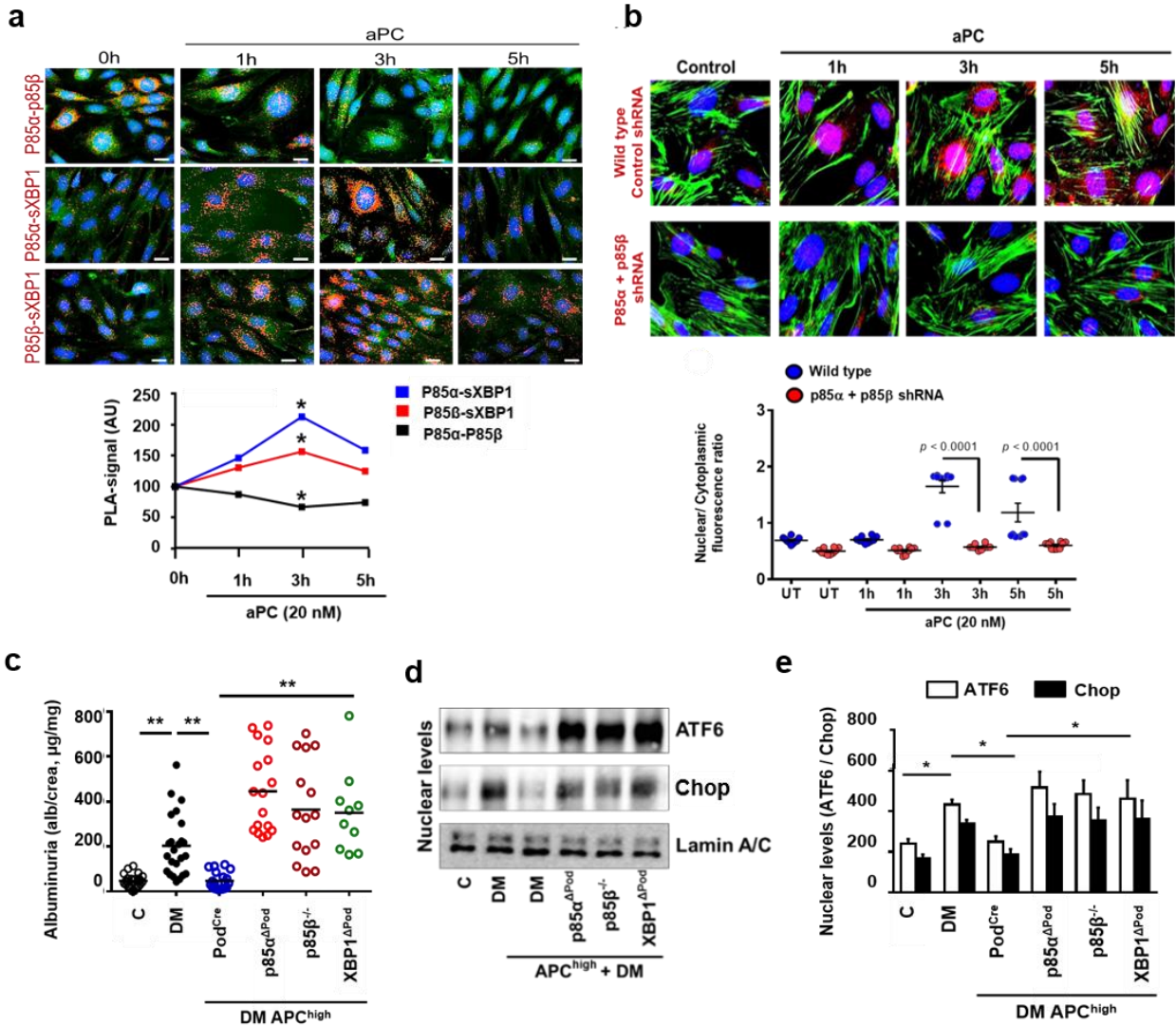


**Figure 21: UPR-reprogramming by aPC depends on p85-sXBP1 signaling**

Treatment with aPC dissociates p85α and p85β protein complexes (**a**, red, top), while promoting interaction of p85α or p85β with sXBP1 (middle and bottom, respectively). Representative immunofluorescence images showing protein complexes (red, proximity ligation assay, PLA). Corresponding line graphs (**a**, below) summarizing PLA positive signals (AU: arbitrary units). PLA complexes (red); nuclear stain DAPI (blue); actin cytoskeleton-phalloidin staining (green). Representative immunofluorescence images showing colocalization of sXBP1 (red) with nuclear DAPI stain (blue) and actin cytoskeleton (phalloidin: green) in wild type (control shRNA treated) and knockdown (p85α+p85β shRNA treated) mouse podocytes (**b**). When compared to control shRNA treated cells, p85α+p85β shRNA treated cells showed marked reduction in nuclear sXBP1 levels post aPC treatment. Dot plot (**b**, below) shows time-dependent nuclear cytoplasmic fluorescence ratio reflecting subcellular localization of sXBP1 following aPC treatments. dNP in APC<sup>high</sup> mice without (Pod<sup>Cre</sup>) or with podocyte specific p85α- or sXBP1- or constitutive p85β-deficiency. Dot plot summarizing albuminuria (**c**)

and representative immunoblots (d) and bar graph (e) showing nuclear levels of ER transcription factors in renal cortex samples. Mean  $\pm$  SEM of at least 3 independent repeat experiments (a-b) or at least 10 (c) or 8 (d-e) mice per group; \* $P$ <0.05, \*\* $P$ <0.01 (a-b: t-test; c, e: ANOVA).

#### 4.10. aPC signals through G-protein coupled receptors to induce UPR in podocytes

Insulin signals through INSR to stimulate the PI3K pathway and the lack of INSR in podocytes upregulates ER stress and induces cell death in dNP. In podocytes, aPC's cytoprotective effect requires PAR3<sup>118</sup>. aPC failed to promote nuclear translocation of sXBP1 in PAR3 knockdown podocytes establishing that PAR3 is required for aPC mediated UPR reprogramming in podocytes (Fig. 22a). PAR3 is considered signaling incompetent and requires PAR1 as co-receptor on murine podocytes<sup>111</sup>. Accordingly, PAR1 knockdown abolished aPC's effect on nuclear translocation of sXBP1 (Fig. 22b). Hence, the adaptive UPR induced by insulin and aPC employs the same intracellular signaling hub but structurally disjunct receptor mechanisms.

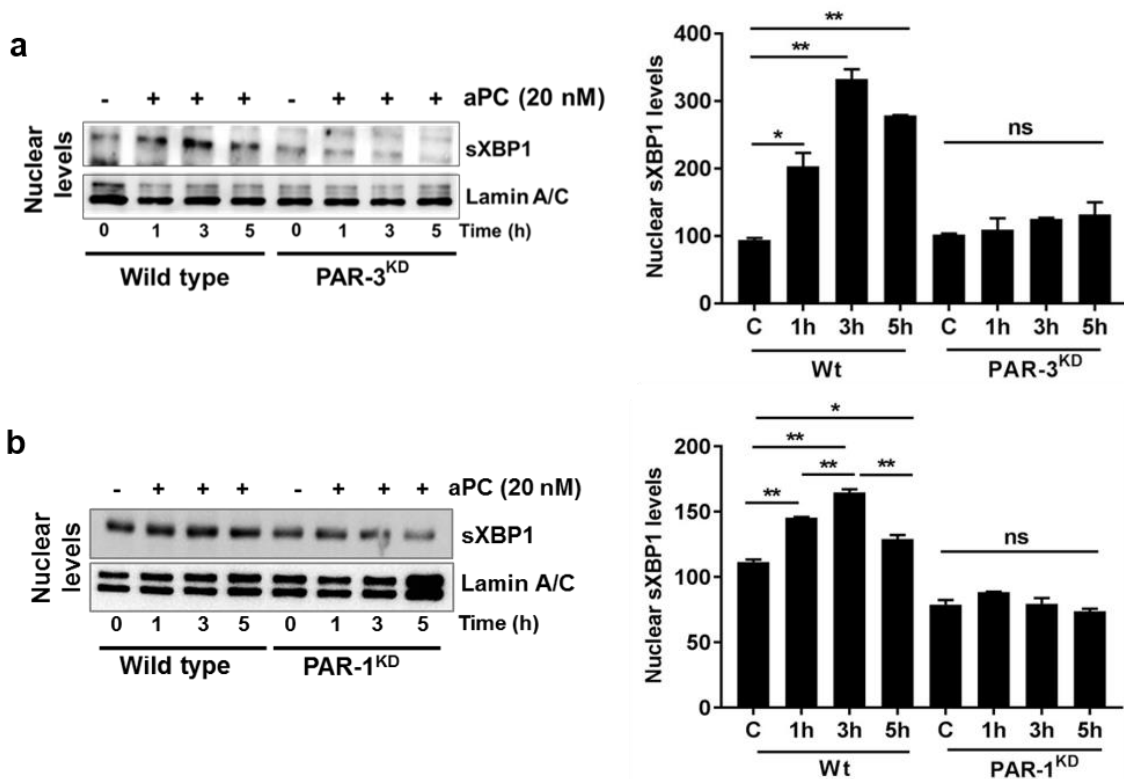


Figure 22: aPC induced nuclear translocation of sXBP1 requires both PAR-3 and PAR-1 receptors

Representative immunoblots and bar graphs showing nuclear levels of sXBP1 in wild type (Wt) and PAR-3 knockdown (PAR-3<sup>KD</sup>) (a), and in wild type (Wt) and PAR-1 knockdown (PAR-1<sup>KD</sup>) (b) mouse podocytes at indicated time points after treatment with aPC (20 nM). Mean ± SEM of at least 3 independent repeat experiments; \**P*<0.05, \*\**P*<0.01 (a, b: t-test).

#### 4.11. Insulin and aPC concordantly regulate XBP1-dependent gene-expression

Considering the signaling redundancy of insulin and aPC via XBP1 we hypothesized that aPC induces XBP1 target genes and intracellular pathways similar to insulin in podocytes. To this end we determined genome-wide XBP1 targeted genes by chromatin immunoprecipitation and whole genome sequencing (Chip-seq) in resting podocytes exposed to insulin or aPC (**Fig. 23a**). Analysis of sXBP1 enriched regions that cover 500 bp upstream and downstream of transcription start sites (TSS) of ~19000 known mouse genes revealed enrichment of agonist-specific (insulin: 344; aPC: 695) and overlapping (insulin + aPC: 1874) XBP1 targets (**Fig. 23b-e**). Filtering of concordant UPR genes revealed that both aPC and insulin typically enriched XBP1 at the proximal promoters of chaperones involved in protein binding and folding (Canx, Cct7, Edem1, Rpn1, Dnajb9, Erp44, Hspa5), components of ER-associated protein degradation (ERAD: Herpud1, Htra2, Vcp, Rfn5), transcription factors (Creb3, Srebf2 and ATF4) and the apoptotic regulator “Bax”<sup>147</sup> which in addition to mitochondrial dysfunction also modulates the UPR (**Fig. 23f**). To specifically determine the impact of sXBP1 enrichment on UPR regulation we performed UPR-pathway-specific expression analyses. Both aPC and insulin suppressed most XBP1-enriched genes while inducing Srebf2, a gene regulating cholesterol metabolism (**Fig. 23g**). Concomitant treatment of resting podocytes with insulin and aPC resulted in an additive induction of gene expression of only few genes (e.g. Sec63, UFD1), while in most cases gene expression remained the same (e.g. Dnajc3, Edem1, Eif2a) (**Fig. 23h**). This corroborates the conclusion that aPC and insulin induce gene expression largely through the same pathway. However, in contrast to insulin, aPC selectively induced components of ERAD (Htra2, Herpud1, Vcp), protein binding and folding (Rpn1, Canx, Cct7, Hspa2, Dnajb9, Erp44), and the transcription factor ATF4, emphasizing involvement of agonist-specific (aPC vs. insulin) regulatory mechanisms for ER-proteostasis. These data demonstrate that aPC and insulin *via* nuclear translocation

of sXBP1 target largely overlapping genes involved in the regulation of energy expenditure, metabolism, and ER-function in podocytes.

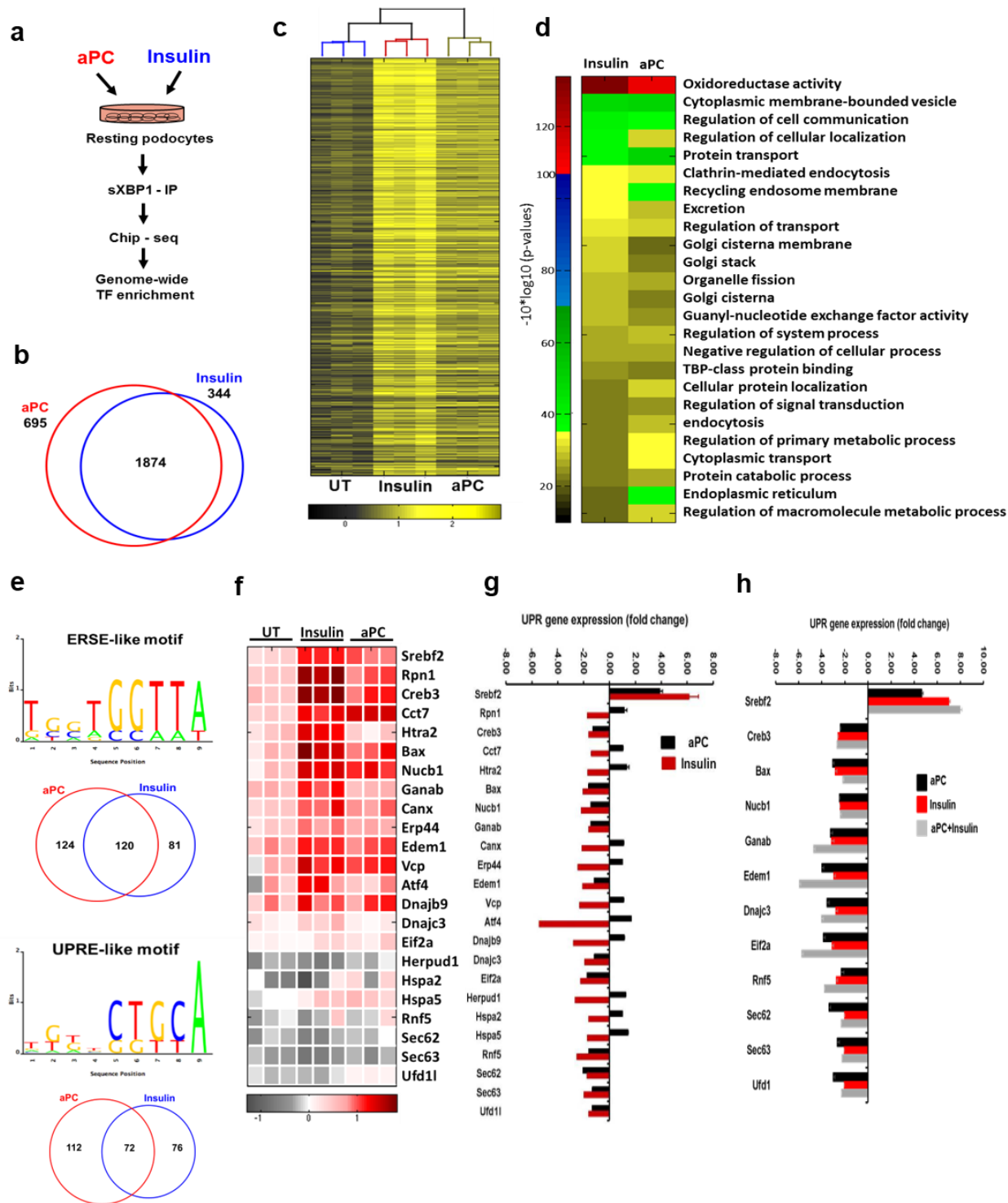


**Figure 23: Insulin and aPC-dependent XBP1 regulatory networks linked to UPR regulation**

Schematic illustration of methodology employed to identify homeostatic agonist-specific XBP1-targets (a). Venn diagram (b) and heat map (c) showing common genes that were significantly enriched after treatment with insulin or aPC versus

untreated (UT). Heat map showing condition-specific enriched pathways highly relevant for regulation of proteostasis (**d**). Candidate ERSE-like and UPR-like regulatory motifs that are overrepresented in UPR target promoters (**e**). Venn diagrams show respective condition-specific proportions. Heat map summarizes enrichment of condition-specific concordant UPR-genes (**f**), their impact on regulation of UPR-gene expression (**g**;  $n=3$ ; mean  $\pm$  SEM, untreated vs. insulin or aPC treated), and the impact of concomitant insulin and aPC treatment on UPR gene expression (**h**;  $n=3$ ; mean  $\pm$  SEM, untreated vs. insulin, aPC or insulin and aPC treated).

## 5. Discussion

### 5.1 Induction of the UPR and rescue of insulin signaling in podocytes in dNP

While the intimate relationship of DM and DKD is well-established, some studies have also demonstrated an association of the metabolic syndrome (hallmarked by impaired insulin signaling and insulin resistance) and an increased risk of kidney disease<sup>8,148</sup>. For DKD several mechanisms, such as increased ROS, inflammation, or altered adipokine levels have been proposed<sup>149-152</sup>, but mechanistic insights into impairment of renal function in association with the metabolic syndrome remained scarce at best. Our study establishes a direct mechanistic link between defective insulin signaling and impaired renal function. Insulin deficiency (STZ model, reflecting T1DM) or impaired insulin signaling (db/db model, reflecting T2DM) cause a maladaptive ER-stress response in podocytes through the dissociation of sXBP1 from the PI3K regulatory subunits, p85 $\alpha$  and p85 $\beta$ . The loss of this association inhibits nuclear sXBP1 translocation and the subsequent loss in activation of UPR chaperones leading to persistent and maladaptive ER-stress and eventually impaired kidney function (**Fig. 21f, g**). The disease progression, as indicated by increasing albuminuria, is closely associated with a progressive and maladaptive change in the molecular signature of the ER transcription factors (**Fig. 9c-g & 10 a-d**). This conclusion is supported by the results obtained in diabetic mice with a podocyte-specific knockout of the insulin receptor, mimicking the reduced insulin signaling seen in T2DM patients, who are insulin resistant and develop dNP even during normoglycemic conditions<sup>16</sup>. These results provide a strong rationale for the limited success of glycemic control to avoid DKD progression<sup>153,154</sup>. Beyond insulin's role in stimulating glucose uptake and metabolism, insulin signaling in podocytes maintains ER homeostasis. Therefore, improving blood glucose control is expected to only partially restore renal function, illustrating the need for new therapeutic approaches targeting cytoprotective signaling nodes as identified here in addition to restoring normoglycemia<sup>155</sup>.

The altered pathophysiological features are also evident in our analyses of non-diabetic  $INSR^{\Delta Pod}$  mice glomeruli, with slight but significantly elevated albuminuria when compared to non-diabetic wild type mice, with fewer WT-1 positive podocytes in the glomeruli and significantly reduced expression of podocin in the renal cortices indicating to a loss in



glomerular filtration barrier, suggesting a physiological function of insulin signaling in podocytes (**Fig. 18a, e-g**).

Manifestation of diabetic nephropathy has been associated with elevated levels of soluble thrombomodulin (reflecting endothelial dysfunction and impaired PC-activation) and reduced levels of aPC with vascular complications such as dNP. The current data identify a new and unexpected function of the coagulation system and in particular of the endothelial derived TM-aPC system. Using mouse models of dNP in mice with genetically impaired PC activation secondary to a targeted point mutation in the TM gene (**Fig. 17a**) we observed an aggravation of indices reflecting diabetic nephropathy in parallel to the increase in ER stress compared to the non-diabetic controls (**Fig. 17f-i**). Subsequently, when the TM<sup>Pro/Pro</sup> mice were crossed with transgenic mouse line with an aPC- gain of function (APC<sup>high</sup> mice), the indices of dNP were alleviated simultaneously with the induction of an adaptive UPR (increased levels of nuclear sXBP, reduced ATF6 and CHOP). The observations made in these genetic mouse models could result from the systemic genetic modifications in all cell types, particularly in the endothelial cells, and may not be specific to the glomerular compartment. It is quite possible that aPC does not need to be generated locally, but rather exerts a true hormone-like activity, improving glomerular function even if generated at distal sites. Importantly, the molecular fingerprint observed (**Fig. 17b-h**) in podocytes are characteristic of defective insulin signaling, corroborating the hormone-like activity of aPC in regard to renal ER-homeostasis. Additional analyses examining the insulin pathway and its impairment in the genetically impaired PC activation mouse model merits further investigation.

The serine-protease aPC conveys nephroprotective effects in animal models of acute and chronic kidney diseases<sup>104,105,131</sup>. In diabetic mice, aPC protects podocytes and glomerular endothelial cells from glucose induced dysfunction. aPC treatment restores nuclear sXBP1 levels and prevents the ATF6 and CHOP dependent maladaptive UPR in diabetic podocyte-specific insulin receptor floxed mice (**Fig. 18h**). The same effect is also observed in obesity induced insulin resistant db/db mice, resembling T2DM, when treated with aPC (**Fig. 19f**). The physiological relevance of aPC for UPR reprogramming via p85-dependent sXBP1 nuclear translocation *in vivo* was further confirmed in diabetic APC<sup>high</sup>

mice with conditional podocyte specific deletion of XBP1 or p85 $\alpha$  or with constitutive p85 $\beta$  deficiency (**Fig. 21c-e**).

Similar to aPC, the bile acid derivative and chemical chaperone TUDCA alleviated ER stress, simultaneously improving the indices of diabetic nephropathy in mice (**Fig. 19**). While the treatment with SGLT2 inhibitor normalized blood glucose levels in diabetic mice and ameliorated the glomerular features of dNP (**Fig. 12a-g**), it was not as effective a treatment as TUDCA or aPC (**Fig. 12, 18 & 19**), both of which restored adaptive UPR and protected the glomerular epithelial cells from the damaging effects of hyperglycemia. These data indicate, that glucose control with SGLT2 inhibitors, which are thought to convey additional nephroprotective effects, do not provide full or sufficient nephroprotection, but approaches restoring ER-homeostasis, such as aPC or chemical chaperons such as TUDCA, may constitute novel therapeutic approaches to dNP.

## **5.2 Glomerular filtration barrier is maintained by sXBP1 in podocytes**

The function of sXBP1 in the constitutive maintenance of ER function has been established<sup>156-159</sup>. Our study describes for the first time the requirement of XBP1 for maintaining homeostasis in glucose stressed renal cells (podocytes) (**Fig. 12 & 13**). Under normal physiologic conditions, the spliced form of XBP1 is known to be present at extremely low levels in tissues, including the liver<sup>94</sup>. The relative abundance of nuclear sXBP1 in non-diabetic glomeruli in our study (**Fig. 8b**) indicates a constitutive-homeostatic function of this UPR signaling arm and ER- transcription factor, raising questions about its underlying regulatory mechanisms in podocytes.

Genome-wide ChIP sequencing of sXBP1-targeted genes in resting podocytes revealed that both aPC and insulin (**Fig. 23**) typically enriched sXBP1 at the proximal promoters of chaperones involved in protein binding and folding, inhibition of global translation, ER-associated protein degradation machinery as well as some specific transcription factors such as Creb3, Srebf2 and ATF4. Erp44<sup>160</sup> is a ER chaperone necessary for proper folding of nascent proteins to be prepared for secretory purpose. This protein from the early secretory pathway (component of the ER-Golgi signaling) further implicates a function of podocytes as highly secretory cells. Thus, podocytes experience a constant,

yet physiologically normal ER burden intrinsically linked to their secretory nature<sup>161-163</sup>. Additionally, Erp44 has been shown to function as a redox-regulated trap for maintaining blood pressure during periods of systemic inflammation through regulation of the enzyme Erp1. Erp1 is known to regulate angiotensin II metabolism indicating local regulation of the renin-angiotensin system<sup>164</sup>. Erp1 was another sXBP1 targeted gene identified in the genome-wide ChIP sequencing in podocytes<sup>165</sup>. Thus, the ChIP sequencing data points not only to an important role of podocytes as secretory cells but possibly to a mode of intercellular communication through secretion of factors that regulates cellular homeostasis within the glomeruli. An important caveat is that ChIP sequencing was not performed on podocytes exposed to high glucose. Yet, the *in vivo* models of DM highlighted the critical function of nuclear sXBP1 in maintaining podocyte homeostasis in dNP (**Fig. 13-21**).

While we didn't observe an induction of the PERK-eIF2 $\alpha$  pathway in the renal cortices of the diabetic mice (**Fig. 11**), ChIP sequencing analysis in podocytes showed that sXBP1 was enriched at the promoter region of the ATF4 gene (**Fig. 23f, g**). Interestingly, we did not detect nuclear ATF4 in the renal cortex lysates of diabetic mice (**Fig. 9c, 11c, d**). Since, both sXBP1 and ATF6 are already known to regulate each other's expression and functions<sup>71-73</sup>, it wouldn't be surprising if ATF6 and sXBP1 together or individually interact with ATF4 regulating its stability. ATF4's nuclear function as a transcription factor could be dependent on its crosstalk with the other two arms of the UPR. Additionally, we detected transcriptional regulation of various components of the ubiquitin-dependent proteasome by insulin and aPC in our Chip-seq data. ATF4 is known to associate and colocalize with the  $\beta$ -transducin repeat-containing protein ( $\beta$ TrCP), part of the Skp1/Cullin/F-box protein (SCF) ubiquitin ligase complexes that tightly regulates its stability and its transcriptional activity in the nucleus<sup>166</sup>. Further examination of nuclear lysates from diabetic renal cortices treated with MG132 would help shed light on why we failed to detect changes of ATF4 in the nucleus. MG132, a proteasome inhibitor, would increase the stability of any ubiquitin-conjugated ATF4. ATF4, which, is a key regulator of mitochondrial unfolded protein response (UPR<sup>Mt</sup>) as well as integrated stress response (ISR) in mammalian cells<sup>167</sup>, is known to activate the expression of cytoprotective genes that reprogram cellular metabolism through mitochondrial stress response. Thus,

stimulation of the mitochondrial UPR and stress response through the activation of ATF4 could be a secondary response of the podocytes to hyperglycemia-induced ER stress.

Both aPC and insulin induce *Srebf2*<sup>168</sup>, a gene regulating cholesterol metabolism, lipid biosynthesis, glucose and fatty acid metabolism (**Fig. 23f-h**). The transcriptional regulation of *Srebf2* and other lipid biosynthetic enzymes and scaffold proteins such as acylCoA synthase (*Acsl*), and Syntaxin 17 (*Stx17*)<sup>169</sup>, point to a potential role of aPC and insulin in regulating proteins that are localized at the mitochondria-associated membranes (MAMs)<sup>170</sup>. Concomitant treatment of resting podocytes with insulin and aPC resulted in an additive induction in the expression of only few genes e.g. *Sec63*, *UFD1*, involved in the transport of precursor polypeptides across the ER lumen as well as ubiquitin-dependent proteolytic pathway (**Fig. 23h**). Control of protein modifications and transportation further underscores that ER- signaling and its regulation in podocytes is essential in maintaining physiological function as a glomerular barrier. The results from the expression analyses corroborate the finding that aPC and insulin induce gene expression *via* nuclear translocation of sXBP1 targeting largely overlapping genes involved in the regulation of ER-homeostasis in podocytes.

Advances in our understanding of podocyte biology from various studies<sup>171-176</sup> have yielded transformative insights regarding glomerular function in health and disease. Therefore, investigating differential transcriptional, proteomic, and metabolomics signatures of podocytes in health and disease will be essential for the identification of novel pathophysiological pathways and molecules contributing to the variability of disease progression, providing new insights into potential novel therapeutic and diagnostic avenues<sup>177,178</sup>.

## 6. Conclusion

Our study establishes a direct mechanistic link between defective insulin signaling in podocytes and impaired kidney function. Furthermore, our investigations have established a common intracellular signaling hub for insulin and a coagulation protease, aPC, which can be exploited for the development of new therapeutic approaches. The maladaptive ER-response in dNP is characterized by a disparate regulation of the tripartite-UPR, which is mechanistically linked to glomerular dysfunction and hallmarked by impaired sXBP1 nuclear translocation and enhanced ATF6 and CHOP signaling. The genetic ablation or functional inactivation of this pathway in murine models of T1DM (lack of insulin) or T2DM (impaired insulin signaling secondary to insulin resistance) promote a maladaptive UPR. Signaling *via* the XBP1 – branch of the UPR is required for adaptive and cytoprotective ER-response in podocytes under hyperglycemic stress. We uncovered that impaired cytoprotective signaling via the XBP1 branch in dNP can be rescued by aPC. Exposure of podocytes to aPC temporally induces nuclear translocation of sXBP1 independent of IRE1 $\alpha$  activation, while the nuclear levels of ATF6 and CHOP remain unchanged, mimicking insulin's effect. aPC promoted complex formation of p85 $\alpha$ /p85 $\beta$  with sXBP1 reminiscent of insulin signaling. While a hormone-like role of coagulation proteases has been proposed previously<sup>179,180</sup>, this study provides for the first time conclusive evidence that coagulation proteases can rescue defective hormone signaling, as the adaptive UPR induced by insulin and aPC employs the same intracellular signaling hub (**Fig. 24**). Importantly, in the presence of impaired insulin signaling, as observed in the most frequent form of DM (T2DM), the PAR-aPC signaling pathway remains intact, and substituting the agonist aPC or an aPC mimetic or interfering with the intracellular signaling pathway may allow circumvention of impaired insulin signaling.

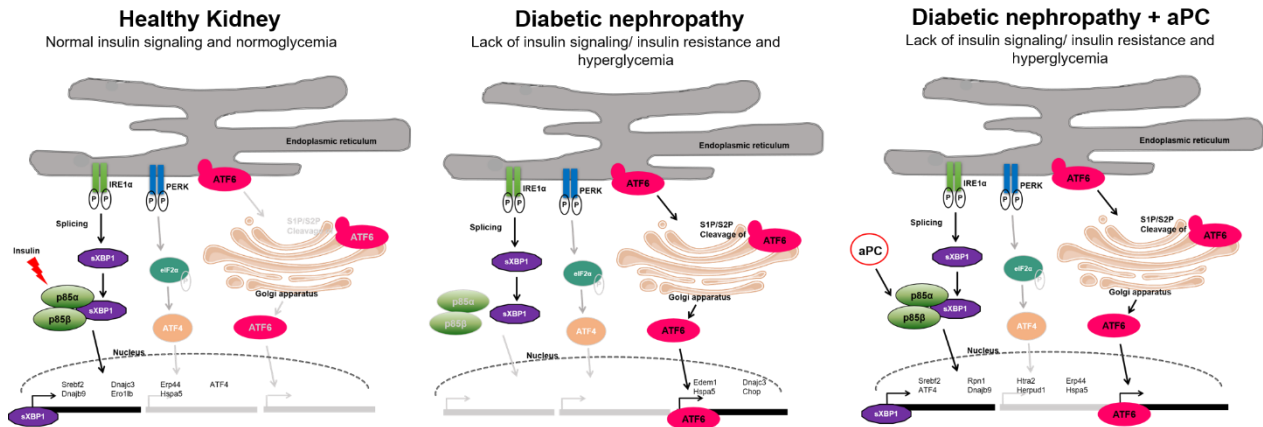


**Figure 24: Proposed model of cytoprotective signaling of insulin and aPC in podocytes in dNP.** Under normal physiological conditions, insulin maintains ER proteostasis via nuclear translocation of sXBP1 in podocytes. The loss of insulin signaling under hyperglycemic conditions disrupts this homeostatic pathway contributing to ER stress. Prolonged ER stress leads to the activation of the cell death machinery and loss of podocytes. Analogous to insulin, aPC is able to induce nuclear translocation of sXBP1 through its interaction with p85 $\alpha$  and p85 $\beta$  in the absence of insulin signaling. Nuclear sXBP1 activates the transcription of UPR chaperones and ERAD components that enable podocytes to resume its normal function within the glomeruli.

## 6. Zusammenfassung

Diese Studie zeigt eine direkte Verbindung zwischen defekter Insulinsignalkaskaden in Podozyten und einer eingeschränkten Nierenfunktion. Unsere Untersuchungen etablieren ein weit verbreitetes intrazelluläres Signalzentrum für Insulin und der Gerinnungsprotease aPC, welches in Abwesenheit eines physiologischen Insulinsignals für therapeutische Zwecke beeinflusst werden kann. Die mechanistische Verbindung zwischen Insulinsignalkaskaden und ER-Stress und die pathophysiologische Relevanz dieser Reaktionswege innerhalb der diabetischen Nephropathie (dNP) wurden hervorgehoben. Die genetische Manipulation oder die funktionelle Inaktivierung die insulin Reaktionsweges in T1DM- (Insulinmangel) und T2DM- (Insulinresistenz) Mausmodellen begünstigen eine maladaptive UPR, welche innerhalb der dNP durch eine gestörte nukleäre sXBP1-Translokation bei gleichzeitig gesteigerter ATF6- und CHOP- Expression gekennzeichnet ist. Signale über den sXBP1-Arm des UPR werden für adaptive ER-Reaktionen in Podozyten unter hyperglykämischem Stress benötigt. Wir enthüllten einen adaptiven UPR-Weg, welcher durch die Gerinnungsprotease aPC reguliert wird und dadurch gestörte Insulinsignalkaskaden verbessern kann und das Überleben von Podozyten sicherstellen kann. Während hormonähnliche Funktionen der Gerinnungsproteasen bereits kürzlich vorgeschlagen wurden<sup>179,180</sup>, haben wir in dieser Studie schlüssige Beweise dafür, dass Gerinnungsproteasen defekte Hormonsignalkaskaden durch die Induktion des adaptiven UPR wiederherstellen können. Die Exposition von Podozyten mit aPC führte temporär zu einer Induktion der nukleären Translokation von sXBP1 unabhängig von einer vorherigen IRE-1-Aktivierung, bei gleichbleibenden nukleären ATF6- und CHOP-Konzentrationen. Dies käme einer nachahmenden Insulinwirkung gleich. Darüber hinaus begünstigt aPC eine komplexe Bildung von p85 $\alpha$  und p85 $\beta$  mit sXBP1, welche an Insulinsignalkaskaden erinnert. Aus diesen Gründen eröffnet die sowohl durch Insulin, als auch aPC induzierte adaptive UPR denselben zentralen intrazellulären Signalweg (**Abb. 24**). Vorhandene Defekte in der Insulinsignalkaskade, wie im DM (T2DM), zeigten, dass der PAR-aPC Signalweg intakt bleibt. APC-Agonisten, aPC-Mimetika oder Eingriffe in den intrazellulären Signalweg könnten so gestörtes Insulinsignaling umgehen.

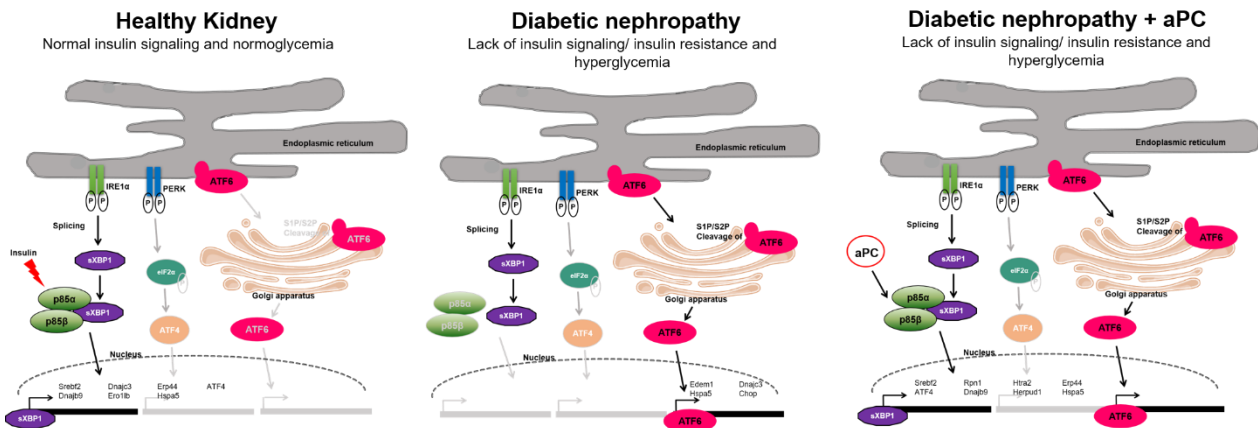


**Figure 24: Schematische Darstellung des zytoprotectiven Signalweges des Insulins und aPC in Podozyten bei dNP.** Unter normalen physiologischen Bedingungen stabilisiert Insulin die ER – Proteostase mittels Translokation von sXBP1 im Podozyten. Durch Verlust des Insulinsignalweges unter hyperglykämischen Bedingungen wird die Homeostase gestört und so ER-Stress induziert. Anhaltender ER-Stress führt zur Aktivierung der Zelltodmaschienerie und zum Verlust von Podozyten. Analog zu Insulin ist aPC in der Lage die Translokation von sXBP1 in den Zellkern zu induzieren, indem es mit p85 $\alpha$  und p85 $\beta$  in der Abwesenheit vom Insulin (Signalweg) interagiert. Nukleäres sXBP1 aktiviert somit die Transkription der UPR- Chaperone und der ERAD Komponenten, wodurch die Podozyten ihre normale Funktion innerhalb der Glomeruli wiedererlangen.



## 7. Future Outlook

Our study unravels the importance of sXBP1 in maintaining cellular and metabolic homeostasis in the glomerular compartment of the kidney in dNP. ER stress and mitochondrial oxidative stress have been implicated in the etiology of insulin resistance associated with T2DM, but the mechanism of their interaction remain poorly defined, in particular in the context of renal disease. While the importance of the transcription factor sXBP1 is well-established in ER quality control (QC), including unfolded protein response (UPR) and ER-associated degradation (ERAD), it's role in mitochondrial UPR (UPR<sup>Mt</sup>) and QC is yet to be clarified.

Among the genome-wide CHIP sequencing data, we observed several mitochondrial (Mt) proteases and UPR<sup>Mt</sup> chaperones apparently regulated by sXBP1 that could be integral mediators of the ER-Mt crosstalk. sXBP1, a key regulator of the UPR, appears to be engaged in the transcriptional activation or repression of redox-sensitive mitochondrial intermembrane space (IMS) import machinery proteins as well as mitochondrial matrix quality control proteases such as Chchd4 (the mammalian homolog of the yeast mitochondrial disulfide relay system carrier Mia40), Clpx, Clpp, Lonp1, and Clptm1. Additionally, sXBP1 seems to regulate the transcription of several of the mitochondrial respiratory chain complex chaperones such as Cox5a, Cox14, Cox16, and Ccs, as well as key metabolic regulators, Esrrb and Esrrg.

Estrogen-related receptors b and g (Esrrb and Esrrg) share similarities to the estrogen receptors  $\alpha$  and  $\beta$  but their functions are unknown. Esrrb and Esrrg are orphan receptors that are known to bind to estrogen response elements in the absence of the ligand estrogen, and transcriptionally activate reporter genes. Furthermore, they are critical regulators of mitochondrial biogenesis and fatty acid oxidation through association with peroxisome proliferator-activated receptor gamma coactivator 1-alpha (PGC-1 $\alpha$ <sup>181</sup>). Esrrb has recently been shown to synergistically regulate somatic cell reprogramming in coordination with Zic3 transcription factor<sup>182</sup>. Esrrb induces transcription of genes involved in oxidative phosphorylation, specifically, components of the electron transport chain (ETC)<sup>182</sup>. While the PERK-ATF4 pathway has been known to be at the intersection of ER

response and mitochondrial oxidative stress response<sup>79</sup>, more recently, IRE1 $\alpha$ <sup>183</sup> has been shown to function as a housekeeping gene at the ER-mitochondria contact points, it remains to be investigated whether Estrogen-related receptors involve UPR regulators in regulating the crosstalk between ER and mitochondria..

Over the last decade, it has become evident that mitochondria and ER networks are interconnected, not just sharing structural and functional interactions essential for the maintenance of cellular homeostasis, but also sharing signaling mediators that help to relieve metabolic stresses as well as maintain cytoplasmic and mitochondrial proteostasis. Both the ER and mitochondria interact through contact points known as mitochondria-associated membranes (MAMs), in order to exchange lipids and Ca<sup>2+</sup>, and regulate cellular homeostasis. This crosstalk becomes dysregulated in diabetes, which contributes to the already existing ER-mitochondria miscommunication persisting in a hyperglycemic state<sup>184,185</sup>. Our results from the podocyte-specific genome-wide ChIP sequencing may identify potential mediators of this crosstalk and help illustrate the role of MAMs as glucose sensors that adapt to cellular bioenergetics<sup>186</sup>.

Since insulin has already been shown to increase the crosstalk between the Mt membrane proteins and the ER in hepatocytes<sup>184</sup>, coagulation proteases such as aPC may additionally regulate the ER-mitochondria interaction and communication, contributing to the control of metabolic functions involved in the control of glucose homeostasis. To adapt to any pathological conditions that influence decreased mitochondrial activity, the organelle has evolved to increase the synthesis of nuclear-encoded mitochondrial chaperones and proteases to facilitate normal functionality. Although, the mitochondria possess an independent genome considered to be a remnant of its symbiotic bacterial ancestry<sup>187</sup>, the mitochondrial and the nuclear genomes have evolved to coordinate complex cellular functions. Thus, the mitochondrial - ER communication enables the cell to coordinate a regulated cellular plan of action via the nucleus to bring about cellular and metabolic homeostasis. Our investigations into aPC's regulation of ER stress in dNP makes it imperative to consider the role of XBP1 in transcriptionally regulating genes that modulate both mitochondrial UPR and endoplasmic reticulum UPR. Moreover, since our study establishes the role of activated protein C in rescuing podocytes from the

detrimental effects of hyperglycemia, it would be interesting to analyze how aPC regulates the ER-MAMs under physiological as well as pathological conditions in the kidney and in other metabolic tissues.

## 8. References

1. Chawla A, Chawla R, Jaggi S. Microvascular and macrovascular complications in diabetes mellitus: Distinct or continuum? *Indian J Endocrinol Metab.* 2016;20(4):546-551.
2. Gross JL, de Azevedo MJ, Silveiro SP, Canani LH, Caramori ML, Zelmanovitz T. Diabetic nephropathy: diagnosis, prevention, and treatment. *Diabetes Care.* 2005;28(1):164-176.
3. Cade WT. Diabetes-related microvascular and macrovascular diseases in the physical therapy setting. *Phys Ther.* 2008;88(11):1322-1335.
4. Shen Z, Fang Y, Xing T, Wang F. Diabetic Nephropathy: From Pathophysiology to Treatment. *J Diabetes Res.* 2017;2017:2379432.
5. Gheith O, Farouk N, Nampoory N, Halim MA, Al-Otaibi T. Diabetic kidney disease: world wide difference of prevalence and risk factors. *J Nephroarmacol.* 2016;5(1):49-56.
6. Gnudi L, Coward RJM, Long DA. Diabetic Nephropathy: Perspective on Novel Molecular Mechanisms. *Trends Endocrinol Metab.* 2016;27(11):820-830.
7. Chatterjee S, Khunti K, Davies MJ. Type 2 diabetes. *Lancet.* 2017;389(10085):2239-2251.
8. Ahlqvist E, Storm P, Karajamaki A, et al. Novel subgroups of adult-onset diabetes and their association with outcomes: a data-driven cluster analysis of six variables. *Lancet Diabetes Endocrinol.* 2018;6(5):361-369.
9. Doshi SM, Friedman AN. Diagnosis and Management of Type 2 Diabetic Kidney Disease. *Clin J Am Soc Nephrol.* 2017;12(8):1366-1373.
10. Brownlee M. The pathobiology of diabetic complications: a unifying mechanism. *Diabetes.* 2005;54(6):1615-1625.
11. Wolf G, Chen S, Ziyadeh FN. From the periphery of the glomerular capillary wall toward the center of disease: podocyte injury comes of age in diabetic nephropathy. *Diabetes.* 2005;54(6):1626-1634.
12. Ghaderian SB, Hayati F, Shayanpour S, Beladi Mousavi SS. Diabetes and end-stage renal disease; a review article on new concepts. *J Renal Inj Prev.* 2015;4(2):28-33.

13. Triplitt CL. Understanding the kidneys' role in blood glucose regulation. *Am J Manag Care*. 2012;18(1 Suppl):S11-16.
14. Reiser J, Altintas MM. Podocytes. *F1000Res*. 2016;5.
15. Tiwari S, Sharma N, Gill PS, et al. Impaired sodium excretion and increased blood pressure in mice with targeted deletion of renal epithelial insulin receptor. *Proc Natl Acad Sci U S A*. 2008;105(17):6469-6474.
16. Welsh GI, Hale LJ, Eremina V, et al. Insulin signaling to the glomerular podocyte is critical for normal kidney function. *Cell Metab*. 2010;12(4):329-340.
17. Coward RJ, Welsh GI, Yang J, et al. The human glomerular podocyte is a novel target for insulin action. *Diabetes*. 2005;54(11):3095-3102.
18. Tonneijck L, Muskiet MH, Smits MM, et al. Glomerular Hyperfiltration in Diabetes: Mechanisms, Clinical Significance, and Treatment. *J Am Soc Nephrol*. 2017;28(4):1023-1039.
19. Bankir L, Roussel R, Bouby N. Protein- and diabetes-induced glomerular hyperfiltration: role of glucagon, vasopressin, and urea. *Am J Physiol Renal Physiol*. 2015;309(1):F2-23.
20. Lin YC, Chang YH, Yang SY, Wu KD, Chu TS. Update of pathophysiology and management of diabetic kidney disease. *J Formos Med Assoc*. 2018;117(8):662-675.
21. Evans M, Palaka E, Furuland H, et al. The value of maintaining normokalaemia and enabling RAASi therapy in chronic kidney disease. *BMC Nephrol*. 2019;20(1):31.
22. Badal SS, Danesh FR. New insights into molecular mechanisms of diabetic kidney disease. *Am J Kidney Dis*. 2014;63(2 Suppl 2):S63-83.
23. Lindenmeyer MT, Rastaldi MP, Ikehata M, et al. Proteinuria and hyperglycemia induce endoplasmic reticulum stress. *J Am Soc Nephrol*. 2008;19(11):2225-2236.
24. Ising C, Koehler S, Braehler S, et al. Inhibition of insulin/IGF-1 receptor signaling protects from mitochondria-mediated kidney failure. *EMBO Mol Med*. 2015;7(3):275-287.
25. DeFronzo RA, Ferrannini E, Groop L, et al. Type 2 diabetes mellitus. *Nat Rev Dis Primers*. 2015;1:15019.

26. Parving HH, Lambers-Heerspink H, de Zeeuw D. Empagliflozin and Progression of Kidney Disease in Type 2 Diabetes. *N Engl J Med*. 2016;375(18):1800-1801.
27. Rajagopalan S, Brook R. Canagliflozin and Cardiovascular and Renal Events in Type 2 Diabetes. *N Engl J Med*. 2017;377(21):2098-2099.
28. de Boer IH. Liraglutide and Renal Outcomes in Type 2 Diabetes. *N Engl J Med*. 2017;377(22):2198.
29. Navarro-Gonzalez JF, Mora-Fernandez C, Muros de Fuentes M, et al. Effect of pentoxifylline on renal function and urinary albumin excretion in patients with diabetic kidney disease: the PREDIAN trial. *J Am Soc Nephrol*. 2015;26(1):220-229.
30. Pergola PE, Raskin P, Toto RD, et al. Bardoxolone methyl and kidney function in CKD with type 2 diabetes. *N Engl J Med*. 2011;365(4):327-336.
31. Ipp E, Genter P, Childress K. Semaglutide and Cardiovascular Outcomes in Patients with Type 2 Diabetes. *N Engl J Med*. 2017;376(9):890-891.
32. Groop PH, Cooper ME, Perkovic V, Emser A, Woerle HJ, von Eynatten M. Linagliptin lowers albuminuria on top of recommended standard treatment in patients with type 2 diabetes and renal dysfunction. *Diabetes Care*. 2013;36(11):3460-3468.
33. Lin SL, Chen RH, Chen YM, et al. Pentoxifylline attenuates tubulointerstitial fibrosis by blocking Smad3/4-activated transcription and profibrogenic effects of connective tissue growth factor. *J Am Soc Nephrol*. 2005;16(9):2702-2713.
34. Bakris GL, Ruilope LM, McMorn SO, et al. Rosiglitazone reduces microalbuminuria and blood pressure independently of glycemia in type 2 diabetes patients with microalbuminuria. *J Hypertens*. 2006;24(10):2047-2055.
35. Lin SL, Chen YM, Chiang WC, Tsai TJ, Chen WY. Pentoxifylline: a potential therapy for chronic kidney disease. *Nephrology (Carlton)*. 2004;9(4):198-204.
36. Mosenzon O, Leibowitz G, Bhatt DL, et al. Effect of Saxagliptin on Renal Outcomes in the SAVOR-TIMI 53 Trial. *Diabetes Care*. 2017;40(1):69-76.
37. Bakris GL. Role for beta-blockers in the management of diabetic kidney disease. *Am J Hypertens*. 2003;16(9 Pt 2):7S-12S.

38. Chen PM, Lai TS, Chen PY, et al. Renoprotective effect of combining pentoxifylline with angiotensin-converting enzyme inhibitor or angiotensin II receptor blocker in advanced chronic kidney disease. *J Formos Med Assoc.* 2014;113(4):219-226.
39. de Zeeuw D, Agarwal R, Amdahl M, et al. Selective vitamin D receptor activation with paricalcitol for reduction of albuminuria in patients with type 2 diabetes (VITAL study): a randomised controlled trial. *Lancet.* 2010;376(9752):1543-1551.
40. Agarwal R, Acharya M, Tian J, et al. Antiproteinuric effect of oral paricalcitol in chronic kidney disease. *Kidney Int.* 2005;68(6):2823-2828.
41. Williams ME, Bolton WK, Khalifah RG, Degenhardt TP, Schotzinger RJ, McGill JB. Effects of pyridoxamine in combined phase 2 studies of patients with type 1 and type 2 diabetes and overt nephropathy. *Am J Nephrol.* 2007;27(6):605-614.
42. Brosius FC, Tuttle KR, Kretzler M. JAK inhibition in the treatment of diabetic kidney disease. *Diabetologia.* 2016;59(8):1624-1627.
43. Tuttle KR, Bakris GL, Toto RD, McGill JB, Hu K, Anderson PW. The effect of ruboxistaurin on nephropathy in type 2 diabetes. *Diabetes Care.* 2005;28(11):2686-2690.
44. Li Z, Liu X, Wang B, et al. Pirfenidone suppresses MAPK signalling pathway to reverse epithelial-mesenchymal transition and renal fibrosis. *Nephrology (Carlton).* 2017;22(8):589-597.
45. Noor A, Taher MA. Combination therapy (131I and carbimazole) of toxic diffuse goitre. *J Assoc Physicians India.* 1989;37(11):733-734.
46. Kirkman MS, Mahmud H, Korytkowski MT. Intensive Blood Glucose Control and Vascular Outcomes in Patients with Type 2 Diabetes Mellitus. *Endocrinol Metab Clin North Am.* 2018;47(1):81-96.
47. Ward CGagiAD. Glycogenolysis and glycogenesis. 2014 Aug 13; rev. no. 13:<https://www.diapedia.org/metabolism-and-hormones/51040851111/glycogenolysis-and-glycogenesis>.
48. S. Bhatt RNK. *Significance of Organ Crosstalk in Insulin*

*Resistance and Type 2 Diabetes.* Elsevier Inc; 2013.

49. Taniguchi CM, Emanuelli B, Kahn CR. Critical nodes in signalling pathways: insights into insulin action. *Nat Rev Mol Cell Biol.* 2006;7(2):85-96.

50. Boucher J, Kleinridders A, Kahn CR. Insulin receptor signaling in normal and insulin-resistant states. *Cold Spring Harb Perspect Biol.* 2014;6(1).
51. Siddle K. Signalling by insulin and IGF receptors: supporting acts and new players. *J Mol Endocrinol.* 2011;47(1):R1-10.
52. Guo S. Insulin signaling, resistance, and the metabolic syndrome: insights from mouse models into disease mechanisms. *J Endocrinol.* 2014;220(2):T1-T23.
53. Hallgren R, Bohman SO, Fredens K. Activated eosinophil infiltration and deposits of eosinophil cationic protein in renal allograft rejection. *Nephron.* 1991;59(2):266-270.
54. Muniyappa R, Montagnani M, Koh KK, Quon MJ. Cardiovascular actions of insulin. *Endocr Rev.* 2007;28(5):463-491.
55. Kubena KS. Metabolic syndrome in adolescents: issues and opportunities. *J Am Diet Assoc.* 2011;111(11):1674-1679.
56. Johnson AM, Olefsky JM. The origins and drivers of insulin resistance. *Cell.* 2013;152(4):673-684.
57. Reaven G. The metabolic syndrome or the insulin resistance syndrome? Different names, different concepts, and different goals. *Endocrinol Metab Clin North Am.* 2004;33(2):283-303.
58. Steinberger J, Daniels SR, Eckel RH, et al. Progress and challenges in metabolic syndrome in children and adolescents: a scientific statement from the American Heart Association Atherosclerosis, Hypertension, and Obesity in the Young Committee of the Council on Cardiovascular Disease in the Young; Council on Cardiovascular Nursing; and Council on Nutrition, Physical Activity, and Metabolism. *Circulation.* 2009;119(4):628-647.
59. Wilson C. Diabetes: ACCORD: 5-year outcomes of intensive glycemic control. *Nat Rev Endocrinol.* 2011;7(6):314.
60. Ozcan U, Cao Q, Yilmaz E, et al. Endoplasmic reticulum stress links obesity, insulin action, and type 2 diabetes. *Science.* 2004;306(5695):457-461.
61. Dokken BB, Saengsirisuwan V, Kim JS, Teachey MK, Henriksen EJ. Oxidative stress-induced insulin resistance in rat skeletal muscle: role of glycogen synthase kinase-3. *Am J Physiol Endocrinol Metab.* 2008;294(3):E615-621.



62. Evans JL, Maddux BA, Goldfine ID. The molecular basis for oxidative stress-induced insulin resistance. *Antioxid Redox Signal*. 2005;7(7-8):1040-1052.
63. Riboulet-Chavey A, Pierron A, Durand I, Murdaca J, Giudicelli J, Van Obberghen E. Methylglyoxal impairs the insulin signaling pathways independently of the formation of intracellular reactive oxygen species. *Diabetes*. 2006;55(5):1289-1299.
64. Hirosumi J, Tuncman G, Chang L, et al. A central role for JNK in obesity and insulin resistance. *Nature*. 2002;420(6913):333-336.
65. Jager J, Gremeaux T, Cormont M, Le Marchand-Brustel Y, Tanti JF. Interleukin-1beta-induced insulin resistance in adipocytes through down-regulation of insulin receptor substrate-1 expression. *Endocrinology*. 2007;148(1):241-251.
66. Walter P, Ron D. The unfolded protein response: from stress pathway to homeostatic regulation. *Science*. 2011;334(6059):1081-1086.
67. Corazzari M, Gagliardi M, Fimia GM, Piacentini M. Endoplasmic Reticulum Stress, Unfolded Protein Response, and Cancer Cell Fate. *Front Oncol*. 2017;7:78.
68. Kanekura K, Ma X, Murphy JT, Zhu LJ, Diwan A, Urano F. IRE1 prevents endoplasmic reticulum membrane permeabilization and cell death under pathological conditions. *Sci Signal*. 2015;8(382):ra62.
69. Hetz C. The unfolded protein response: controlling cell fate decisions under ER stress and beyond. *Nat Rev Mol Cell Biol*. 2012;13(2):89-102.
70. Promlek T, Ishiwata-Kimata Y, Shido M, Sakuramoto M, Kohno K, Kimata Y. Membrane aberrancy and unfolded proteins activate the endoplasmic reticulum stress sensor Ire1 in different ways. *Mol Biol Cell*. 2011;22(18):3520-3532.
71. Yoshida H, Matsui T, Yamamoto A, Okada T, Mori K. XBP1 mRNA is induced by ATF6 and spliced by IRE1 in response to ER stress to produce a highly active transcription factor. *Cell*. 2001;107(7):881-891.
72. Yoshida H, Oku M, Suzuki M, Mori K. pXBP1(U) encoded in XBP1 pre-mRNA negatively regulates unfolded protein response activator pXBP1(S) in mammalian ER stress response. *J Cell Biol*. 2006;172(4):565-575.
73. Yoshida H, Uemura A, Mori K. pXBP1(U), a negative regulator of the unfolded protein response activator pXBP1(S), targets ATF6 but not ATF4 in proteasome-mediated degradation. *Cell Struct Funct*. 2009;34(1):1-10.

74. Brown M, Strudwick N, Suwara M, et al. An initial phase of JNK activation inhibits cell death early in the endoplasmic reticulum stress response. *J Cell Sci.* 2016;129(12):2317-2328.
75. Winnay JN, Boucher J, Mori MA, Ueki K, Kahn CR. A regulatory subunit of phosphoinositide 3-kinase increases the nuclear accumulation of X-box-binding protein-1 to modulate the unfolded protein response. *Nat Med.* 2010;16(4):438-445.
76. Maurel M, Chevet E, Tavernier J, Gerlo S. Getting RIDD of RNA: IRE1 in cell fate regulation. *Trends Biochem Sci.* 2014;39(5):245-254.
77. Minamino T, Komuro I, Kitakaze M. Endoplasmic reticulum stress as a therapeutic target in cardiovascular disease. *Circ Res.* 2010;107(9):1071-1082.
78. Pakos-Zebrucka K, Koryga I, Mnich K, Lujic M, Samali A, Gorman AM. The integrated stress response. *EMBO Rep.* 2016;17(10):1374-1395.
79. Fusakio ME, Willy JA, Wang Y, et al. Transcription factor ATF4 directs basal and stress-induced gene expression in the unfolded protein response and cholesterol metabolism in the liver. *Mol Biol Cell.* 2016;27(9):1536-1551.
80. Flamment M, Hajduch E, Ferre P, Fougelle F. New insights into ER stress-induced insulin resistance. *Trends Endocrinol Metab.* 2012;23(8):381-390.
81. Wu J, Zhang R, Torreggiani M, et al. Induction of diabetes in aged C57B6 mice results in severe nephropathy: an association with oxidative stress, endoplasmic reticulum stress, and inflammation. *Am J Pathol.* 2010;176(5):2163-2176.
82. Lee J, Ozcan U. Unfolded protein response signaling and metabolic diseases. *J Biol Chem.* 2014;289(3):1203-1211.
83. Yamamoto K, Yoshida H, Kokame K, Kaufman RJ, Mori K. Differential contributions of ATF6 and XBP1 to the activation of endoplasmic reticulum stress-responsive cis-acting elements ERSE, UPRE and ERSE-II. *J Biochem.* 2004;136(3):343-350.
84. Yan W, Frank CL, Korth MJ, et al. Control of PERK eIF2alpha kinase activity by the endoplasmic reticulum stress-induced molecular chaperone P58IPK. *Proc Natl Acad Sci U S A.* 2002;99(25):15920-15925.
85. Iurlaro R, Munoz-Pinedo C. Cell death induced by endoplasmic reticulum stress. *FEBS J.* 2016;283(14):2640-2652.

86. Kadowaki H, Nishitoh H. Signaling pathways from the endoplasmic reticulum and their roles in disease. *Genes (Basel)*. 2013;4(3):306-333.
87. Gestwicki JE, Garza D. Protein quality control in neurodegenerative disease. *Prog Mol Biol Transl Sci*. 2012;107:327-353.
88. Boland B, Yu WH, Corti O, et al. Promoting the clearance of neurotoxic proteins in neurodegenerative disorders of ageing. *Nat Rev Drug Discov*. 2018;17(9):660-688.
89. Iwawaki T, Akai R, Kohno K, Miura M. A transgenic mouse model for monitoring endoplasmic reticulum stress. *Nat Med*. 2004;10(1):98-102.
90. Lee AH, Heidtman K, Hotamisligil GS, Glimcher LH. Dual and opposing roles of the unfolded protein response regulated by IRE1alpha and XBP1 in proinsulin processing and insulin secretion. *Proc Natl Acad Sci U S A*. 2011;108(21):8885-8890.
91. Harding HP, Zeng H, Zhang Y, et al. Diabetes mellitus and exocrine pancreatic dysfunction in *perk*<sup>-/-</sup> mice reveals a role for translational control in secretory cell survival. *Mol Cell*. 2001;7(6):1153-1163.
92. Zhang W, Feng D, Li Y, Iida K, McGrath B, Cavener DR. PERK EIF2AK3 control of pancreatic beta cell differentiation and proliferation is required for postnatal glucose homeostasis. *Cell Metab*. 2006;4(6):491-497.
93. Delepine M, Nicolino M, Barrett T, Golamaully M, Lathrop GM, Julier C. EIF2AK3, encoding translation initiation factor 2-alpha kinase 3, is mutated in patients with Wolcott-Rallison syndrome. *Nat Genet*. 2000;25(4):406-409.
94. Park SW, Zhou Y, Lee J, et al. The regulatory subunits of PI3K, p85alpha and p85beta, interact with XBP-1 and increase its nuclear translocation. *Nat Med*. 2010;16(4):429-437.
95. Ozcan L, Ergin AS, Lu A, et al. Endoplasmic reticulum stress plays a central role in development of leptin resistance. *Cell Metab*. 2009;9(1):35-51.
96. Clegg DJ, Gotoh K, Kemp C, et al. Consumption of a high-fat diet induces central insulin resistance independent of adiposity. *Physiol Behav*. 2011;103(1):10-16.
97. Won JC, Jang PG, Namkoong C, et al. Central administration of an endoplasmic reticulum stress inducer inhibits the anorexigenic effects of leptin and insulin. *Obesity (Silver Spring)*. 2009;17(10):1861-1865.

98. Ozcan U, Yilmaz E, Ozcan L, et al. Chemical chaperones reduce ER stress and restore glucose homeostasis in a mouse model of type 2 diabetes. *Science*. 2006;313(5790):1137-1140.
99. Kars M, Yang L, Gregor MF, et al. Tauroursodeoxycholic Acid may improve liver and muscle but not adipose tissue insulin sensitivity in obese men and women. *Diabetes*. 2010;59(8):1899-1905.
100. Xiao C, Giacca A, Lewis GF. Sodium phenylbutyrate, a drug with known capacity to reduce endoplasmic reticulum stress, partially alleviates lipid-induced insulin resistance and beta-cell dysfunction in humans. *Diabetes*. 2011;60(3):918-924.
101. Kobayashi K, Forte TM, Taniguchi S, Ishida BY, Oka K, Chan L. The db/db mouse, a model for diabetic dyslipidemia: molecular characterization and effects of Western diet feeding. *Metabolism*. 2000;49(1):22-31.
102. Burke SJ, Batdorf HM, Burk DH, et al. db/db Mice Exhibit Features of Human Type 2 Diabetes That Are Not Present in Weight-Matched C57BL/6J Mice Fed a Western Diet. *J Diabetes Res*. 2017;2017:8503754.
103. Rieusset J. Contribution of mitochondria and endoplasmic reticulum dysfunction in insulin resistance: Distinct or interrelated roles? *Diabetes Metab*. 2015;41(5):358-368.
104. Isermann B, Vinnikov IA, Madhusudhan T, et al. Activated protein C protects against diabetic nephropathy by inhibiting endothelial and podocyte apoptosis. *Nat Med*. 2007;13(11):1349-1358.
105. Bock F, Shahzad K, Vergnolle N, Isermann B. Activated protein C based therapeutic strategies in chronic diseases. *Thromb Haemost*. 2014;111(4):610-617.
106. Gil-Bernabe P, D'Alessandro-Gabazza CN, Toda M, et al. Exogenous activated protein C inhibits the progression of diabetic nephropathy. *J Thromb Haemost*. 2012;10(3):337-346.
107. Bock F, Shahzad K, Wang H, et al. Activated protein C ameliorates diabetic nephropathy by epigenetically inhibiting the redox enzyme p66Shc. *Proc Natl Acad Sci U S A*. 2013;110(2):648-653.

108. Yamaji K, Wang Y, Liu Y, et al. Activated protein C, a natural anticoagulant protein, has antioxidant properties and inhibits lipid peroxidation and advanced glycation end products formation. *Thromb Res.* 2005;115(4):319-325.
109. Adams RL, Bird RJ. Review article: Coagulation cascade and therapeutics update: relevance to nephrology. Part 1: Overview of coagulation, thrombophilias and history of anticoagulants. *Nephrology (Carlton).* 2009;14(5):462-470.
110. Monroe DM, Key NS. The tissue factor-factor VIIa complex: procoagulant activity, regulation, and multitasking. *J Thromb Haemost.* 2007;5(6):1097-1105.
111. Madhusudhan T, Kerlin BA, Isermann B. The emerging role of coagulation proteases in kidney disease. *Nat Rev Nephrol.* 2016;12(2):94-109.
112. Griffin JH, Zlokovic BV, Mosnier LO. Activated protein C: biased for translation. *Blood.* 2015;125(19):2898-2907.
113. Mosnier LO, Zlokovic BV, Griffin JH. Cytoprotective-selective activated protein C therapy for ischaemic stroke. *Thromb Haemost.* 2014;112(5):883-892.
114. Muller F, Mutch NJ, Schenk WA, et al. Platelet polyphosphates are proinflammatory and procoagulant mediators in vivo. *Cell.* 2009;139(6):1143-1156.
115. Bjorkqvist J, Nickel KF, Stavrou E, Renne T. In vivo activation and functions of the protease factor XII. *Thromb Haemost.* 2014;112(5):868-875.
116. Hollenberg MD, Compton SJ. International Union of Pharmacology. XXVIII. Proteinase-activated receptors. *Pharmacol Rev.* 2002;54(2):203-217.
117. Adams MN, Ramachandran R, Yau MK, et al. Structure, function and pathophysiology of protease activated receptors. *Pharmacol Ther.* 2011;130(3):248-282.
118. Madhusudhan T, Wang H, Straub BK, et al. Cytoprotective signaling by activated protein C requires protease-activated receptor-3 in podocytes. *Blood.* 2012;119(3):874-883.
119. Soh UJ, Dores MR, Chen B, Trejo J. Signal transduction by protease-activated receptors. *Br J Pharmacol.* 2010;160(2):191-203.
120. Ostrowska E, Reiser G. The protease-activated receptor-3 (PAR-3) can signal autonomously to induce interleukin-8 release. *Cell Mol Life Sci.* 2008;65(6):970-981.

121. Madhusudhan T, Wang H, Ghosh S, et al. Signal integration at the PI3K-p85-XBP1 hub endows coagulation protease activated protein C with insulin-like function. *Blood*. 2017;130(12):1445-1455.
122. Duran-Salgado MB, Rubio-Guerra AF. Diabetic nephropathy and inflammation. *World J Diabetes*. 2014;5(3):393-398.
123. Julia S, James U. Direct Oral Anticoagulants: A Quick Guide. *Eur Cardiol*. 2017;12(1):40-45.
124. Stacy ZA, Richter SK. Direct oral anticoagulants for stroke prevention in atrial fibrillation: treatment outcomes and dosing in special populations. *Ther Adv Cardiovasc Dis*. 2018;12(9):247-262.
125. Dockendorff C, Aisiku O, Verplank L, et al. Discovery of 1,3-Diaminobenzenes as Selective Inhibitors of Platelet Activation at the PAR1 Receptor. *ACS Med Chem Lett*. 2012;3(3):232-237.
126. Aisiku O, Peters CG, De Ceunynck K, et al. Parmodulins inhibit thrombus formation without inducing endothelial injury caused by vorapaxar. *Blood*. 2015;125(12):1976-1985.
127. Dowal L, Sim DS, Dilks JR, et al. Identification of an antithrombotic allosteric modulator that acts through helix 8 of PAR1. *Proc Natl Acad Sci U S A*. 2011;108(7):2951-2956.
128. De Ceunynck K, Peters CG, Jain A, et al. PAR1 agonists stimulate APC-like endothelial cytoprotection and confer resistance to thromboinflammatory injury. *Proc Natl Acad Sci U S A*. 2018;115(5):E982-E991.
129. Refice C, Loriga R, Pompa MN, et al. P030. Global postural rehabilitation and migraine: a pilot-study. *J Headache Pain*. 2015;16(Suppl 1):A116.
130. Nieman MT. Protease-activated receptors in hemostasis. *Blood*. 2016;128(2):169-177.
131. Nazir S, Gadi I, Al-Dabet MM, et al. Cytoprotective activated protein C averts Nlrp3 inflammasome-induced ischemia-reperfusion injury via mTORC1 inhibition. *Blood*. 2017;130(24):2664-2677.
132. Mosnier LO, Gale AJ, Yegneswaran S, Griffin JH. Activated protein C variants with normal cytoprotective but reduced anticoagulant activity. *Blood*. 2004;104(6):1740-1744.

133. Mosnier LO, Yang XV, Griffin JH. Activated protein C mutant with minimal anticoagulant activity, normal cytoprotective activity, and preservation of thrombin activable fibrinolysis inhibitor-dependent cytoprotective functions. *J Biol Chem.* 2007;282(45):33022-33033.
134. Lazic D, Sagare AP, Nikolakopoulou AM, Griffin JH, Vassar R, Zlokovic BV. 3K3A-activated protein C blocks amyloidogenic BACE1 pathway and improves functional outcome in mice. *J Exp Med.* 2019;216(2):279-293.
135. Williams PD, Zlokovic BV, Griffin JH, Pryor KE, Davis TP. Preclinical safety and pharmacokinetic profile of 3K3A-APC, a novel, modified activated protein C for ischemic stroke. *Curr Pharm Des.* 2012;18(27):4215-4222.
136. Dong W, Wang H, Shahzad K, et al. Activated Protein C Ameliorates Renal Ischemia-Reperfusion Injury by Restricting Y-Box Binding Protein-1 Ubiquitination. *J Am Soc Nephrol.* 2015;26(11):2789-2799.
137. Breyer MD, Bottinger E, Brosius FC, 3rd, et al. Mouse models of diabetic nephropathy. *J Am Soc Nephrol.* 2005;16(1):27-45.
138. Madhusudhan T, Wang H, Dong W, et al. Defective podocyte insulin signalling through p85-XBP1 promotes ATF6-dependent maladaptive ER-stress response in diabetic nephropathy. *Nat Commun.* 2015;6:6496.
139. Wang H, Madhusudhan T, He T, et al. Low but sustained coagulation activation ameliorates glucose-induced podocyte apoptosis: protective effect of factor V Leiden in diabetic nephropathy. *Blood.* 2011;117(19):5231-5242.
140. Jaskolski F, Mülle C, Manzoni OJ. An automated method to quantify and visualize colocalized fluorescent signals. *J Neurosci Methods.* 2005;146(1):42-49.
141. Kistler AD, Caicedo A, Abdulreda MH, et al. In vivo imaging of kidney glomeruli transplanted into the anterior chamber of the mouse eye. *Sci Rep.* 2014;4:3872.
142. Tian X, Kim JJ, Monkley SM, et al. Podocyte-associated talin1 is critical for glomerular filtration barrier maintenance. *J Clin Invest.* 2014;124(3):1098-1113.
143. Wei Jiang RH, Mengping Wei, Chenhong Li, Zilong Qiu, Xiaofei Yang & Chen Zhang. An optimized method for high-titer lentivirus preparations without ultracentrifugation. *Scientific Reports.* 2015;5.
144. Kutner RH, Zhang XY, Reiser J. Production, concentration and titration of pseudotyped HIV-1-based lentiviral vectors. *Nat Protoc.* 2009;4(4):495-505.

145. Li H, Handsaker B, Wysoker A, et al. The Sequence Alignment/Map format and SAMtools. *Bioinformatics*. 2009;25(16):2078-2079.
146. Pepke S, Wold B, Mortazavi A. Computation for ChIP-seq and RNA-seq studies. *Nat Methods*. 2009;6(11 Suppl):S22-32.
147. Hetz C, Bernasconi P, Fisher J, et al. Proapoptotic BAX and BAK modulate the unfolded protein response by a direct interaction with IRE1alpha. *Science*. 2006;312(5773):572-576.
148. Nashar K, Egan BM. Relationship between chronic kidney disease and metabolic syndrome: current perspectives. *Diabetes Metab Syndr Obes*. 2014;7:421-435.
149. Haller H, Ji L, Stahl K, Bertram A, Menne J. Molecular Mechanisms and Treatment Strategies in Diabetic Nephropathy: New Avenues for Calcium Dobesilate-Free Radical Scavenger and Growth Factor Inhibition. *Biomed Res Int*. 2017;2017:1909258.
150. Reidy K, Kang HM, Hostetter T, Susztak K. Molecular mechanisms of diabetic kidney disease. *J Clin Invest*. 2014;124(6):2333-2340.
151. Johnson DW, Armstrong K, Campbell SB, et al. Metabolic syndrome in severe chronic kidney disease: Prevalence, predictors, prognostic significance and effects of risk factor modification. *Nephrology (Carlton)*. 2007;12(4):391-398.
152. Sharma K, Ramachandrarao S, Qiu G, et al. Adiponectin regulates albuminuria and podocyte function in mice. *J Clin Invest*. 2008;118(5):1645-1656.
153. Cherney DZI, Odutayo A, Verma S. A Big Win for Diabetic Kidney Disease: CREDENCE. *Cell Metab*. 2019;29(5):1024-1027.
154. Yang J, Zhou Y, Guan Y. PPARgamma as a therapeutic target in diabetic nephropathy and other renal diseases. *Curr Opin Nephrol Hypertens*. 2012;21(1):97-105.
155. Vial G, Chauvin MA, Bendridi N, et al. Imeglimin normalizes glucose tolerance and insulin sensitivity and improves mitochondrial function in liver of a high-fat, high-sucrose diet mice model. *Diabetes*. 2015;64(6):2254-2264.
156. Lee AH, Iwakoshi NN, Glimcher LH. XBP-1 regulates a subset of endoplasmic reticulum resident chaperone genes in the unfolded protein response. *Mol Cell Biol*. 2003;23(21):7448-7459.



157. Acosta-Alvear D, Zhou Y, Blais A, et al. XBP1 controls diverse cell type- and condition-specific transcriptional regulatory networks. *Mol Cell*. 2007;27(1):53-66.
158. Kaser A, Lee AH, Franke A, et al. XBP1 links ER stress to intestinal inflammation and confers genetic risk for human inflammatory bowel disease. *Cell*. 2008;134(5):743-756.
159. Sha H, He Y, Yang L, Qi L. Stressed out about obesity: IRE1alpha-XBP1 in metabolic disorders. *Trends Endocrinol Metab*. 2011;22(9):374-381.
160. Watanabe S, Harayama M, Kanemura S, Sitia R, Inaba K. Structural basis of pH-dependent client binding by ERp44, a key regulator of protein secretion at the ER-Golgi interface. *Proc Natl Acad Sci U S A*. 2017;114(16):E3224-E3232.
161. Chen YM, Kikkawa Y, Miner JH. A missense LAMB2 mutation causes congenital nephrotic syndrome by impairing laminin secretion. *J Am Soc Nephrol*. 2011;22(5):849-858.
162. Clement LC, Avila-Casado C, Mace C, et al. Podocyte-secreted angiopoietin-like-4 mediates proteinuria in glucocorticoid-sensitive nephrotic syndrome. *Nat Med*. 2011;17(1):117-122.
163. Chugh SS, Clement LC, Mace C. New insights into human minimal change disease: lessons from animal models. *Am J Kidney Dis*. 2012;59(2):284-292.
164. Li JJ, Kwak SJ, Jung DS, et al. Podocyte biology in diabetic nephropathy. *Kidney Int Suppl*. 2007(106):S36-42.
165. Hisatsune C, Ebisui E, Usui M, et al. ERp44 Exerts Redox-Dependent Control of Blood Pressure at the ER. *Mol Cell*. 2015;58(6):1015-1027.
166. Lassot I, Segeral E, Berlioz-Torrent C, et al. ATF4 degradation relies on a phosphorylation-dependent interaction with the SCF(betaTrCP) ubiquitin ligase. *Mol Cell Biol*. 2001;21(6):2192-2202.
167. Quiros PM, Prado MA, Zamboni N, et al. Multi-omics analysis identifies ATF4 as a key regulator of the mitochondrial stress response in mammals. *J Cell Biol*. 2017;216(7):2027-2045.
168. Madison BB. Srebp2: A master regulator of sterol and fatty acid synthesis. *J Lipid Res*. 2016;57(3):333-335.

169. Kimura H, Arasaki K, Ohsaki Y, et al. Syntaxin 17 promotes lipid droplet formation by regulating the distribution of acyl-CoA synthetase 3. *J Lipid Res.* 2018;59(5):805-819.
170. Bradley RM, Marvyn PM, Aristizabal Henao JJ, et al. Acylglycerophosphate acyltransferase 4 (AGPAT4) is a mitochondrial lysophosphatidic acid acyltransferase that regulates brain phosphatidylcholine, phosphatidylethanolamine, and phosphatidylinositol levels. *Biochim Biophys Acta.* 2015;1851(12):1566-1576.
171. Beck LH, Jr., Bonegio RG, Lambeau G, et al. M-type phospholipase A2 receptor as target antigen in idiopathic membranous nephropathy. *N Engl J Med.* 2009;361(1):11-21.
172. Kanda S, Horita S, Yanagihara T, Shimizu A, Hattori M. M-type phospholipase A2 receptor (PLA2R) glomerular staining in pediatric idiopathic membranous nephropathy. *Pediatr Nephrol.* 2017;32(4):713-717.
173. Tomas NM, Beck LH, Jr., Meyer-Schwesinger C, et al. Thrombospondin type-1 domain-containing 7A in idiopathic membranous nephropathy. *N Engl J Med.* 2014;371(24):2277-2287.
174. Cara-Fuentes G, Segarra A, Silva-Sanchez C, et al. Angiotensin-like-4 and minimal change disease. *PLoS One.* 2017;12(4):e0176198.
175. Bertelli R, Bonanni A, Caridi G, Canepa A, Ghiggeri GM. Molecular and Cellular Mechanisms for Proteinuria in Minimal Change Disease. *Front Med (Lausanne).* 2018;5:170.
176. Horowitz LM, Rosenberg SE, Ureno G, Kalehzan BM, O'Halloran P. Psychodynamic formulation, consensual response method, and interpersonal problems. *J Consult Clin Psychol.* 1989;57(5):599-606.
177. Mariani LH, Pendergraft WF, 3rd, Kretzler M. Defining Glomerular Disease in Mechanistic Terms: Implementing an Integrative Biology Approach in Nephrology. *Clin J Am Soc Nephrol.* 2016;11(11):2054-2060.
178. Lin JS, Susztak K. Podocytes: the Weakest Link in Diabetic Kidney Disease? *Curr Diab Rep.* 2016;16(5):45.

179. Ramachandran R, Hollenberg MD. Proteinases and signalling: pathophysiological and therapeutic implications via PARs and more. *Br J Pharmacol.* 2008;153 Suppl 1:S263-282.
180. Badeanlou L, Furlan-Freguia C, Yang G, Ruf W, Samad F. Tissue factor-protease-activated receptor 2 signaling promotes diet-induced obesity and adipose inflammation. *Nat Med.* 2011;17(11):1490-1497.
181. Zamora M, Villena JA. Targeting mitochondrial biogenesis to treat insulin resistance. *Curr Pharm Des.* 2014;20(35):5527-5557.
182. Sone M, Morone N, Nakamura T, et al. Hybrid Cellular Metabolism Coordinated by Zic3 and Esrrb Synergistically Enhances Induction of Naive Pluripotency. *Cell Metab.* 2017;25(5):1103-1117 e1106.
183. Carreras-Sureda A, Jana F, Urra H, et al. Non-canonical function of IRE1alpha determines mitochondria-associated endoplasmic reticulum composition to control calcium transfer and bioenergetics. *Nat Cell Biol.* 2019;21(6):755-767.
184. Tubbs E, Theurey P, Vial G, et al. Mitochondria-associated endoplasmic reticulum membrane (MAM) integrity is required for insulin signaling and is implicated in hepatic insulin resistance. *Diabetes.* 2014;63(10):3279-3294.
185. Simmen T, Tagaya M. Organelle Communication at Membrane Contact Sites (MCS): From Curiosity to Center Stage in Cell Biology and Biomedical Research. *Adv Exp Med Biol.* 2017;997:1-12.
186. Rieusset J. The role of endoplasmic reticulum-mitochondria contact sites in the control of glucose homeostasis: an update. *Cell Death Dis.* 2018;9(3):388.
187. Chandel NS. Evolution of Mitochondria as Signaling Organelles. *Cell Metab.* 2015;22(2):204-206.

## 9. Acknowledgement

I dedicate this doctoral thesis to **Dr. Jayanti Sen**, who was the seed of my inspiration for pursuing a career in the field of molecular biology and research. I know wherever she is, she must be extremely pleased to see how far I have come.

I am extremely grateful to my doctoral father and guide, **Prof. Dr. Berend Isermann**, for supporting me at every step of the way through my journey as a research scientist. He has been extremely encouraging and helped me navigate the difficult phases of my doctoral journey. I have learnt more from him in the past 3 years than all my years of being in this field of work. Under his supervision, I have grown as a scientist and as an individual. Thank you, Berend.

In my journey to attaining Ph.D., I cannot forget **Dr. Thati Madhusudhan's** contributions. He taught me laboratory/ experimental skills and challenged me scientifically, sometimes as a supervisor and other times as a friend.

In the last 5 years, since I moved to Magdeburg and started my Ph.D. in AG Isermann, I have had the greatest opportunities to work alongside some incredible people, who have become much more than colleagues. **Evelyn Amrita**, my first girlfriend in MD. She and I joined AG Isermann around the same time. Evelyn is a woman after my own heart, independent, honest, full of integrity, sincere, dedicated and self-respecting. She has been an inspiration and I try to emulate her attitude towards life every day. I admire her deeply. Whenever I lack motivation, I reflect on Evelyn's famous words of encouragement to me, "passing clouds!". **Dr. Al-Dabet Moh'd Mohanad** was my very shy, sweet and understanding office colleague. Pure at heart, kind, chivalrous, courteous, sensitive, talented and a superior human being, we all should strive to be. Al-Dabet's wife, Ala, and their 2 daughters, Dana and Dima, became my family. I knew that anytime I felt low and unhappy, they would be available to shower me with love and cheer me up. I am so glad I got a chance to meet such a beautiful family and such unadulterated, pure souls. I wish Al-Dabet, Ala, Dana and Dima all the prosperity and happiness. **Haroon Sheikh** was a brief member of AG Isermann but in the short duration he was here, he became a true friend, always there to help and be a shoulder to cry on. Soft-spoken, sensitive, and intelligent, Haroon is a brilliant individual. I have seen him smile through all his struggles and overcome all difficulties life throws in his path. Haroon, you will remain a friend forever. **Sumra Nazir**, although our friendship began well along after we became colleagues, I have seen your growth as an individual and a scientist. I have learnt so much from just observing you. Sumra is tremendously pure at heart, honest, dedicated, loyal, values friendship and is a strong, independent and self-respecting individual. She is my sister from another mother and will remain so no matter where we are in life. I hope Sumra, you and I, will be able to look back at our experiences and laugh at the dark times we have managed to overcome together. I will always be there for you, a phone call or a message away. **Dr. Juliane Wolter**, you were my senior when I joined Isermann lab, but we became friends towards the time you were finishing your Ph.D. Our dinner outings, movie outings and meetings outside the lab have been breaths of fresh air and helped dilute the stress of Ph.D life. Easy going, helpful, thoughtful, kind and friendly, I have always seen Juliane laugh and smile. Thank you for all our times together, I cherish our walks and heart-to-heart conversations. **Ahmed Elwakiel** joined AG Isermann several

years after I joined the lab, but his quiet, patient and tolerant attitude towards life and science has been qualities of extreme admiration for me. I have enjoyed his journal club presentations a lot. He is an immensely talented scientist and an incredibly talented teacher. I hope he continues teaching since he can make any topic very simple and easy to understand. Thank you, Ahmed, for all your sincere advices, for helping see things from a different vantage point and for always speaking your mind with me. True and honest human beings are a rare find in this World. Thank you for being critical and supportive. **Ruma (Makarova), Frau Deneser and Julia (Judin)**, have been my source of strength when I have found myself alone and dull in lab. They have been affectionate, kind, considerate, helpful and guided me whenever I have needed it. Having them in the lab has been a real asset. All 3 of you have enriched my life. I am deeply grateful to you for your company, support, and for always lending me a kind ear. **Dr. Ronald Biemann and Dr. Kathleen Biemann** were the first colleagues and family I turned to for help when I was facing difficulties in my personal life. I will forever be grateful to the both for being there for me when I needed good and trustworthy friends around me. I am deeply grateful to Ronald and Kathleen for their kindness and friendship

I am not very good at expressing my love openly to my parents, **Mr. Viswa Ghosh and Mrs. Bhaswati Ghosh** and my sister, **Udita Ghosh**. Yet I know they know and understand my innermost feelings. I have survived through it all knowing they believe in me and are always going to be there. I don't think I have words to express how fortunate I am that I am their daughter. I hope to be born as my parents' child again. I wish I had more of their talents and goodness, although my sister has inherited the larger share of that. Udita Ghosh is the best gift my parents gave me although I didn't realize this growing up. I have and I continue to learn a lot from her. My life would be completely empty and utterly boring without her. Gratitude, love and respect are very trivial words when I try to express what I feel for these 3 people. They will always remain my true critics and best guides through every phase of life. They are the ones who push me to do better; to fight for the right things, to never give up; to continue to learn and grow in every aspect of life; to be simple and yet not a simpleton; to pay attention to intricate details, and to think from the heart! After these 3, when I try to define 'family', **Sharang** comes to mind, my husband and partner. My doctoral journey and our relationship began around the same time. His sacrifices and investments in my doctorate degree have been almost equal to my own. I believe I moved to Jena for only 10 months because I had to meet Sharang and become integral part of each other's journeys. He is everything I lack and wish I had/ was. He is my friend, my dance partner, my pride, my entertainment and my laughter, my critic, my guide, my confidant and my connect to the World outside of science. He is my happiness and my 'home away from home'. To my **grandparents (Sengupta and Ghosh)**, our memories together are a constant source of affection, positivity, strength and guiding lights in my life.

To my Sharma family (**Renuka, Jayamala, Sanjay, Shashi, Shivam and Raghav**), I am grateful to you all for accepting me into your life and your family. You have brought diversity and colorful relationships into my life. Thank you for letting me be who I am and showering me with affection, love and blessings. In this world of hatred and jealousy, you each continue to bind us together into one family unit through love.

**Dr. Alok Sinha**, took me in for a month-long summer internship at NIPGR (J.N.U, New Delhi, India) when I was still finding my way in the field of research. As my boss and guide initially, and later as a friend, he has been and always will be an inspiration. The month I spent in his lab helped me solidify my determination to continue in the path towards a doctoral degree. An immensely talented scientist, he gave me a chance to prove to myself that I was capable of undertaking the challenges of this career. Whenever I have needed guidance, he has been one email away. I will always be indebted to him.

Lastly, I would like to mention all those people who have been an integral part of my journey and my life- **Mr. Robey, Ms. Hayes, Mr. Oakes, Mr. Wilson, Mrs. Robinson and all my teachers at ISSH** (Tokyo, Japan), **Dr. Isona Kakuchi, Dr. Kamolika Roy, Dr. Divya Vangala, Dr. Divya Kanneganti, Prof. Dr. Ruibao Ren** (Brandeis University), **Dr. Benjamin Cuiffo, Dr. Eri Verter, Dr. Ana Ivonne Vazquez Armendariz, Dr. Philipp Stavowy** (DHZ, Berlin), **Dr. Clara Lemos, Dr. Ibrahim Soeguet** (Istanbul, Turkey), **Kuheli Banerjee, Dr. Manisha Juneja, Dr. Katyayni Vinnakota, Dr. Manmeet S. Bedi, Dr. Varunika Goyal, Tunikipati family** (Texas, U.S.A), **Dhar family** (Toronto, Canada), **Banerjea family** (Nairobi, Kenya), and **Kanneganti family** (Stoneham, U.S.A). Thank you for adding much value, love and friendships to my life, I am who I am because of all of you. You have been fundamental to my personal and professional successes.

## 10. Declaration

Ich erkläre, dass ich die der Medizinischen Fakultät der Otto-von-Guericke-Universität zur Promotion eingereichte Dissertation mit dem Titel

**The regulation of endoplasmic reticulum stress by activated protein C in diabetic nephropathy**

im Institut für Klinische Chemie und Pathobiochemie der Medizinischen Fakultät der Otto-von-Guericke-Universität Magdeburg

mit Unterstützung durch Prof. Dr. med. Berend Isermann

ohne sonstige Hilfe durchgeführt und bei der Abfassung der Dissertation keine anderen als die dort aufgeführten Hilfsmittel benutzt habe.

Bei der Abfassung der Dissertation sind Rechte Dritter nicht verletzt worden.

Ich habe diese Dissertation bisher an keiner in- oder ausländischen Hochschule zur Promotion eingereicht. Ich übertrage der Medizinischen Fakultät das Recht, weitere Kopien meiner Dissertation herzustellen und zu vertreiben.

Magdeburg, den

(Sanchita Ghosh)

Unterschrift

## 11. Curriculum Vitae and list of publications

### 11.1 Curriculum Vitae

#### PERSONAL INFORMATION:

Name: Sanchita Ghosh  
Address: Otto-von-Guericke-University (OvGU) Magdeburg  
Medical Faculty / Institute of Clinical Chemistry and Pathobiochemistry  
Leipziger strasse 44  
39120 Magdeburg  
Tel: +49 176 7217766  
Email: **sanchita.ghosh@med.ovgu.de & sanchita.g87@gmail.com**  
Born: 20.05.1987  
Nationality: Indian

---

#### EDUCATION:

Title of qualification: **PhD student**, Institute of Clinical Chemistry and Pathobiochemistry (IKCP)  
Dates: April 2014- to date  
Name of institution: Otto-von-Guericke University (Medical Faculty), Magdeburg (Germany)

Title of qualification: **Master of Science in Molecular Medicine (final grade 88%)**  
Dates: October 2010- September 2012  
Name of institution: Charité Medical University (Research Hospital), Berlin (Germany)



Title of qualification: **Bachelor of Science in Biology**  
Dates: August 2005- May 2009  
Name of institution: Brandeis University, Waltham, Massachusetts (U.S.A)

Title of qualification: **International High School Graduate Diploma** (International high school curriculum with additional Advance Placement courses in Calculus AB & BC, English literature, Biology, Chemistry, Art and Theory of Knowledge), Rating Distinction (90%)  
Dates: August 2001- June 2005  
Name of institution: International School of Sacred Heart, Tokyo (Japan)

---

#### **POSTER PRESENTATIONS (selected):**

**Ghosh S**, Madhusudhan T, Wang H, et al. (July 2017). Spatiotemporal modulation of the protease activated receptors signaling protects against diabetic nephropathy. Poster session presented at the 63<sup>rd</sup> Annual SSC Meeting of the ISTH - Congress: International Society on Thrombosis and Haemostasis, Berlin, Germany.

**Ghosh S**, Madhusudhan T, Moh'd Mohanad A, et al. (November 2016). *Hormone-like function of coagulation protease rescues defective insulin signaling in the kidney*. Poster session presented at the annual Kidney Week of the American Society of Nephrology in Chicago, IL, USA

---

#### **SCIENTIFIC ACTIVITIES, AWARDS & FELLOWSHIPS:**

Participated in Grant Proposal Writing Workshop organized by the Graduate Academy, OvGU (Medical Faculty) - 4<sup>th</sup> & 5<sup>th</sup> of February 2019, Magdeburg, Germany.

Participated in Career Day 2018- Perspectives for Women in Life Sciences- organized by the OvGU, EKFK (Else Kröner Forschungskolleg), CBBS (Centre for Behavioral Brain Sciences) and Lin (Leibniz Institute for Neurobiology Magdeburg) – 14<sup>th</sup> of June 2018, Magdeburg, Germany.

Best Poster, at the the 63<sup>rd</sup> Annual SSC Meeting of the ISTH - Congress: International Society on Thrombosis and Haemostasis - July 2017, Berlin, Germany.

Winner of scientific photo contest "Impression of Inflammation" organized by the Health Sciences Campus OvGU (Medical Faculty) – 2015, Magdeburg, Germany.

Participated in "Introduction into animal experimental methods" and was certified for animal handling/ experiments, at OvGU (Medical Faculty) - 2015, Magdeburg, Germany.

Awardee of the Aspire Student Training grant from the Helmholtz Graduate School of Molecular Cell Biology at the Max-Delbrück-Center (MDC), Berlin- competitive scholarship supporting outstanding students of molecular life sciences who wish to receive training in one of the MDC's excellent research groups - 2012 (February to July), Berlin, Germany.

Worked as a research student for 6 months on a project title, "The role of MACC1 in colorectal cancers" in the lab of Prof. Dr. Ulrike Stein at the Max-Delbrück-Center (MDC) – January to August 2012, Berlin, Germany.

Worked as research student for 3 months on a project titled, "Furin-dependent proNGF maturation determines apoptosis or integrins- associated migration of vascular smooth muscle cells in atherosclerosis in the lab of Dr. med. Philipp Stawowy at the Deutsches Herzzentrum (DHZ) – August to December 2011, Berlin, Germany.

Awardee of the Alumni and Friends Scholarship (Brandeis University) - Combination of scholarship and employment to cover the full tuition and living costs for the duration of study- August 2005 - May 2009, Waltham (MA), U.S.A.

Dean's List- is an academic honor attributed to students whose semester GPA is 3.50 or higher (on a scale of 1.00 to 4.00, with 4.00 representing the highest percentage achievable). To be eligible, the student must have taken at least 3 full courses (12 credit hours) for a letter grade, and not have received a grade of D (laboratory courses and Physical exercise courses inclusive) - 2005 & 2008 (August to December), Waltham (MA), U.S.A.

## 11.2 List of publications

Madhusudhan T\*, **Ghosh S\***, Wang H\*, Dong W, Gupta D, Stoyanov S, Elwakiel A, Moh'd Mohanad A, Krishnan S, Kohli S, Biemann R, Nazir S, Zimmermann S, Mathews A, Gadi I, Rana R, Frey H, Moeller MJ, Schaefer L, Esmon CT, Reiser J, Rezaie AR, Ruf W, and Isermann B. Podocyte integrin- $\beta$ 3 and activated protein C coordinately restrict RhoA signaling and ameliorate diabetic nephropathy. **JASN**. 2019 (in revision).

(\* All authors contributed equally to this work). *IF:9.11*

Shahzad K, **Ghosh S**, Mathew A, and Isermann B. 'Endoplasmic reticulum stress and apoptosis in diabetic nephropathy', in Gnudi L (ed.), *Methods in Molecular Biology*. Springer Nature.(in process).

Nazir S, Gadi I, Moh'd Mohanad A, Elwakiel A, Kohli S, **Ghosh S**, Manoharan J, Ranjan S, Bock F, Braun-Dullaes RC, Esmon CT, Huber TB, Camerer E, Dockendorff C, Griffin JH, Isermann B, and Shahzad K. Cytoprotective activated protein C averts Nlrp3 inflammasome-induced ischemia-reperfusion injury via mTORC1 inhibition. **Blood**. 2017;130(24):2664-2677. *IF:13.16*

Marquardt A, Moh'd Mohanad A, **Ghosh S**, Kohli S, Manoharan J, ElWakiel A, Gadi I, Bock F, Nazir S, Wang H, Lindquist J, Nawroth PP, Madhusudhan T, Mertens P, Shahzad K, and Isermann B. FXR-agonism protects against diabetic tubulopathy -add-on effect on top of ACE-inhibition. **J Am Soc Nephrol**. November 2017. *IF:8.98*

Madhusudhan T\*, Wang H\*, **Ghosh S\***, Dong W, Kumar V, Moh'd Mohanad A, Manoharan J, Bock F, Kohli S, Marquardt A, Shahzad K, Müller AJ, Esmon CT, Nawroth PP, Reiser J, Chavakis T, Ruf W, and Isermann B. Signal integration at the PI3K-p85-XBP1 hub endows coagulation protease activated protein C with insulin like function. **Blood**. 2017;130(12):1445-1455.

(\* All authors contributed equally to this work). *IF:13.16*

Shahzad K, BockF, Moh'd Mohanad A, Gadi I, Kohli S, Nazir S, **Ghosh S**, Ranjan S, Wang H, Madhusudhan T, Nawroth PP, and Isermann B. Caspase-1, but Not Caspase-3, Promotes Diabetic Nephropathy. **J Am Soc Nephrol**. 2016;(27): 2270–2275. *IF: 8.98*

Madhusudhan T, Wang H, Dong W, **Ghosh S**, Bock F, Thangapandi VR, Ranjan S, Wolter J, Kohli S, Shahzad K, Heidel F, Krueger M, Schwenger V, Moeller MJ, Kalinski T, Reiser J, Chavakis T, and Isermann B. Defective podocyte insulin signalling through p85-XBP1 promotes ATF6-dependent maladaptive ER-stress response in diabetic nephropathy. **Nat Commun**. 2015;6:6496. *IF:12.35*

Urband D, Lorenz J, Meyborg H, **Ghosh S**, Kintscher U, Kaufmann J, Fleck E, Kappert K, and Stawowy P. Proprotein convertase furin enhances survival and migration of vascular

smooth muscle cells via processing of pro-nerve growth factor. *J Biochem.* 2013;153(2):197-207. *IF:2.58*